

Supplementary Information

Identification of common variants associated with human hippocampal and intracranial volumes

Jason L. Stein*, Sarah E. Medland*, Alejandro Arias Vasquez*, Derrek P. Hibar*, Rudy E. Senstad, Anderson M. Winkler, Roberto Toro, Katja Appel, Richard Bartecek, Ørjan Bergmann, Manon Bernard, Andrew A. Brown, Dara M. Cannon, Mallar Chakravarty, Andrea Christoforou, Martin Domin, Oliver Grimm, Marisa Hollinshead, Avram J. Holmes, Georg Homuth, Jouke-Jan Hottenga, Camilla Langan, Lorna M. Lopez, Narelle K. Hansell, Kristy S. Hwang, Sungeun Kim, Gonzalo Laje, Phil H. Lee, Xinmin Liu, Eva Loth, Anbarasu Lourdusamy, Susana Muñoz Maniega, Morten Mattingsdal, Sebastian Mohnke, Kwangsik Nho, Allison C. Nugent, Carol O'Brien, Martina Papmeyer, Benno Pütz, Adaikalavan Ramasamy, Jerod Rasmussen, Mark Rijpkema, Shannon L. Risacher, J. Cooper Roddey, Emma J. Rose, Mina Ryten, Li Shen, Emma Sprooten, Eric Strengman, Alexander Teumer, Daniah Trabzuni, Jessica Turner, Kristel van Eijk, Theo G.M. van Erp, Marie-Jose van Tol, Katharina Wittfeld, Christiane Wolf, Saskia Woudstra, Andre Aleman, Saud Alhusaini, Laura Almasy, Elisabeth B. Binder, David G. Brohawn, Rita M. Cantor, Melanie A. Carless, Aiden Corvin, Michael Czisch, Joanne E. Curran, Gail Davies, Marcio A. A. de Almeida, Norman Delanty, Chantal Depondt, Ravi Duggirala, Thomas D. Dyer, Susanne Erk, Jesen Fagerness, Peter T. Fox, Nelson B. Freimer, Michael Gill, Harald H.H. Göring, Donald J. Hagler, David Hoehn, Florian Holsboer, Martine Hoogman, Norbert Hosten, Neda Jahanshad, Matthew P. Johnson, Dalia Kasperaviciute, Jack W. Kent, Jr., Peter Kochunov, Jack L. Lancaster, Stephen M. Lawrie, David C. Liewald, René Mandl, Mar Matarin, Manuel Mattheisen, Eva Meisenzahl, Ingrid Melle, Eric K. Moses, Thomas W. Mühlleisen, Matthias Nauck, Markus M. Nöthen, Rene L. Olvera, Massimo Pandolfo, G. Bruce Pike, Ralf Puls, Ivar Reinvang, Miguel E. Rentería, Marcella Rietschel, Joshua L. Roffman, Natalie A. Royle, Dan Rujescu, Jonathan Savitz, Hugo G. Schnack, Knut Schnell, Nina Seiferth, Colin Smith, Vidar M. Steen, Maria C. Valdés Hernández, Martijn Van den Heuvel, Nic J. van der Wee, Neeltje E.M. Van Haren, Joris A. Veltman, Henry Völzke, Robert Walker, Lars T. Westlye, Christopher D. Whelan, Ingrid Agartz, Dorret I. Boomsma, Gianpiero L. Cavalleri, Anders M. Dale, Srdjan Djurovic, Wayne C. Drevets, Peter Hagoort, Jeremy Hall, Andreas Heinz, Clifford R. Jack, Jr., Tatiana M. Foroud, Stephanie Le Hellard, Fabio Macciardi, Grant W. Montgomery, Jean Baptiste Poline, David J. Porteous, Sanjay M. Sisodiya, John M. Starr, Jessika Sussmann, Arthur W. Toga, Dick J. Veltman, Henrik Walter, Michael W. Weiner, the Alzheimer's Disease Neuroimaging Initiative, EPIGEN Consortium, IMAGEN Consortium, Saguenay Youth Study Group, Joshua C. Bis, M. Arfan Ikram, Albert V. Smith, Vilmundur Gudnason, Christophe Tzourio, Meike W. Vernooij, Lenore J. Launer, Charles DeCarli, Sudha Seshadri, for the CHARGE Consortium, Ole A. Andreassen, Liana G. Apostolova, Mark E. Bastin, John Blangero, Han G. Brunner, Randy L. Buckner, Sven Cichon, Giovanni Coppola, Greig I. de Zubiray, Ian J. Deary, Gary Donohoe, Eco J.C. de Geus, Thomas Espeseth, Guillén Fernández, David C. Glahn, Hans J. Grabe, John Hardy, Hilleke E. Hulshoff Pol, Mark Jenkinson, René S. Kahn, Colm McDonald, Andrew M. McIntosh, Francis J. McMahon, Katie L. McMahon, Andreas Meyer-Lindenberg, Derek W. Morris, Bertram Müller-Myhsok, Thomas E. Nichols, Roel A. Ophoff, Tomas Paus, Zdenka Pausova, Brenda W. Penninx, Steven G. Potkin, Philipp G. Sämann, Andrew J. Saykin, Gunter Schumann, Jordan W. Smoller, Joanna M. Wardlaw, Michael E. Weale, Nicholas G. Martin#, Barbara Franke#, Margaret J. Wright#, Paul M. Thompson#, for the Enhancing Neuroimaging Genetics through Meta-Analysis (ENIGMA) Consortium

Note this document is hyperlinked. Please click on a subheading below to navigate to that section of the document. A hyperlinked contents page is provided at the start of each subsection.

CONTENTS

Supplementary Note	2
Supplementary Figures	9
Supplementary Tables	50

Supplementary Note

1. Haplotype analysis

We conducted haplotype analyses in two samples, SHIP (N=800) and SHIP-Trend (N=871) using directly genotyped SNPs. These two samples were genotyped on Affy 6.0 and Illumina Human Omni 2.5M chips, which do not have the same SNP coverage in the associated region. Residuals of average bilateral hippocampal volume, after adjusting for intracranial volume and other covariates included in all analyses (sex, age, age², sex × age, sex × age², and 4 MDS components), were used as the phenotype of interest. Haplotype analyses were conducted in PLINK using the --proxy-assoc command.

In the SHIP sample, alleles at rs7294919 showed association in the context of a 4-SNP haplotype comprised of rs7972948, rs4767469, rs7294919, rs7133290 ($P=0.0214$). In addition, no haplotypes excluding rs7294919 led to stronger association results, although association with rs7133290 ($r^2=0.965$ to rs7294919) gave similar results to rs7294919 alone ($P=0.0524$).

In the SHIP-Trend sample, alleles at rs7294919 showed association in the context of a 4-SNP haplotype comprised of rs9669553, rs7294919, SNP12-115816539, and rs4766810 ($P=0.0446$). In addition, haplotypes excluding rs7294919 led to similar association results, though a slightly stronger signal was observed with rs4766810 ($r^2=0.518$ to rs7294919; $P=0.00601$).

These findings imply that rs7294919 was well tagged by surrounding SNPs and that genotyping error was not causing spurious results, as association was still found after removing rs7294919. In addition, we can conclude from this analysis that the causal variant lies within the haplotype block defined by the SNPs above and is well tagged by rs7294919.

2. PBMC eQTLs

We looked for potential regulatory signals of rs7294919 in peripheral blood mononuclear cells (PBMCs), and we identified additional *cis*-associations. Interestingly, no evidence of association with *TESC* was seen in PBMCs in the Mexican-American GOBS cohort ($P=0.386$) or in 80 samples within SNPEexpress ($P=0.453$). Rather, strong associations of rs7294919 were seen with expression of *LOC283454* ($P=8.52\times 10^{-6}$) and *HRK* ($P=2.84\times 10^{-5}$) within the GOBS sample (N=1224)⁷¹. Significant associations were also seen for *C12orf49* ($P=0.0053$) and *FBXW8* ($P=0.0078$). Although not a perfect proxy for brain, these significant *cis*-effects from blood-derived tissue suggest additional positional candidate genes for future examination.

3. Consortium Authors:

The following authors are included under the Alzheimer's Disease Neuroimaging Initiative (ADNI):

Michael Weiner (UC San Francisco), Paul Aisen (UC San Diego), Ronald Petersen (Mayo Clinic, Rochester), Clifford R. Jack, Jr. (Mayo Clinic, Rochester), William Jagust (UC Berkeley), John Q. Trojanowski (U Pennsylvania), Arthur W. Toga (UCLA), Laurel Beckett (UC Davis), Robert C. Green (Brigham and Women's Hospital / Harvard Medical School), Andrew J. Saykin (Indiana University), John Morris (Washington University St. Louis); **ADNI 2 Private Partner Scientific Board (PPSB) Chair:** Enchi Liu (Janssen Alzheimer Immunotherapy); **Data and Publication Committee (DPC):** Robert C. Green (Brigham and Women's Hospital/Harvard Medical School (Chair)); **Resource Allocation Review Committee:** Tom Montine (University of Washington (Chair)); **Clinical Core Leaders:** Ronald Petersen (Mayo Clinic, Rochester), Paul Aisen (UC San Diego); **Clinical Informatics and Operations:** Anthony Gamst (UC San Diego), Ronald G. Thomas (UC San Diego), Michael Donohue (UC San Diego), Sarah Walter (UC San Diego), Devon Gessert (UC San Diego), Tamie Sather (UC San Diego); **Biostatistics Core Leaders and Key Personnel:** Laurel Beckett (UC Davis), Danielle Harvey (UC Davis), Anthony Gamst (UC San Diego), Michael Donohue (UC San Diego), John Kornak (UC Davis); **MRI Core Leaders and Key Personnel:** Clifford R. Jack, Jr. (Mayo Clinic, Rochester), Anders Dale (UC San Diego), Matthew Bernstein (Mayo Clinic, Rochester), Joel Felmlee (Mayo Clinic, Rochester), Nick Fox (University of London), Paul Thompson (UCLA School of Medicine), Norbert Schuff (UCSF), Gene Alexander (Banner Alzheimer's Institute), Charles DeCarli (UC Davis); **PET Core Leaders and Key Personnel:** William Jagust (UC Berkeley), Dan Bandy (Banner Alzheimer's Institute), Robert A. Koeppe (University of Michigan), Norm Foster (University of Utah), Eric M. Reiman (Banner Alzheimer's Institute), Kewei Chen (Banner Alzheimer's Institute), Chet Mathis (University of Pittsburgh); **Neuropathology Core Leaders:** John Morris (Washington University St. Louis), Nigel J. Cairns (Washington University St. Louis), Lisa Taylor-Reinwald (Washington University St. Louis); **Biomarkers Core Leaders and Key Personnel:** J.Q. Trojanowski (UPenn School of Medicine), Les Shaw (UPenn School of Medicine), Virginia M.Y. Lee (UPenn School of Medicine), Magdalena Korecka (UPenn School of Medicine); **Informatics Core Leaders and Key Personnel:** Arthur W. Toga (UCLA), Karen Crawford (UCLA), Scott Neu (UCLA); **Genetics Core Leaders and Key Personnel:** Andrew J. Saykin (Indiana University), Tatiana M. Foroud (Indiana University), Steven Potkin (UC Irvine), Li Shen (Indiana University); **Early Project Development:** Zaven Kachaturian (Radebaugh & Associates (KRA), Inc / Alzheimer's Association's Ronald and Nancy Reagan's Research Institute), Richard Frank (General Electric), Peter J. Snyder (University of Connecticut); **NIA:** Susan Molchan (National Institute on Aging/National Institutes of Health).

ADNI Investigators By Site (FULL ADNI Investigator Lists):

Oregon Health and Science University: Jeffrey Kaye, Joseph Quinn, Betty Lind, Sara Dolen – Past Investigator; **University of Southern California:** Lon S. Schneider, Sonia Pawluczyk, Bryan M. Spann; **University of California--San Diego:** James Brewer, Helen Vanderswag; **University of Michigan:** Judith L. Heidebrink, Joanne L. Lord; **Mayo Clinic, Rochester:** Ronald Petersen, Kris Johnson; **Baylor College of Medicine:** Rachelle S. Doody, Javier Villanueva-Meyer, Munir Chowdhury; **Columbia University Medical Center:** Yaakov Stern, Lawrence S. Honig, Karen L. Bell; **Washington University, St. Louis:** John C. Morris, Beau Ances, Maria Carroll, Sue Leon, Mark A. Mintun – Past Investigator, Stacy Schneider – Past Investigator; **University of Alabama - Birmingham:** Daniel Marson, Randall Griffith, David Clark; **Mount Sinai School of Medicine:** Hillel Grossman, Effie Mitsis, Aliza Romirowsky; **Rush University Medical Center:** Leyla deToledo-Morrell, Raj C. Shah; **Wein Center:** Ranjan Duara, Daniel Varon, Peggy Roberts; **Johns Hopkins University:** Marilyn Albert, Chiadi Onyike, Stephanie Kielb; **New York University:** Henry Rusinek, Mony J de Leon, Lidia Glodzik, Susan De Santi – Past Investigator; **Duke University Medical Center:** P. Murali Doraiswamy, Jeffrey R. Petrella, R. Edward Coleman; **University of Pennsylvania:** Steven E. Arnold, Jason H. Karlawish, David Wolk; **University of Kentucky:** Charles D. Smith, Greg Jicha, Peter Hardy; **University of Pittsburgh:** Oscar L. Lopez, MaryAnn Oakley, Donna M. Simpson; **University of Rochester Medical Center:** Anton P. Porsteinsson, Bonnie S. Goldstein, Kim Martin, Kelly M. Makino – Past Investigator, M. Saleem Ismail – Past Investigator, Connie Brand – Past Investigator; **University of California, Irvine:** Ruth A. Mulnard, Gaby Thai, Catherine Mc-Adams-Ortiz; **University of Texas Southwestern Medical School:** Kyle Womack, Dana Mathews, Mary Quiceno, Ramon Diaz-Arrastia – Past Investigator, Richard King – Past Investigator, Myron Weiner – Past Investigator, Kristen Martin-Cook – Past Investigator, Michael DeVos – Past Investigator; **Emory University:** Allan I. Levey, James J. Lah, Janet S. Cellar; **University of Kansas, Medical Center:** Jeffrey M. Burns, Heather S. Anderson, Russell H. Swerdlow; **University of California, Los Angeles:** Liana Apostolova, Po H. Lu, George Bartzokis – Past Investigator, Daniel H.S. Silverman – Past Investigator; **Mayo Clinic, Jacksonville:** Neill R Graff-Radford (London), Francine Parfitt, Heather Johnson; **Indiana University:** Martin R. Farlow, Ann Marie Hake, Brandy R. Matthews, Scott Herring – Past Investigator, **Yale University School of Medicine:** Christopher H. van Dyck, Richard E. Carson, Martha G. MacAvoy; **McGill Univ., Montreal-Jewish General Hospital:** Howard

Chertkow, Howard Bergman, Chris Hosei; **Sunnybrook Health Sciences, Ontario**: Sandra Black, Bojana Stefanovic, Curtis Caldwell; **U.B.C. Clinic for AD & Related Disorders**: Ging-Yuek Robin Hsiung, Howard Feldman, Benita Mudge, Michele Assaly – Past Investigator; **Cognitive Neurology - St. Joseph's, Ontario**: Andrew Kertesz, John Rogers, Dick Trost; **Cleveland Clinic Lou Ruvo Center for Brain Health**: Charles Bernick, Donna Munic; **Northwestern University**: Diana Kerwin, Marek-Marsel Mesulam, Kristina Lipowski, Chuang-Kuo Wu – Past Investigator, Nancy Johnson – Past Investigator; **Premiere Research Inst (Palm Beach Neurology)**: Carl Sadowsky, Walter Martinez, Teresa Villena; **Georgetown University Medical Center**: Raymond Scott Turner, Kathleen Johnson, Brigid Reynolds; **Brigham and Women's Hospital**: Reisa A. Sperling, Keith A. Johnson, Gad Marshall, Meghan Frey – Past Investigator; **Stanford University**: Jerome Yesavage, Joy L. Taylor, Barton Lane, Allyson Rosen – Past Investigator, Jared Tinklenberg – Past Investigator; **Banner Sun Health Research Institute**: Marwan Sabbagh, Christine Belden, Sandra Jacobson; **Boston University**: Neil Kowall, Ronald Killiany, Andrew E. Budson, Alexander Norbash – Past Investigator, Patricia Lynn Johnson – Past Investigator; **Howard University**: Thomas O. Obisesan, Saba Wolday, Salome K. Bwayo – Past Investigator; **Case Western Reserve University**: Alan Lerner, Leon Hudson, Paula Ogorzki; **University of California, Davis – Sacramento**: Evan Fletcher, Owen Carmichael, John Olichney, Charles DeCarli; **Neurological Care of CNY**: Smita Kittur; **Parkwood Hospital**: Michael Borrie, T-Y Lee, Rob Bartha; **University of Wisconsin**: Sterling Johnson, Sanjay Asthana, Cynthia M. Carlsson; **University of California, Irvine - BIC**: Steven G. Potkin, Adrian Preda, Dana Nguyen; **Banner Alzheimer's Institute**: Pierre Tariot, Adam Fleisher, Stephanie Reeder; **Dent Neurologic Institute**: Vernice Bates, Horacio Capote, Michelle Rainka; **Ohio State University**: Douglas W. Scharre, Maria Kataki; **Albany Medical College**: Earl A. Zimmerman, Dzintra Celmins, Alice D. Brown – Past Investigator; **Hartford Hospital, Olin Neuropsychiatry Research Center**: Godfrey D. Pearlson, Karen Blank, Karen Anderson; **Dartmouth-Hitchcock Medical Center**: Andrew J. Saykin, Robert B. Santulli, Eben S. Schwartz; **Wake Forest University Health Sciences**: Kaycee M. Sink, Jeff D. Williamson, Pradeep Garg, Franklin Watkins – Past Investigator; **Rhode Island Hospital**: Brian R. Ott, Henry Querfurth, Geoffrey Tremont; **Butler Hospital**: Stephen Salloway, Paul Malloy, Stephen Correia; **UC San Francisco**: Howard J. Rosen, Bruce L. Miller; **Medical University South Carolina**: Jacobo Mintzer, Crystal Flynn Longmire, Kenneth Spicer; **St. Joseph's Health Care**: Elizabeth Finger, Irina Rachinsky, John Rogers, Andrew Kertesz – Past Investigator, Dick Drost – Past Investigator.

The following authors are included under the EPIGEN Consortium:

Gianpiero Cavalleri (Department of Molecular and Cellular Therapeutics, the Royal College of Surgeons, Ireland), Saud Alhusaini (Department of Molecular and Cellular Therapeutics, the Royal College of Surgeons, Ireland), Norman Delanty (Department of Molecular and Cellular Therapeutics, the Royal College of Surgeons, Ireland), Christopher Whelan (Department of Molecular and Cellular Therapeutics, the Royal College of Surgeons, Ireland), Sanjay Sisodiya (Department of Clinical and Experimental Epilepsy, Institute of Neurology, University College, London, UK), Dalia Kasperaviciute (Department of Clinical and Experimental Epilepsy, Institute of Neurology, University College, London, UK), Mar Matarin (Department of Clinical and Experimental Epilepsy, Institute of Neurology, University College, London, UK), Chantal Depondt (Department of Neurology, Hopital Erasme, Universite Libre de Bruxelles), David B. Goldstein (The Centre for Genomics and Population Genetics, Duke University Institute for Genome Sciences and Policy, Durham, North Carolina, USA), Erin L. Heinzen (The Centre for Genomics and Population Genetics, Duke University Institute for Genome Sciences and Policy, Durham, North Carolina, USA), Kevin Shianna (The Centre for Genomics and Population Genetics, Duke University Institute for Genome Sciences and Policy, Durham, North Carolina, USA), Rodney Radtke (Department of Medicine, Duke University Medical Center, Durham, North Carolina, USA) and Ruth Ottmann (Departments of Epidemiology, Neurology, and the G.H. Sergievsky Center, Columbia University, New York, NY).

The following authors are included under the IMAGEN Consortium:

Schumann G (King's College London, Institute of Psychiatry, London, UK), Conrod P (King's College London, Institute of Psychiatry, London, UK), Reed L (King's College London, Institute of Psychiatry, London, UK), Barker G (King's College London, Institute of Psychiatry, London, UK), Williams S (King's College London, Institute of Psychiatry, London, UK), Loth E (King's College London, Institute of Psychiatry, London, UK), Struve M (King's College London, Institute of Psychiatry, London, UK), Lourdusamy A (King's College London, Institute of Psychiatry, London, UK), Cattrell A (King's College London, Institute of Psychiatry, London, UK), Nymberg C (King's College London, Institute of Psychiatry, London, UK), Topper L (King's College London, Institute of Psychiatry, London, UK), Smith L (King's College London, Institute of Psychiatry, London, UK), Havatzias S (King's College London, Institute of Psychiatry, London, UK), Stueber K (King's College London, Institute of Psychiatry, London, UK), Mallik C (King's College London, Institute of Psychiatry, London, UK), Stacey D (King's College London, Institute of Psychiatry, London, UK), Peng Wong C (King's College London, Institute of Psychiatry, London, UK), Werts H (King's College London, Institute of Psychiatry, London, UK), Williams S (King's College London, Institute of Psychiatry, London, UK), Andrew C (King's College London, Institute of Psychiatry, London, UK), Desrivieres S (King's College London, Institute

of Psychiatry, London, UK), Heinz A (Department of Psychiatry and Psychotherapy, Universitätsmedizin Berlin, Berlin, Germany), Gallinat J (Department of Psychiatry and Psychotherapy, Universitätsmedizin Berlin, Berlin, Germany), Häke I (Department of Psychiatry and Psychotherapy, Universitätsmedizin Berlin, Berlin, Germany), Ivanov N (Department of Psychiatry and Psychotherapy, Universitätsmedizin Berlin, Berlin, Germany), Klär A (Department of Psychiatry and Psychotherapy, Universitätsmedizin Berlin, Berlin, Germany), Reuter J (Department of Psychiatry and Psychotherapy, Universitätsmedizin Berlin, Berlin, Germany), Palafox C (Department of Psychiatry and Psychotherapy, Universitätsmedizin Berlin, Berlin, Germany), Hohmann C (Department of Psychiatry and Psychotherapy, Universitätsmedizin Berlin, Berlin, Germany), Schilling C (Department of Psychiatry and Psychotherapy, Universitätsmedizin Berlin, Berlin, Germany), Lüdemann K (Department of Psychiatry and Psychotherapy, Universitätsmedizin Berlin, Berlin, Germany), Romanowski A (Department of Psychiatry and Psychotherapy, Universitätsmedizin Berlin, Berlin, Germany), Ströhle A (Department of Psychiatry and Psychotherapy, Universitätsmedizin Berlin, Berlin, Germany), Wolff E (Department of Psychiatry and Psychotherapy, Universitätsmedizin Berlin, Berlin, Germany), Rapp M (Department of Psychiatry and Psychotherapy, Universitätsmedizin Berlin, Berlin, Germany), Ittermann B (Physikalisch-Technische Bundesanstalt, Berlin, Germany), Brühl R (Physikalisch-Technische Bundesanstalt, Berlin, Germany), Ihlenfeld A (Physikalisch-Technische Bundesanstalt, Berlin, Germany), Walaszek B (Physikalisch-Technische Bundesanstalt, Berlin, Germany), Schubert F (Physikalisch-Technische Bundesanstalt, Berlin, Germany), Garavan H (Institute of Neuroscience, Trinity College, Dublin, Ireland), Connolly C (Institute of Neuroscience, Trinity College, Dublin, Ireland), Jones J (Institute of Neuroscience, Trinity College, Dublin, Ireland), Lalor E (Institute of Neuroscience, Trinity College, Dublin, Ireland), McCabe E (Institute of Neuroscience, Trinity College, Dublin, Ireland), Ní Shiothcháin A (Institute of Neuroscience, Trinity College, Dublin, Ireland), Whelan R (Institute of Neuroscience, Trinity College, Dublin, Ireland), Spanagel R (Department of Psychopharmacology, Central Institute of Mental Health, Mannheim, Germany), Leonardi-Essmann F (Department of Psychopharmacology, Central Institute of Mental Health, Mannheim, Germany), Sommer W (Department of Psychopharmacology, Central Institute of Mental Health, Mannheim, Germany), Flor H (Department of Cognitive and Clinical Neuroscience, Central Institute of Mental Health, Mannheim, Germany), Vollstaedt-Klein S (Department of Cognitive and Clinical Neuroscience, Central Institute of Mental Health, Mannheim, Germany), Nees F (Department of Cognitive and Clinical Neuroscience, Central Institute of Mental Health, Mannheim, Germany), Banaschewski T (Department of Child and Adolescent Psychiatry, Central Institute of Mental Health, Mannheim, Germany), Poustka L (Department of Child and Adolescent Psychiatry, Central Institute of Mental Health, Mannheim, Germany), Steiner S (Department of Child and Adolescent Psychiatry, Central Institute of Mental Health, Mannheim, Germany), Mann K (Department of Addictive Behaviour and Addiction Medicine, Mannheim, Germany), Buehler M (Department of Addictive Behaviour and Addiction Medicine, Mannheim, Germany), Rietschel M (Department of Genetic Epidemiology in Psychiatry, Central Institute of Mental Health, Mannheim, Germany), Stolzenburg E (Department of Genetic Epidemiology in Psychiatry, Central Institute of Mental Health, Mannheim, Germany), Schmal C (Department of Genetic Epidemiology in Psychiatry, Central Institute of Mental Health, Mannheim, Germany), Schirmbeck F (Department of Genetic Epidemiology in Psychiatry, Central Institute of Mental Health, Mannheim, Germany), Paus T (Rotman Research Institute, University of Toronto, Ontario, Canada), Gowland P (School of Physics and Astronomy, University of Nottingham, Nottingham, UK), Heym N (School of Psychology, University of Nottingham, Nottingham, UK), Lawrence C (School of Psychology, University of Nottingham, Nottingham, UK), Newman C (School of Psychology, University of Nottingham, Nottingham, UK), Pausova Z (The Hospital for Sick Children, University of Toronto, Ontario, Canada), Smolka M (Technische Universität Dresden, Dresden, Germany), Huebner T (Technische Universität Dresden, Dresden, Germany), Ripke S (Technische Universität Dresden, Dresden, Germany), Mennigen E (Technische Universität Dresden, Dresden, Germany), Muller K (Technische Universität Dresden, Dresden, Germany), Ziesch V (Technische Universität Dresden, Dresden, Germany), Büchel C (Department of Systems Neuroscience, University Medical Center Hamburg-Eppendorf, Hamburg, Germany), Bromberg U (Department of Systems Neuroscience, University Medical Center Hamburg-Eppendorf, Hamburg, Germany), Fadai T (Department of Systems Neuroscience, University Medical Center Hamburg-Eppendorf, Hamburg, Germany), Lueken L (Department of Systems Neuroscience, University Medical Center Hamburg-Eppendorf, Hamburg, Germany), Yacubian J (Department of Systems Neuroscience, University Medical Center Hamburg-Eppendorf, Hamburg, Germany), Finsterbusch J (Department of Systems Neuroscience, University Medical Center Hamburg-Eppendorf, Hamburg, Germany), Martinot JL (Institut National de la Santé et de la Recherche Médicale, Service Hospitalier Frédéric Joliot, Orsay, France), Artiges E (Institut National de la Santé et de la Recherche Médicale, Service Hospitalier Frédéric Joliot, Orsay, France), Bordas N (Institut National de la Santé et de la Recherche Médicale, Service Hospitalier Frédéric Joliot, Orsay, France), de Bourronville S (Institut National de la Santé et de la Recherche Médicale, Service Hospitalier Frédéric Joliot, Orsay, France), Bricaud Z (Institut National de la Santé et de la Recherche Médicale, Service Hospitalier Frédéric Joliot, Orsay, France), Gollier Briand F (Institut National de la Santé et de la Recherche Médicale, Service Hospitalier Frédéric Joliot, Orsay, France), Lemaitre H (Institut National de la Santé et de la Recherche Médicale, Service Hospitalier Frédéric Joliot, Orsay, France), Massicotte J (Institut National de la Santé et de

la Recherche Médicale, Service Hospitalier Frédéric Joliot, Orsay, France), Miranda R (Institut National de la Santé et de la Recherche Médicale, Service Hospitalier Frédéric Joliot, Orsay, France), Paillère Martinot ML (Institut National de la Santé et de la Recherche Médicale, Service Hospitalier Frédéric Joliot, Orsay, France), Penttilä J (Institut National de la Santé et de la Recherche Médicale, Service Hospitalier Frédéric Joliot, Orsay, France), Poline JB (Neurospin, Commissariat à l'Energie Atomique, Paris, France), Barbot A (Neurospin, Commissariat à l'Energie Atomique, Paris, France), Schwartz Y (Neurospin, Commissariat à l'Energie Atomique, Paris, France), Lalanne C (Neurospin, Commissariat à l'Energie Atomique, Paris, France), Frouin V (Neurospin, Commissariat à l'Energie Atomique, Paris, France), Thyreau B (Neurospin, Commissariat à l'Energie Atomique, Paris, France), Dalley J (Department of Experimental Psychology, Behavioural and Clinical Neurosciences Institute, University of Cambridge, Cambridge, UK), Mar A (Department of Experimental Psychology, Behavioural and Clinical Neurosciences Institute, University of Cambridge, Cambridge, UK), Robbins T (Department of Experimental Psychology, Behavioural and Clinical Neurosciences Institute, University of Cambridge, Cambridge, UK), Subramaniam N (Department of Experimental Psychology, Behavioural and Clinical Neurosciences Institute, University of Cambridge, Cambridge, UK), Theobald D (Department of Experimental Psychology, Behavioural and Clinical Neurosciences Institute, University of Cambridge, Cambridge, UK), Richmond N (Department of Experimental Psychology, Behavioural and Clinical Neurosciences Institute, University of Cambridge, Cambridge, UK), de Rover M (Department of Experimental Psychology, Behavioural and Clinical Neurosciences Institute, University of Cambridge, Cambridge, UK), Molander A (Department of Experimental Psychology, Behavioural and Clinical Neurosciences Institute, University of Cambridge, Cambridge, UK), Jordan E (Department of Experimental Psychology, Behavioural and Clinical Neurosciences Institute, University of Cambridge, Cambridge, UK), Robinson E (Department of Experimental Psychology, Behavioural and Clinical Neurosciences Institute, University of Cambridge, Cambridge, UK), Hipolata L (Department of Experimental Psychology, Behavioural and Clinical Neurosciences Institute, University of Cambridge, Cambridge, UK), Moreno M (Department of Experimental Psychology, Behavioural and Clinical Neurosciences Institute, University of Cambridge, Cambridge, UK), Arroyo M (Department of Experimental Psychology, Behavioural and Clinical Neurosciences Institute, University of Cambridge, Cambridge, UK), Stephens D (University of Sussex, Brighton, UK), Ripley T (University of Sussex, Brighton, UK), Crombag H (University of Sussex, Brighton, UK), Pena Y (University of Sussex, Brighton, UK), Lathrop M (Centre National de Genotypage, Evry, France), Zelenika D (Centre National de Genotypage, Evry, France), Heath S (Centre National de Genotypage, Evry, France), Lanzerath D (German Centre for Ethics in Medicine, Bonn (DZEM), Germany), Heinrichs B (German Centre for Ethics in Medicine, Bonn (DZEM), Germany), Spranger T (German Centre for Ethics in Medicine, Bonn (DZEM), Germany), Fuchs B (Gesellschaft fuer Ablauforganisation m.b.H. (Munich) (GABO), Germany), Speiser C (Gesellschaft fuer Ablauforganisation m.b.H. (Munich) (GABO), Germany), Resch F (Klinik für Kinder- und Jugendpsychiatrie, Zentrum für Psychosoziale Medizin, Universitätsklinikum Heidelberg, Germany), Haffner J (Klinik für Kinder- und Jugendpsychiatrie, Zentrum für Psychosoziale Medizin, Universitätsklinikum Heidelberg, Germany), Parzer P (Klinik für Kinder- und Jugendpsychiatrie, Zentrum für Psychosoziale Medizin, Universitätsklinikum Heidelberg, Germany), Brunner R (Klinik für Kinder- und Jugendpsychiatrie, Zentrum für Psychosoziale Medizin, Universitätsklinikum Heidelberg, Germany), Klaassen A (Scito, Paris, France), Klaassen I (Scito, Paris, France), Constant P (PERTIMM, Asnières-Sur-Seine, France), Mignon X (PERTIMM, Asnières-Sur-Seine, France), Thomsen T (NordicNeuroLabs, Bergen, Norway), Zysset S (NordicNeuroLabs, Bergen, Norway), Vestboe A (NordicNeuroLabs, Bergen, Norway), Ireland J (Delosis Ltd, London, UK), Rogers J (Delosis Ltd, London, UK).

The following authors are included under the Saguenay Youth Study (SYS) Group:

Tomas Paus (Rotman Research Institute, University of Toronto, Ontario, Canada), Zdenka Pausova (The Hospital for Sick Children, University of Toronto, Ontario, Canada), Manon Bernard (The Hospital for Sick Children, University of Toronto, Ontario, Canada), Mallar Chakravarty (Rotman Research Institute, University of Toronto, Ontario, Canada), G. Bruce Pike (Montreal Neurological Institute, McGill University, Montreal, Quebec, Canada).

The following authors are included under the CHARGE consortium:

Joshua C. Bis (Cardiovascular Health Research Unit, Department of Medicine, University of Washington, Seattle, WA, USA), Charles DeCarli (Department of Neurology and Center of Neuroscience, University of California at Davis, Sacramento, CA, USA.), Albert Vernon Smith (Icelandic Heart Association, Kopavogur, Iceland ; University of Iceland, Faculty of Medicine, Reykjavik, Iceland), Fedde van der Lijn (Department of Medical Informatics, Erasmus MC University Medical Center, Rotterdam, The Netherlands; Department of Radiology, Erasmus MC University Medical Center, Rotterdam, The Netherlands), Fabrice Crivello (Univ. Bordeaux, Neurofunctional Imaging Group, UMR 5296, F-33000 Bordeaux, France; Centre National de la Recherche Scientifique (CNRS), Neurofunctional Imaging Group, UMR 5296, F-33000 Bordeaux, France; Commissariat à l'Energie Atomique (CEA), Neurofunctional Imaging Group, UMR 5296, F-33000 Bordeaux, France), Myriam Fornage (Brown Foundation Institute of Molecular Medicine, The University of Texas Health

Sciences Center at Houston, Houston, TX, USA; Human Genetics Center School of Public Health, The University of Texas Health Sciences Center at Houston, Houston, TX, USA), Stephanie Debette (INSERM, U708, Neuroepidemiology, F-75013, Paris, France; UPMC Univ Paris 06, UMR_S708, Neuroepidemiology, F-75005, Paris, France; Department of Neurology, Boston University School of Medicine, Boston, MA, USA), Joshua M. Shulman (Program in Translational NeuroPsychiatric Genomics, Institute for the Neurosciences, Department of Neurology, Brigham and Women's Hospital, Boston, MA, USA; Program in Medical and Population Genetics, Broad Institute, Cambridge, MA, USA), Helena Schmidt (Institute of Molecular Biology and Biochemistry, Medical University Graz, Austria), Velandai Srikanth (Stroke and Ageing Research Centre, Southern Clinical School, Department of Medicine, Monash University, Melbourne, Australia; Menzies Research Institute Tasmania, University of Tasmania, Hobart, Australia.), Maaike Schuur (Genetic Epidemiology Unit, Department of Epidemiology, Erasmus MC University Medical Center, Rotterdam, The Netherlands; Department of Neurology, Erasmus MC University Medical Center, Rotterdam, The Netherlands.), Lei Yu (Rush Alzheimer's Disease Center, Rush University Medical Center, Chicago, IL, USA), Seung-Hoan Choi (Department of Biostatistics, Boston University School of Public Health, Boston, MA, USA), Sigurdur Sigurdsson (Icelandic Heart Association, Kopavogur, Iceland), Benjamin F.J. Verhaaren (Department of Radiology, Erasmus MC University Medical Center, Rotterdam, The Netherlands; Department of Epidemiology, Erasmus MC University Medical Center, Rotterdam, The Netherlands), Anita L. DeStefano (Department of Biostatistics, Boston University School of Public Health, Boston, MA, USA; Department of Neurology, Boston University School of Medicine, Boston, MA, USA; The National Heart, Lung and Blood Institute's Framingham Heart Study, Framingham, MA, USA), Jean-Charles Lambert (INSERM Unit 744, Lille, France; Institut Pasteur de Lille, Lille, France; Université Lille Nord de France, Lille, France), Clifford R. Jack Jr. (Department of Radiology, Mayo Clinic, Rochester, MN, USA), Maksim Struchalin (Genetic Epidemiology Unit, Department of Epidemiology, Erasmus MC University Medical Center, Rotterdam, The Netherlands), Jim Stankovich (Menzies Research Institute Tasmania, University of Tasmania, Hobart, Australia), Carla A. Ibrahim-Verbaas (Genetic Epidemiology Unit, Department of Epidemiology, Erasmus MC University Medical Center, Rotterdam, The Netherlands; Department of Neurology, Erasmus MC University Medical Center, Rotterdam, The Netherlands), Debra Fleischman (Rush Alzheimer's Disease Center, Rush University Medical Center, Chicago, IL, USA; Department of Neurological Sciences, Rush University Medical Center, Chicago, IL, USA; Department of Behavioral Sciences, Rush University Medical Center, Chicago, IL, USA), Alex Zijdenbos (Biospective Inc., Montreal, Canada), Tom den Heijer (Department of Neurology, Erasmus MC University Medical Center, Rotterdam, The Netherlands; Department of Epidemiology, Erasmus MC University Medical Center, Rotterdam, The Netherlands; Department of Neurology, Sint Franciscus Gasthuis, Rotterdam, the Netherlands), Bernard Mazoyer (Univ. Bordeaux, Neurofunctional Imaging Group, UMR 5296, F-33000 Bordeaux, France; Centre National de la Recherche Scientifique (CNRS), Neurofunctional Imaging Group, UMR 5296, F-33000 Bordeaux, France; Commissariat à l'Energie Atomique (CEA), Neurofunctional Imaging Group, UMR 5296, F-33000 Bordeaux, France), Laura H. Coker (Division of Public Health Sciences, Wake Forest School of Medicine, Winston-Salem, NC, USA), Christian Enzinger (Department of Neurology, Medical University Graz, Austria), Patrick Danoy (University of Queensland, Diamantina Institute, Princess Alexandra Hospital, Brisbane, Australia), Najaf Amin (Genetic Epidemiology Unit, Department of Epidemiology, Erasmus MC University Medical Center, Rotterdam, The Netherlands), Konstantinos Arfanakis (Rush Alzheimer's Disease Center, Rush University Medical Center, Chicago, IL, USA; Department of Biomedical Engineering, Illinois Institute of Technology, Chicago, IL, USA), Mark A. van Buchem (Department of Radiology, Leiden University Medical Center, Leiden, the Netherlands), Renée F.A.G. de Brujin (Department of Neurology, Erasmus MC University Medical Center, Rotterdam, The Netherlands; Department of Epidemiology, Erasmus MC University Medical Center, Rotterdam, The Netherlands), Alexa Beiser (Department of Biostatistics, Boston University School of Public Health, Boston, MA, USA; Department of Neurology, Boston University School of Medicine, Boston, MA, USA; The National Heart, Lung and Blood Institute's Framingham Heart Study, Framingham, MA, USA), Carole Dufouil (INSERM, U708, Neuroepidemiology, F-75013, Paris, France.), Juebin Huang (Department of Neurology, University of Mississippi Medical Center, Jackson, MS, USA), Margherita Cavalieri (Department of Neurology, Medical University Graz, Austria), Russell Thomson (Menzies Research Institute Tasmania, University of Tasmania, Hobart, Australia), Wiro J. Niessen (Department of Medical Informatics, Erasmus MC University Medical Center, Rotterdam, The Netherlands; Department of Radiology, Erasmus MC University Medical Center, Rotterdam, The Netherlands; Faculty of Applied Sciences, Delft University of Technology, Delft, the Netherlands), Lori B. Chibnik, (Program in Translational NeuroPsychiatric Genomics, Institute for the Neurosciences, Department of Neurology, Brigham and Women's Hospital, Boston, MA, USA; Program in Medical and Population Genetics, Broad Institute, Cambridge, MA, USA) , Gauti K. Gislason (Icelandic Heart Association, Kopavogur, Iceland), Albert Hofman (Department of Epidemiology, Erasmus MC University Medical Center, Rotterdam, The Netherlands), Aleksandra Pikula (Department of Neurology, Boston University School of Medicine, Boston, MA, USA), Philippe Amouyel (INSERM Unit 744, Lille, France; Institut Pasteur de Lille, Lille, France; Université Lille Nord de France, Lille, France; Centre Hospitalier Régional Universitaire de Lille, Lille, France), Kevin B. Freeman (Department of Psychiatry and Human Behavior, University of Mississippi Medical Center, Jackson, MS, USA.), Thanh G.

Phan (Stroke and Ageing Research Centre, Southern Clinical School, Department of Medicine, Monash University, Melbourne, Australia), Ben A. Oostra (Genetic Epidemiology Unit, Department of Epidemiology, Erasmus MC University Medical Center, Rotterdam, The Netherlands; Department of Clinical Genetics, Erasmus MC University Medical Center, Rotterdam, The Netherlands), Michael A. Nalls (Laboratory of Neurogenetics, Intramural Research Program, National Institute of Aging, NIH, Bethesda, MD, USA), Andre G. Uitterlinden (Department of Internal Medicine, Erasmus MC University Medical Center, Rotterdam, the Netherlands), Rhoda Au, (Department of Neurology, Boston University School of Medicine, Boston, MA, USA; The National, Heart, Lung and Blood Institute's Framingham Heart Study, Framingham, MA, USA), Alexis Elbaz (INSERM, U708, Neuroepidemiology, F-75013, Paris, France; UPMC Univ Paris 06, UMR_S708, Neuroepidemiology, F-75005, Paris, France), Richard J. Beare (Stroke and Ageing Research Centre, Southern Clinical School, Department of Medicine, Monash University, Melbourne, Australia; Developmental Imaging Group, Murdoch Children's Research Institute, The Royal Children's Hospital, Flemington Rd, Parkville, Victoria, Australia), John C. van Swieten (Department of Neurology, Erasmus MC University Medical Center, Rotterdam, The Netherlands), Oscar Lopez (Department of Neurology, University of Pittsburgh School of Medicine, Pittsburgh, PA, USA; Department of Psychiatry, University of Pittsburgh School of Medicine, Pittsburgh, PA, USA; Department of Psychology, University of Pittsburgh School of Medicine, Pittsburgh, PA, USA), Tamara B. Harris (Laboratory of Epidemiology, Demography, and Biometry, National Institute of Health, Bethesda, MD, USA), Vincent Chouraki (INSERM Unit 744, Lille, France; Institut Pasteur de Lille, Lille, France; Université Lille Nord de France, Lille, France), Monique M.B. Breteler (Population Health Sciences, German Center for Neurodegenerative Diseases (DZNE), Bonn, Germany; Population Health Sciences, University of Bonn, Bonn, Germany; Department of Epidemiology, Harvard School of Public Health, Harvard University, Boston, MA, USA), Philip L. De Jager (Program in Translational NeuroPsychiatric Genomics, Institute for the Neurosciences, Department of Neurology, Brigham and Women's Hospital, Boston, MA, USA; Program in Medical and Population Genetics, Broad Institute, Cambridge, MA, USA; Harvard Medical School, Boston, MA, USA), James T. Becker (Department of Epidemiology, Harvard School of Public Health, Harvard University, Boston, MA, USA; Harvard Medical School, Boston, MA, USA; Department of Neurology, Mayo Clinic, Rochester, MN, USA), Meike W. Vernooij (Department of Radiology, Erasmus MC University Medical Center, Rotterdam, The Netherlands; Department of Epidemiology, Erasmus MC University Medical Center, Rotterdam, The Netherlands), David Knopman (Department of Neurology, Mayo Clinic, Rochester, MN, USA), Franz Fazekas (Department of Neurology, Medical University Graz, Austria), Philip A. Wolf (Department of Neurology, Boston University School of Medicine, Boston, MA, USA; The National, Heart, Lung and Blood Institute's Framingham Heart Study, Framingham, MA, USA), Aad van der Lugt (Department of Radiology, Erasmus MC University Medical Center, Rotterdam, The Netherlands), Vilmundur Gudnason (Icelandic Heart Association, Kopavogur, Iceland; University of Iceland, Faculty of Medicine, Reykjavik, Iceland), W.T. Longstreth Jr. (Department of Neurology, University of Washington, Seattle, WA, USA; Department of Epidemiology, University of Washington, Seattle, WA, USA), Mathew A. Brown (Diamantina Institute, University of Queensland, Queensland, Australia), David A. Bennett (Rush Alzheimer's Disease Center, Rush University Medical Center, Chicago, IL, USA), Cornelia M. van Duijn (Genetic Epidemiology Unit, Department of Epidemiology, Erasmus MC University Medical Center, Rotterdam, The Netherlands), Thomas H. Mosley (Department of Neurology, University of Mississippi Medical Center, Jackson, MS, USA; Department of Medicine (Geriatrics), University of Mississippi Medical Center, Jackson, MS, USA), Reinhold Schmidt (Department of Neurology, Medical University Graz, Austria), Christophe Tzourio (Univ. Bordeaux, U708, F-33000 Bordeaux, France; INSERM, Neuroepidemiology U708, F-33000, Bordeaux, France), Lenore J. Launer (Laboratory of Epidemiology, Demography, and Biometry, National Institute of Health, Bethesda, MD, USA), M. Arfan Ikram (Department of Radiology, Erasmus MC University Medical Center, Rotterdam, The Netherlands; Netherlands Consortium of Healthy Aging, Leiden, The Netherlands), Sudha Seshadri (Department of Neurology, Boston University School of Medicine, Boston, MA, USA; The National, Heart, Lung and Blood Institute's Framingham Heart Study, Framingham, MA, USA).

The ENIGMA Consortium:

The ENIGMA consortium is a network of research groups whose goal is to facilitate the meta-analysis of neuroimaging data. Consortium members contributing to this paper are listed in the main author list.

Supplementary Figures

Identification of common variants associated with human hippocampal and intracranial volumes

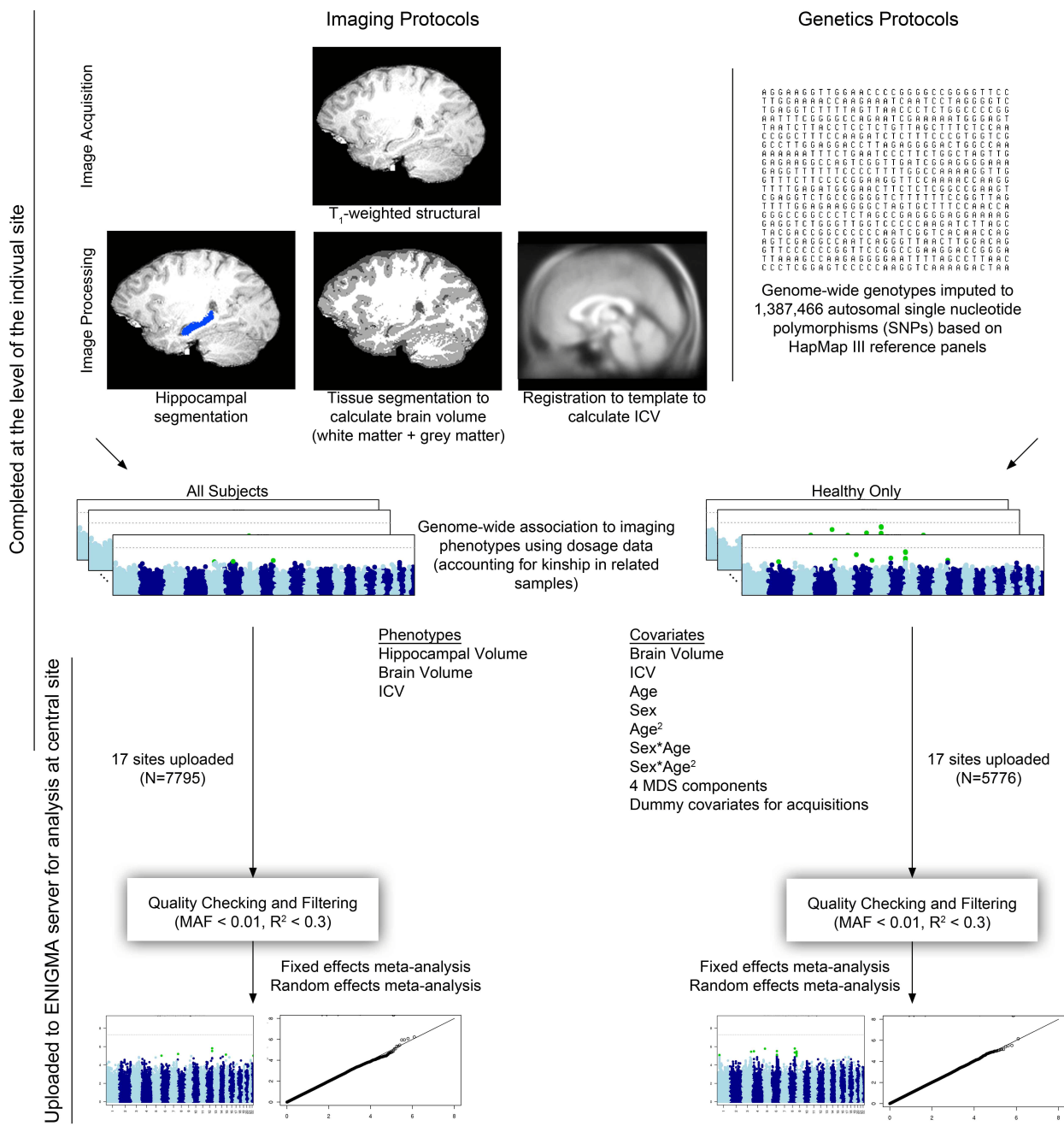
CONTENTS

Supplementary Figure 1: Outline of project methods.	13
Supplementary Figure 2: Distribution of left hippocampal volume in 22 cohorts contributing to the meta-analysis.	14
Supplementary Figure 3: Distribution of right hippocampal volume in 22 cohorts contributing to the meta-analysis.	15
Supplementary Figure 4: The distribution of the ratio of left hippocampal volume to right hippocampal volume for the 22 cohorts contributing to the meta-analysis.	16
Supplementary Figure 5: Distribution of total brain volume in 20 cohorts contributing to the meta-analysis.	17
Supplementary Figure 6: Distribution of estimated total intracranial volume (ICV) in 22 cohorts contributing to the meta-analysis.	18
Supplementary Figure 7: Multi-dimensional scaling plots comparing each population in the discovery sample to HapMap III reference panels of known ancestry.	19
Supplementary Figure 8: Histogram of allele frequency differences between each SNP in the individual cohort and the CEU HapMap III reference.	20
Supplementary Figure 9: Manhattan plots show genome-wide association results from each cohort, using average bilateral hippocampal volume as the phenotype in healthy subjects only, controlling for ICV.	21
Supplementary Figure 10: QQ plots show genome-wide association results from each cohort using average bilateral hippocampal volume as the phenotype, in healthy subjects only, controlling for ICV.	22
Supplementary Figure 11: Manhattan plots show genome-wide association results from each cohort using average bilateral hippocampal volume as a phenotype in all subjects (regardless of diagnosis), controlling for ICV.	23
Supplementary Figure 12: QQ plots show genome-wide association results from each cohort using average bilateral hippocampal volume as the phenotype in all subjects (regardless of diagnosis), controlling for ICV.	24
Supplementary Figure 13: Manhattan plots show genome-wide association results from each cohort using average bilateral hippocampal volume as a phenotype in healthy subjects only, controlling for brain volume.	25

Supplementary Figure 14: QQ plots show genome-wide association results from each cohort using average bilateral hippocampal volume as the phenotype in healthy subjects only, controlling for brain volume.	26
Supplementary Figure 15: Manhattan plots show genome-wide association results from each cohort using average bilateral hippocampal volume as a phenotype in all subjects (regardless of diagnosis), controlling for brain volume.	27
Supplementary Figure 16: QQ plots show genome-wide association results from each cohort using average bilateral hippocampal volume as the phenotype in all subjects (regardless of diagnosis), controlling for brain volume.	28
Supplementary Figure 17: Manhattan plots show genome-wide association results from each cohort using average bilateral hippocampal volume as a phenotype in healthy subjects only, without controlling for ICV or brain volume.	29
Supplementary Figure 18: QQ plots show genome-wide association results from each cohort using average bilateral hippocampal volume as a phenotype in healthy subjects only, without controlling for ICV or brain volume.	30
Supplementary Figure 19: Manhattan plots show genome-wide association results from each cohort using average bilateral hippocampal volume as a phenotype in all subjects (regardless of diagnosis), without controlling for ICV or brain volume.	31
Supplementary Figure 20: QQ plots show genome-wide association results from each cohort using average bilateral hippocampal volume as a phenotype in all subjects (regardless of diagnosis), without controlling for ICV or brain volume.	32
Supplementary Figure 21: Manhattan plots show genome-wide association results from each cohort for total brain volume as a phenotype in healthy subjects only.	33
Supplementary Figure 22: QQ plots showing genome-wide association results from each cohort for total brain volume as a phenotype in healthy subjects only.	34
Supplementary Figure 23: Manhattan plots show genome-wide association results from each cohort using estimated total intracranial volume (ICV) as a phenotype in healthy subjects only.	35
Supplementary Figure 24: QQ plots show genome-wide association results from each cohort using estimated total intracranial volume (ICV) as a phenotype in healthy subjects only.	36
Supplementary Figure 25: Fixed effects meta-analysis of hippocampal volume controlling for estimated intracranial volume and other covariates in healthy subjects only (N=5,776) and in all subjects (N=7,795).	37
Supplementary Figure 26: QQ plots of fixed effects meta-analysis of average bilateral hippocampal volume controlling for ICV and other covariates in healthy subjects only (N=5,776) and all subjects (N=7,795).	37

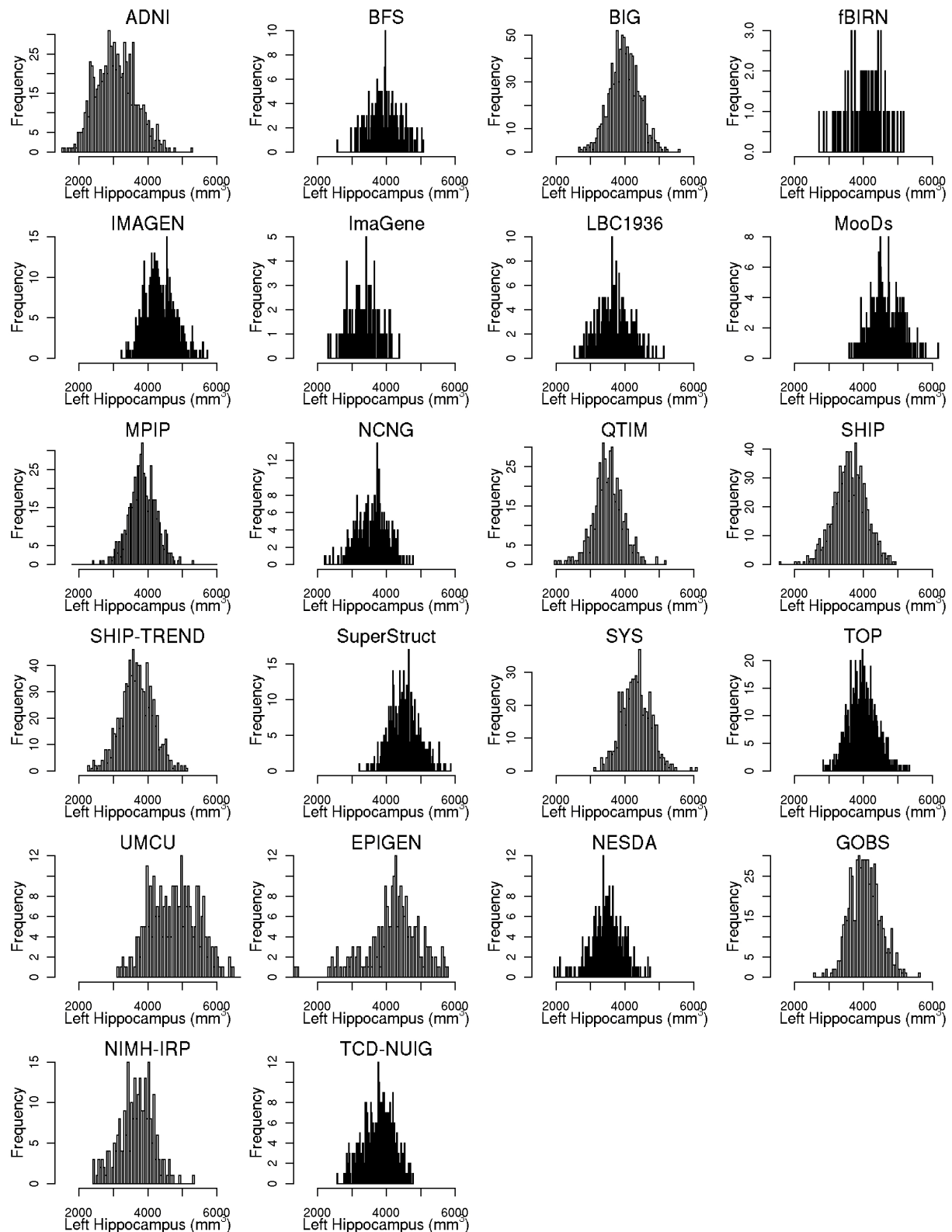
Supplementary Figure 27: Fixed effects meta-analysis of hippocampal volume controlling for brain volume and other covariates in healthy subjects only (N=5,776) and in all subjects (N=7,795).	38
Supplementary Figure 28: QQ plots of the fixed effects meta-analysis of average bilateral hippocampal volume controlling for brain volume and other covariates in healthy subjects only (N=5,776) and in all subjects (N=7,795).	38
Supplementary Figure 29: Fixed effects meta-analysis of hippocampal volume controlling for other covariates in healthy subjects only (N=5,775) and in all subjects (N=7,794).	39
Supplementary Figure 30: QQ plots of fixed effects meta-analysis of average bilateral hippocampal volume controlling for other covariates in healthy subjects only (N=5,775) and in all subjects (N=7,794).	39
Supplementary Figure 31: Fixed effects meta-analysis of estimated intracranial volume and total brain size measures including other covariates in healthy subjects only (N=5,778).	40
Supplementary Figure 32: QQ plots of fixed effects meta-analysis using total brain size measures as phenotypes including other covariates in healthy subjects only (N=5,778).	40
Supplementary Figure 33: Random effects meta-analysis of hippocampal volume controlling for estimated intracranial volume and other covariates in healthy subjects only (N=5,776) and in all subjects (N=7,795).	41
Supplementary Figure 34: QQ plots of random effects meta-analysis of hippocampal volume controlling for estimated intracranial volume and other covariates in healthy subjects only (N=5,776) and in all subjects (N=7,795).	41
Supplementary Figure 35: Random effects meta-analysis of hippocampal volume controlling for brain volume and other covariates in healthy subjects only (N=5,776) and in all subjects (N=7,795).	42
Supplementary Figure 36: QQ plots of random effects meta-analysis of hippocampal volume controlling for brain volume and other covariates in healthy subjects only (N=5,776) and in all subjects (N=7,795).	42
Supplementary Figure 37: Random effects meta-analysis of hippocampal volume controlling for other covariates in healthy subjects only (N=5,775) and in all subjects (N=7,794).	43
Supplementary Figure 38: QQ plots of random effects meta-analysis of hippocampal volume controlling for other covariates in healthy subjects only (N=5,775) and in all subjects (N=7,794).	43
Supplementary Figure 39: Random effects meta-analysis of estimated intracranial volume and total brain size measures including other covariates in healthy subjects only (N=5,778).	44

Supplementary Figure 40: QQ plots of random effects meta-analysis of total brain size measures including other covariates in healthy subjects only (N=5,778).	44
Supplementary Figure 41: QQ plot of ICV associations for 175 SNPs previously identified as strongly associated with height.	45
Supplementary Figure 42: QQ plot of hippocampal volume associations controlling for intracranial volume and other covariates in all subjects for 175 SNPs previously identified as strongly associated with height.	46
Supplementary Figure 43: QQ plot of hippocampal volume associations controlling for other covariates without a measure of head size in all subjects for SNPs previously identified as strongly associated with height.	47
Supplementary Figure 44: Structural equation models of the association among rs10784502, height, and ICV.	48



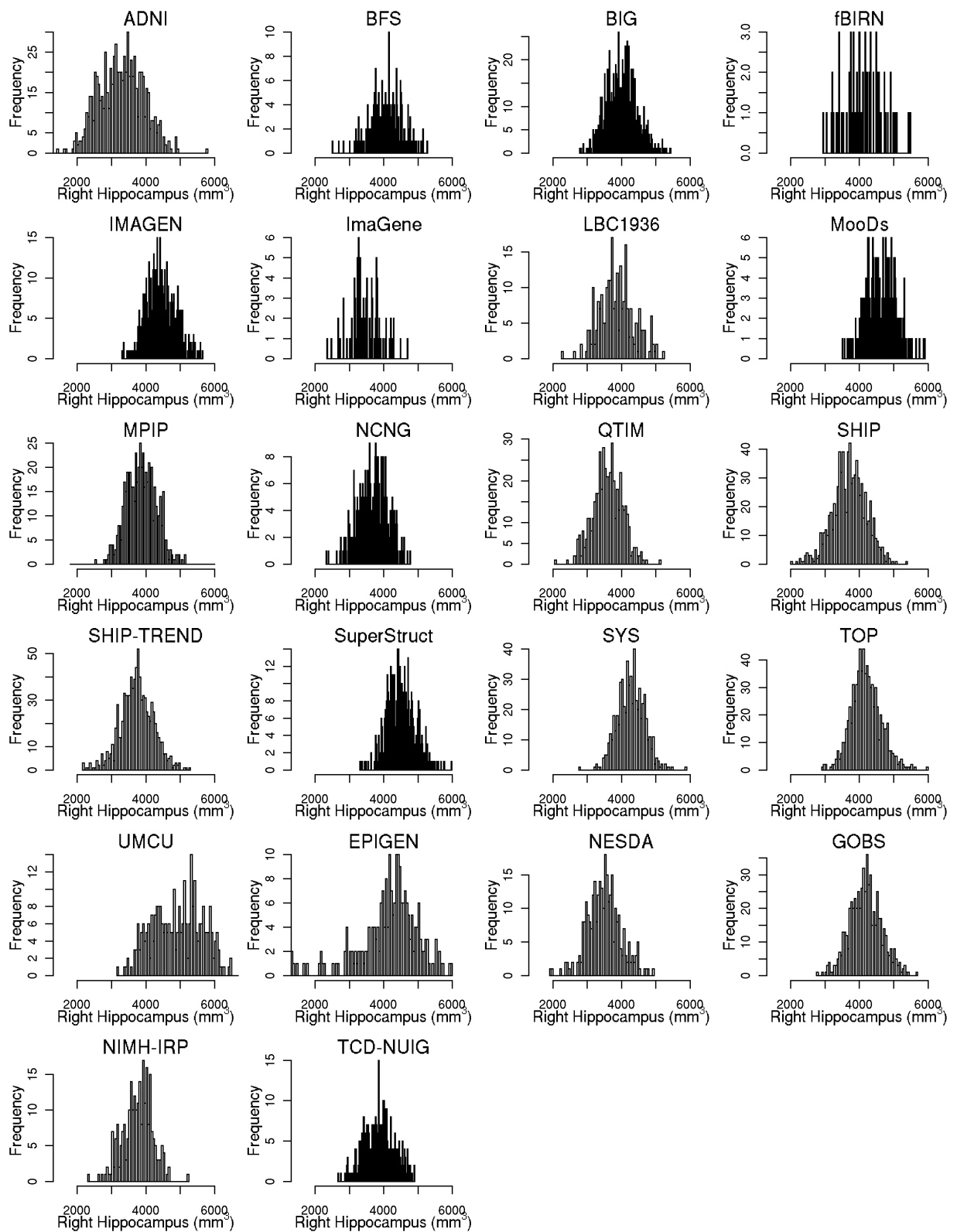
Supplementary Figure 1: Outline of project methods.

Imaging protocols detailing methods for segmenting the hippocampus and brain volume were provided; estimated total Intracranial Volume (ICV) was calculated through registration to a template. Protocols were provided for genome-wide imputation to the HapMap III reference panels. Genome-wide association was conducted using all subjects, and separately using only healthy subjects. GWAS analyses examined bilateral average hippocampal volume, brain volume, and ICV. Segmentation, imputation, and association were conducted at the level of the individual site. GWAS summary statistics were uploaded to a central server for additional quality checking and meta-analysis. Seventeen sites participated in the discovery stage including N=7,795 subjects regardless of diagnosis (all subjects) and N=5,776 subjects when restricting analyses to healthy subjects only. Both fixed effects and random effects meta-analyses were conducted across all contributing samples. Replication was attempted on SNPs of interest found in this analysis.



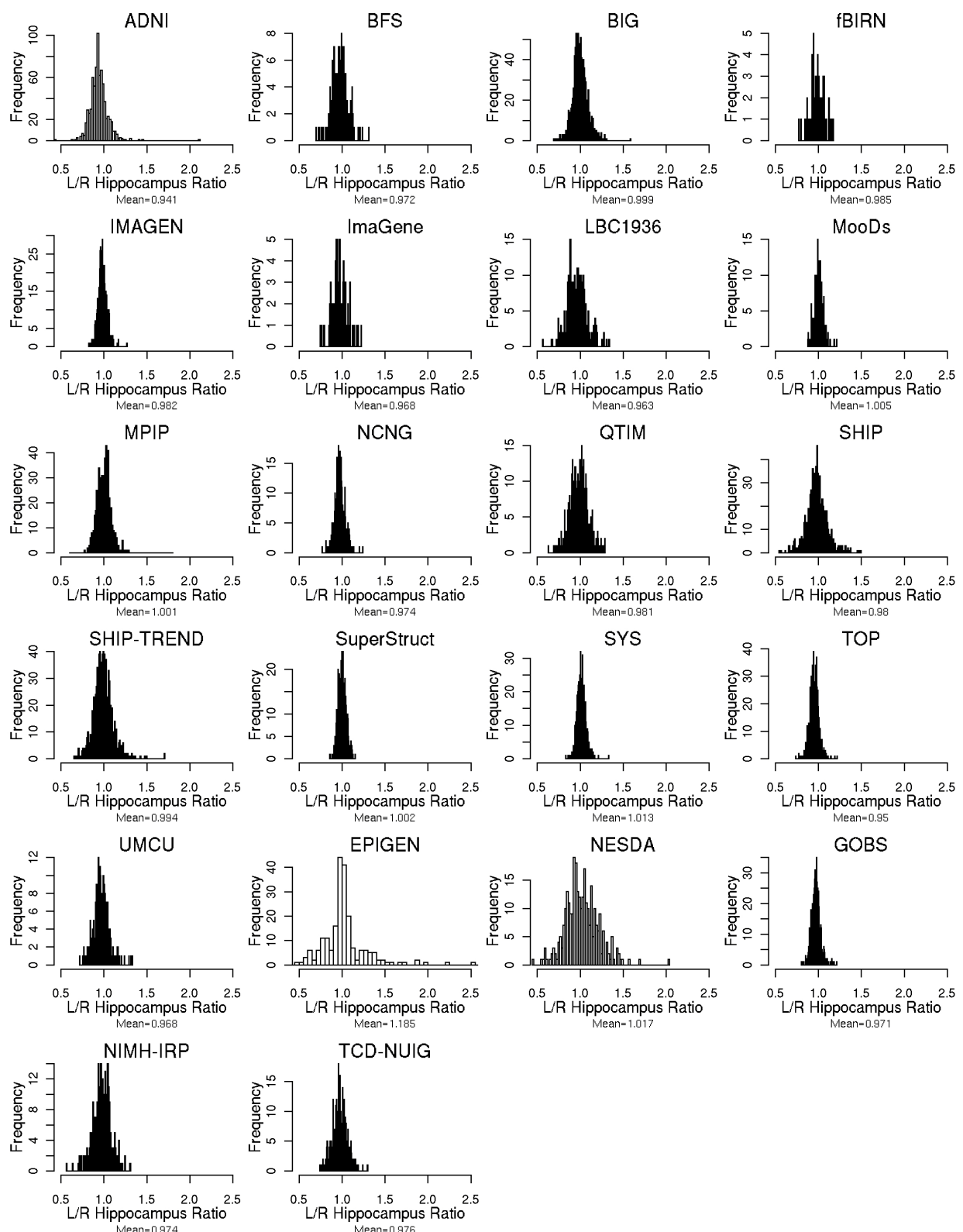
Supplementary Figure 2: Distribution of left hippocampal volume in 22 cohorts contributing to the meta-analysis.

To standardize the histograms, the distribution in each sample is presented using 100 bins. Outliers in these distributions were manually quality checked and removed from further analyses if poorly segmented. Histograms show all subjects used in the analysis (poorly segmented phenotypic values are not included).



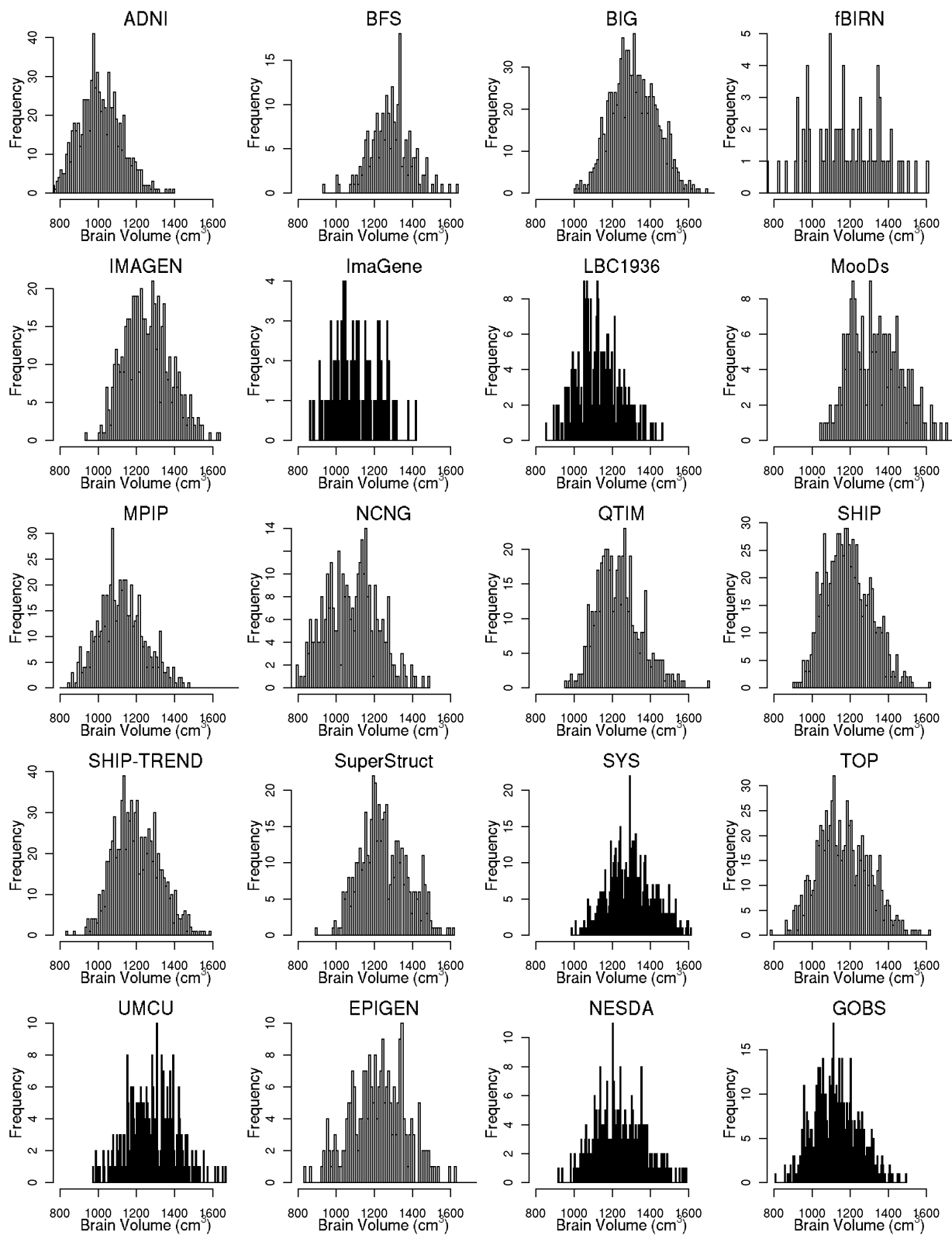
Supplementary Figure 3: Distribution of right hippocampal volume in 22 cohorts contributing to the meta-analysis.

Methods are as described in **Supplementary Figure 2**.



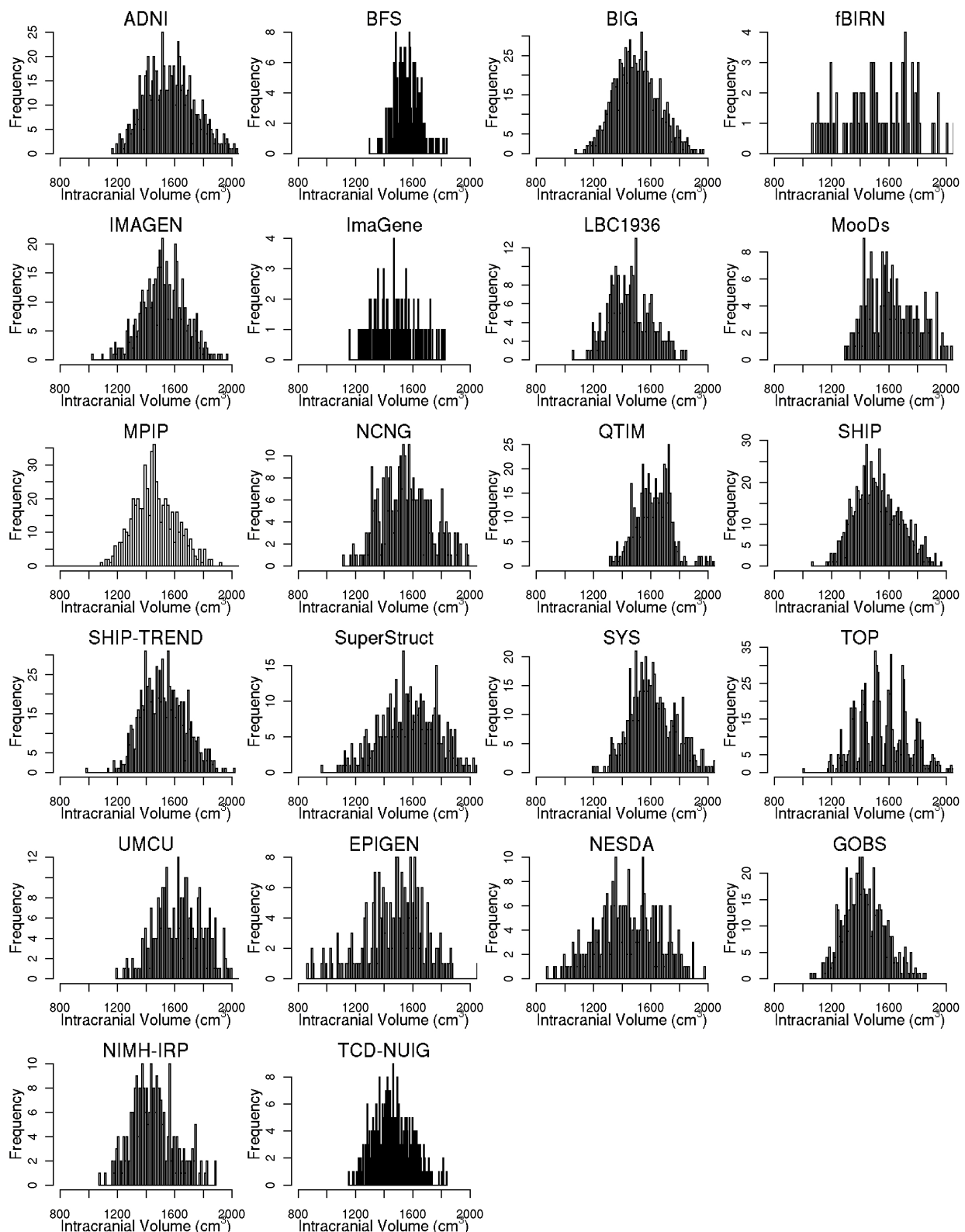
Supplementary Figure 4: The distribution of the ratio of left hippocampal volume to right hippocampal volume for the 22 cohorts contributing to the meta-analysis.

Means are approximations derived from the midpoints of the bins. As neurologically normal adults¹⁻³ and children⁴⁻⁶ have significantly larger right than left hippocampi, on average, the mean L/R ratio is usually < 1. Outliers in these histograms proved to be useful for identifying segmentation errors. Histograms presented here show all subjects used in the analysis (poorly segmented phenotypic values are not included). EPIGEN includes patients with epilepsy who have a higher ratio than the boundaries of the x-axis used here, which gives a larger histogram bin width.



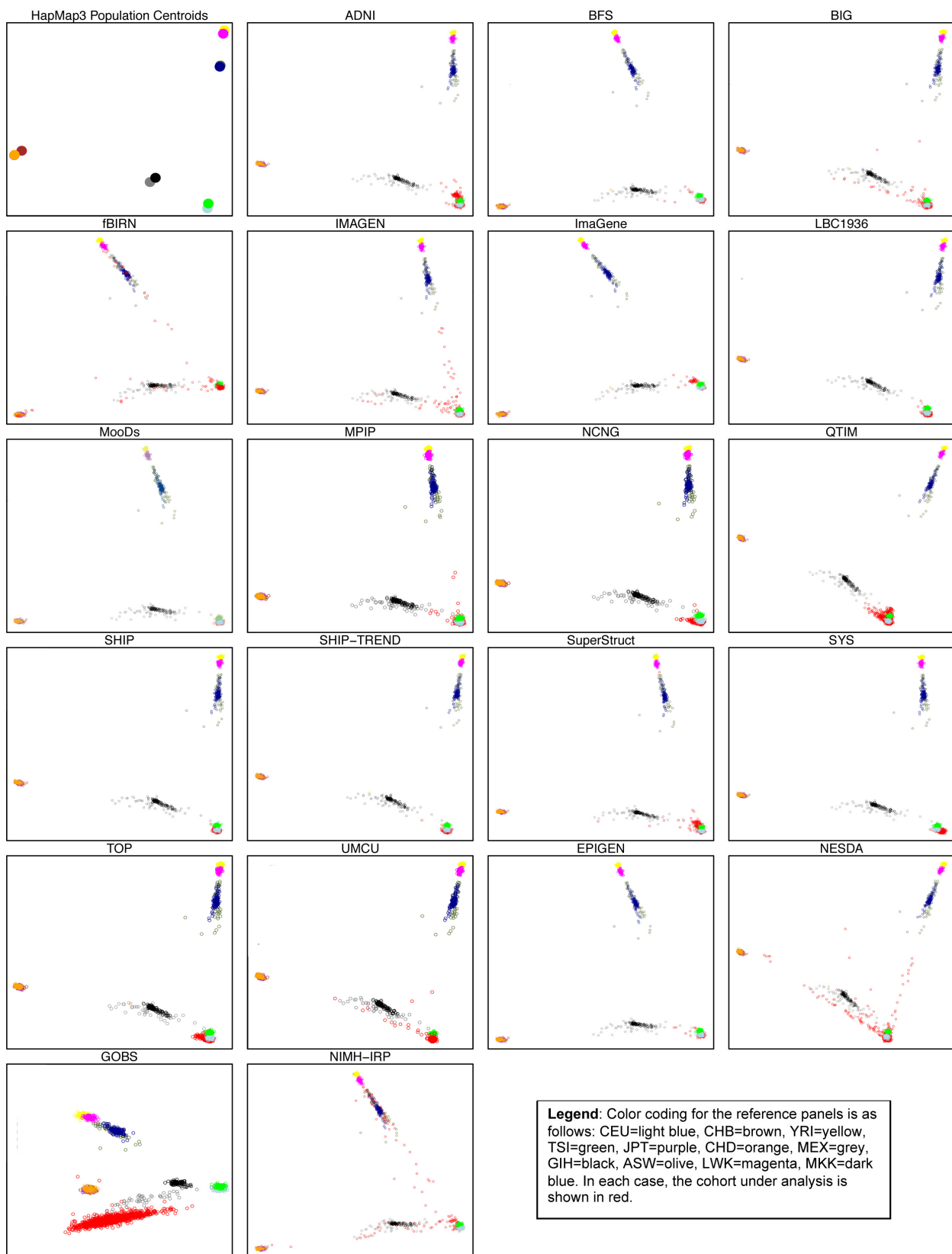
Supplementary Figure 5: Distribution of total brain volume in 20 cohorts contributing to the meta-analysis.

Brain volumes were calculated by segmenting gray and white matter excluding cerebrospinal fluid. Outliers in these distributions were manually quality checked and removed from further analyses if poorly segmented. Histograms show all subjects used in the analysis (poorly segmented phenotypic values are not included). The NIMH-IRP and TCD-NUIG replication samples did not have segmented brain volumes.



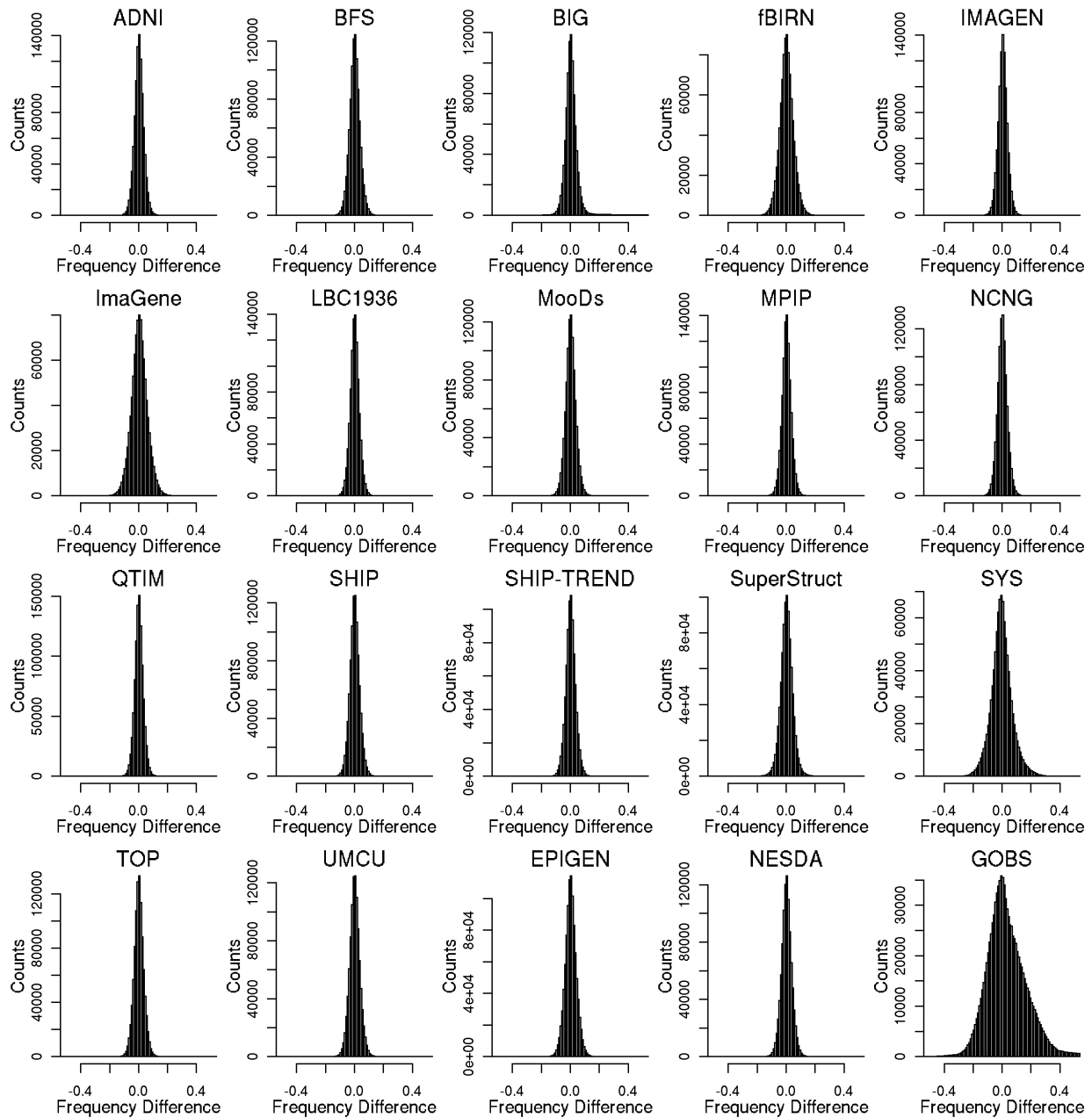
Supplementary Figure 6: Distribution of estimated total Intracranial Volume (ICV) in 22 cohorts contributing to the meta-analysis.

ICV was calculated by warping each brain to a standard template via linear registration. The degree of warping may be used to estimate percent change relative to that template and subsequently estimated volume when the template volume is known. Outliers in these distributions were manually quality checked and removed from further analyses if poorly registered (and are not included in these figures).



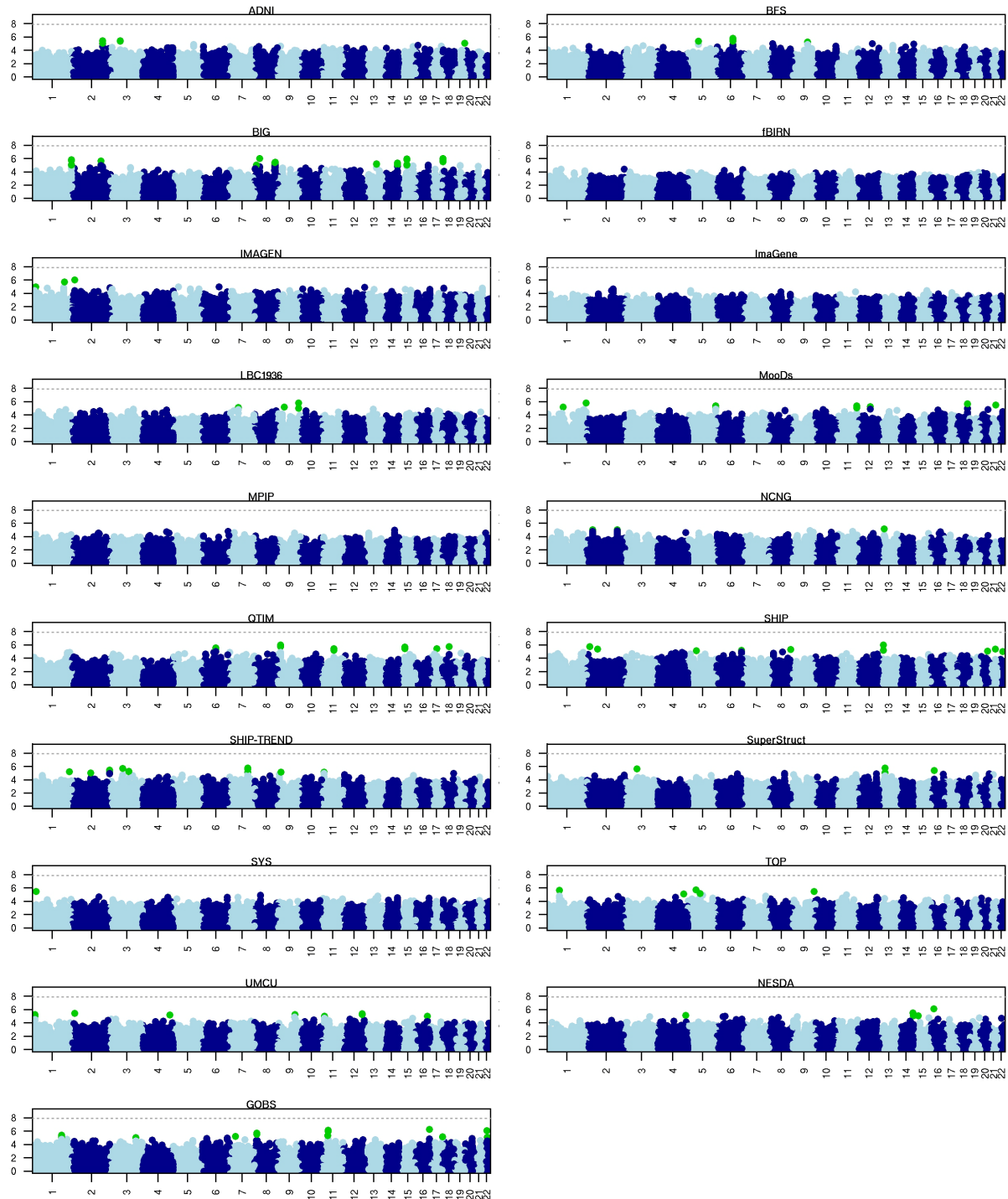
Supplementary Figure 7: Multi-dimensional scaling plots comparing each population in the discovery sample to HapMap III reference panels of known ancestry.

The centroid of each HapMap III reference panel is shown in the first panel for clarity and is plotted against the axis of the BIG sample.



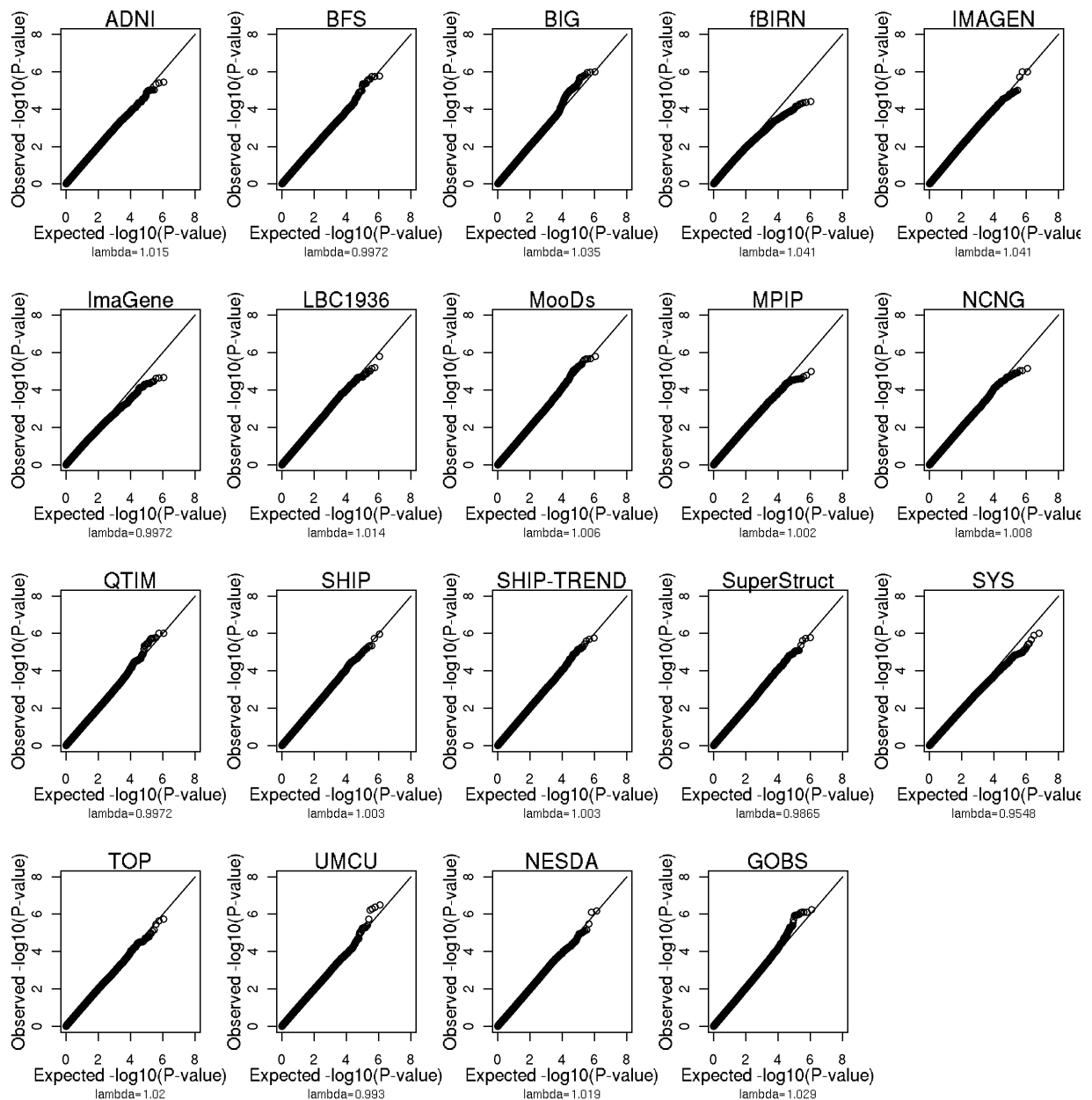
Supplementary Figure 8: Histogram of allele frequency differences between each SNP in the individual cohort and the CEU HapMap III reference.

Histograms centered on zero with little variance imply that the CEU population was an appropriate reference panel for imputation. The GOBS sample is composed of Mexican-Americans: the MEX HapMap III reference panel was used for imputation in this sample, but the difference from the CEU reference is shown here for comparison.



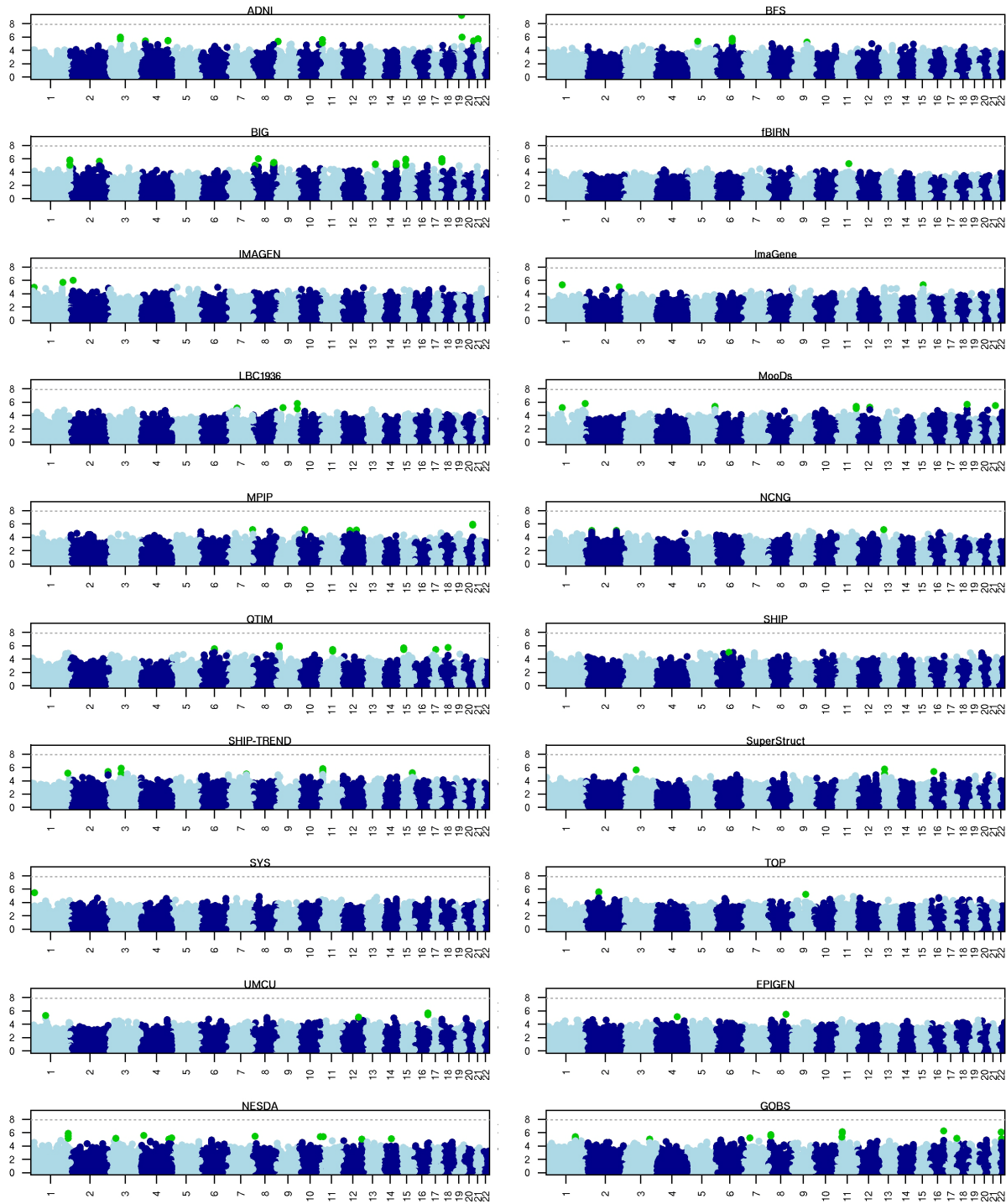
Supplementary Figure 9: Manhattan plots show genome-wide association results from each cohort, using average bilateral hippocampal volume as the phenotype in healthy subjects only.

Association models statistically controlled for the effects of ICV, age, sex, age², age×sex interaction, age²×sex interaction, 4 MDS components, and dummy variables for different scanner or acquisition sequences (when needed). The dotted line representing genome-wide significance is set at $P=1.25\times10^{-8}$.



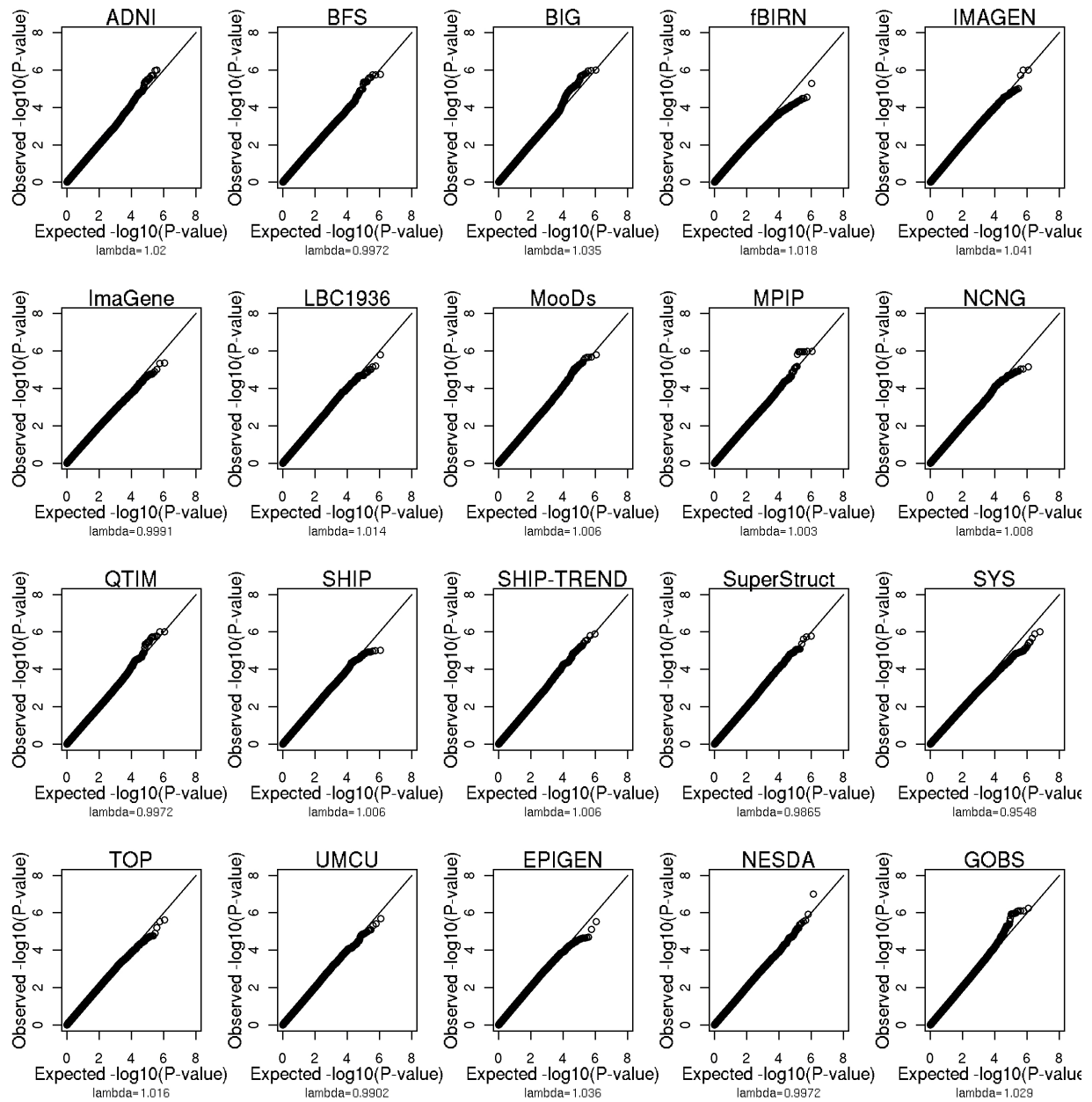
Supplementary Figure 10: QQ plots show genome-wide association results from each cohort using average bilateral hippocampal volume as the phenotype, in healthy subjects only.

Association models statistically controlled for the effects of ICV, age, sex, age^2 , age \times sex interaction, $age^2\times$ sex interaction, 4 MDS components, and dummy variables for different scanner or acquisition sequences (when needed). Lambda values in each sample are all near 1, indicating no inflation of test-statistics.



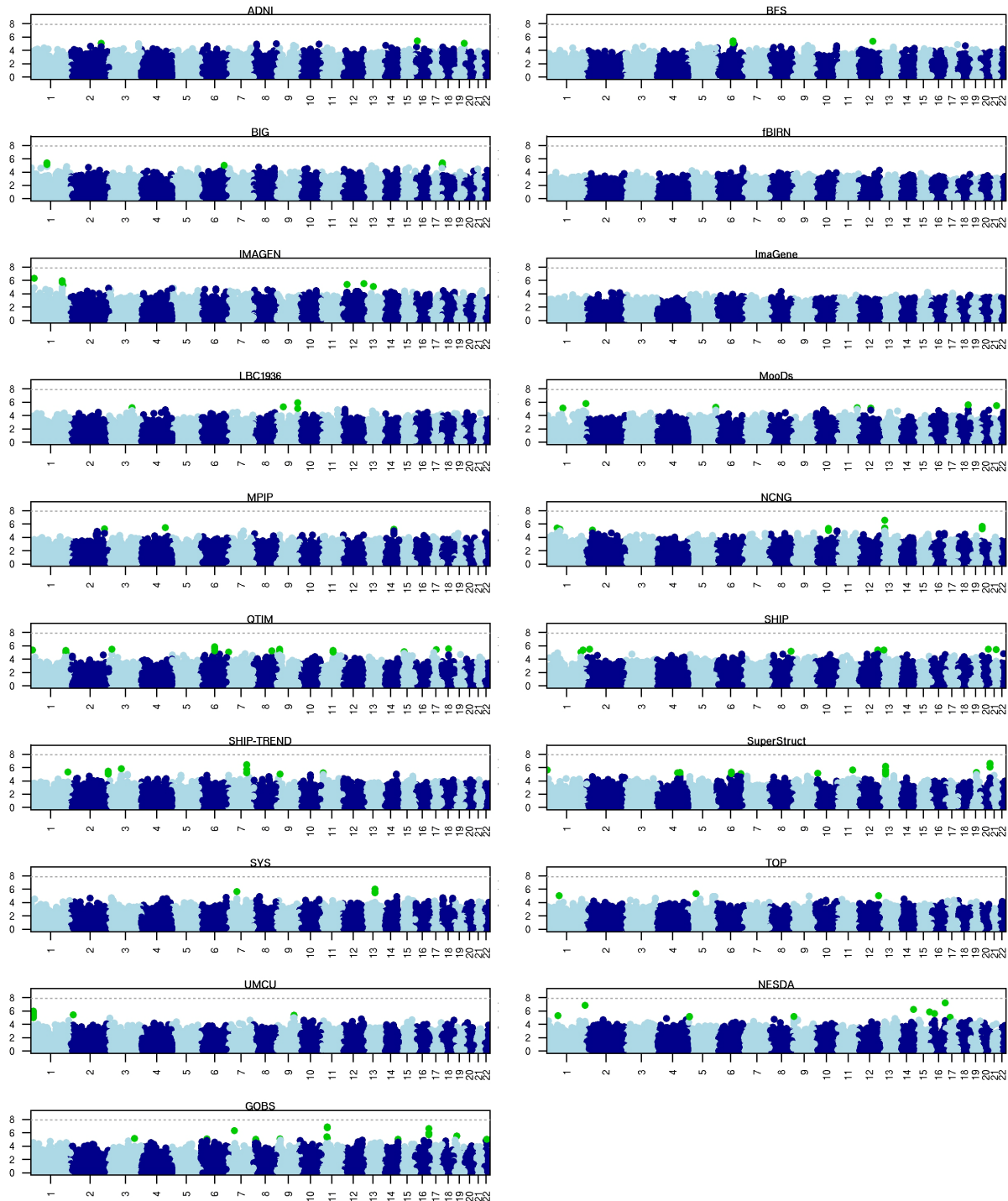
Supplementary Figure 11: Manhattan plots show genome-wide association results from each cohort using average bilateral hippocampal volume as a phenotype in all subjects (regardless of diagnosis).

Association models controlled for the effects of ICV, age, sex, age^2 , $age \times sex$ interaction, $age^2 \times sex$ interaction, 4 MDS components, and dummy variables for different scanner or acquisition sequence (when needed). The genome-wide significant locus (rs2075650; $P = 5.482 \times 10^{-10}$) in the ADNI sample on chromosome 19 represents a locus in LD with the *APOE* ε4 allele known to be associated with late-onset Alzheimer's disease.



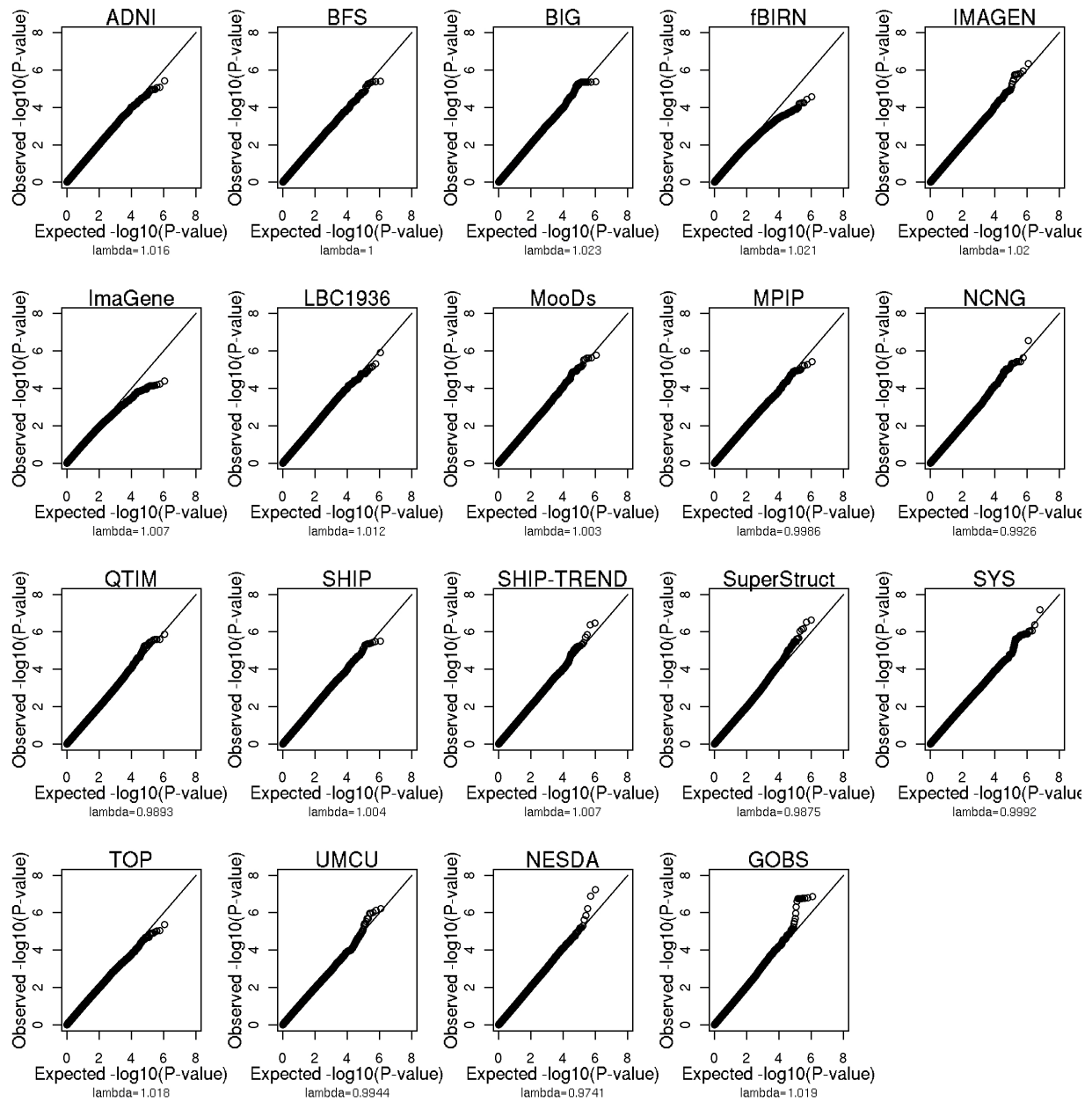
Supplementary Figure 12: QQ plots show genome-wide association results from each cohort using average bilateral hippocampal volume as the phenotype in all subjects (regardless of diagnosis).

Association models statistically controlled for the effects of ICV, age, sex, age², age×sex interaction, age²×sex interaction, 4 MDS components, and dummy variables for different scanner or acquisition sequences (when needed). Lambda values in each sample are all near 1 indicating no inflation of test-statistics.



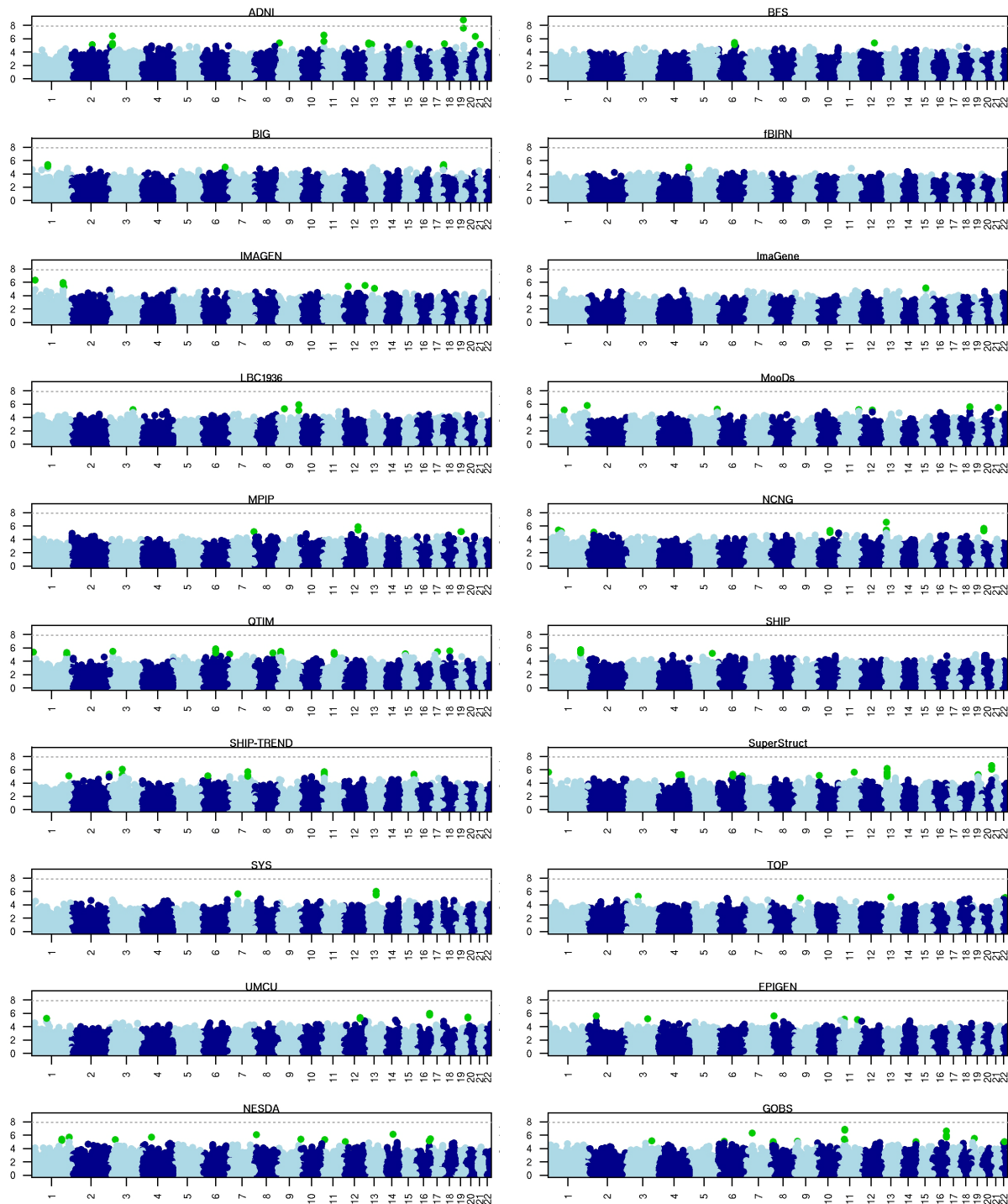
Supplementary Figure 13: Manhattan plots show genome-wide association results from each cohort using average bilateral hippocampal volume as a phenotype in healthy subjects only.

Association models statistically controlled for the effects of **brain volume**, age, sex, age^2 , age \times sex interaction, $age^2\times$ sex interaction, 4 MDS components, and dummy variables for different scanner or acquisition sequences (when needed).



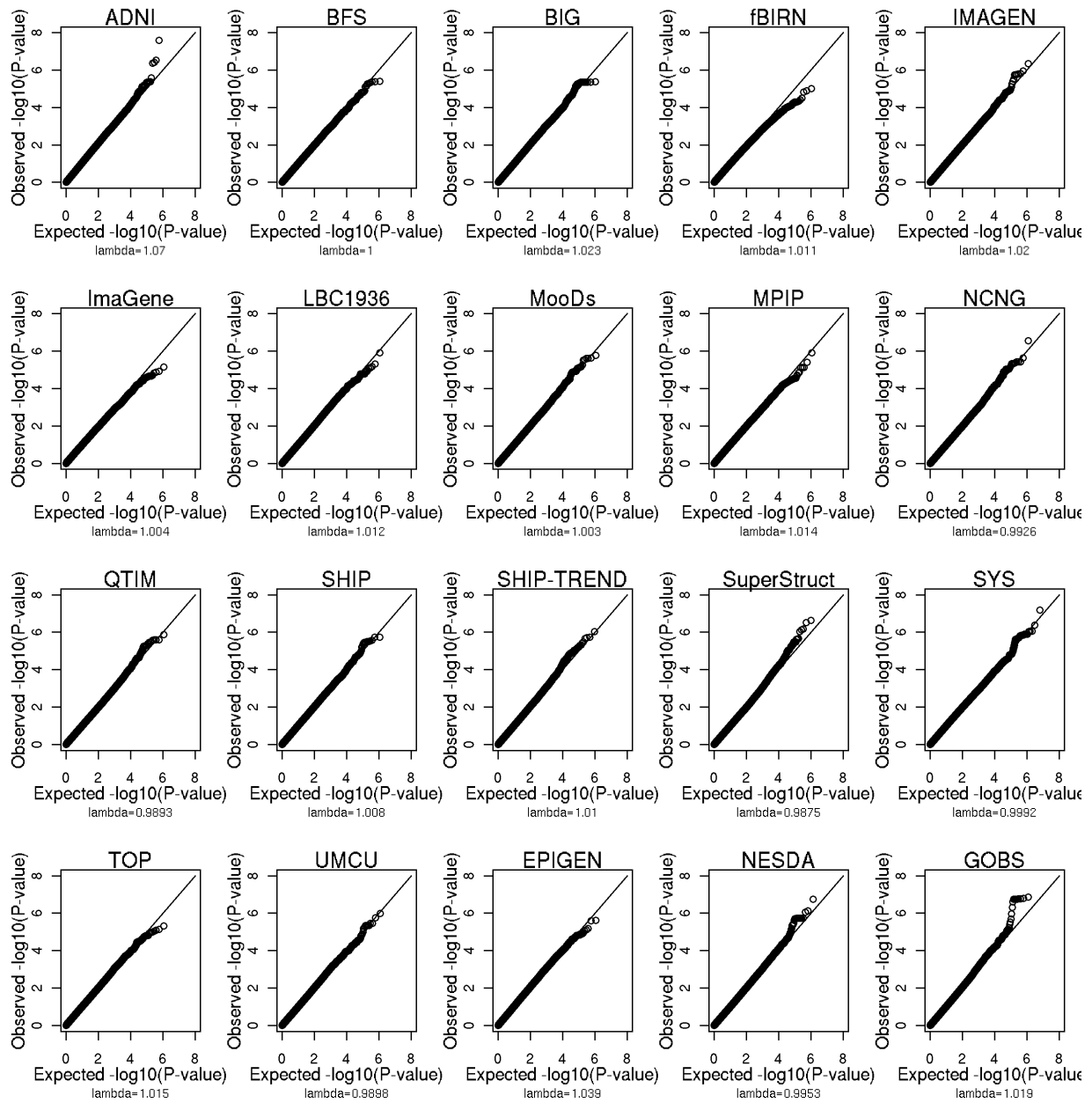
Supplementary Figure 14: QQ plots show genome-wide association results from each cohort using average bilateral hippocampal volume as the phenotype in healthy subjects only.

Association models statistically controlled for the effects of **brain volume**, age, sex, age^2 , $age \times sex$ interaction, $age^2 \times sex$ interaction, 4 MDS components, and dummy variables for different scanner or acquisition sequences (when needed). Lambda values in each sample are all near 1 indicating no inflation of test-statistics.



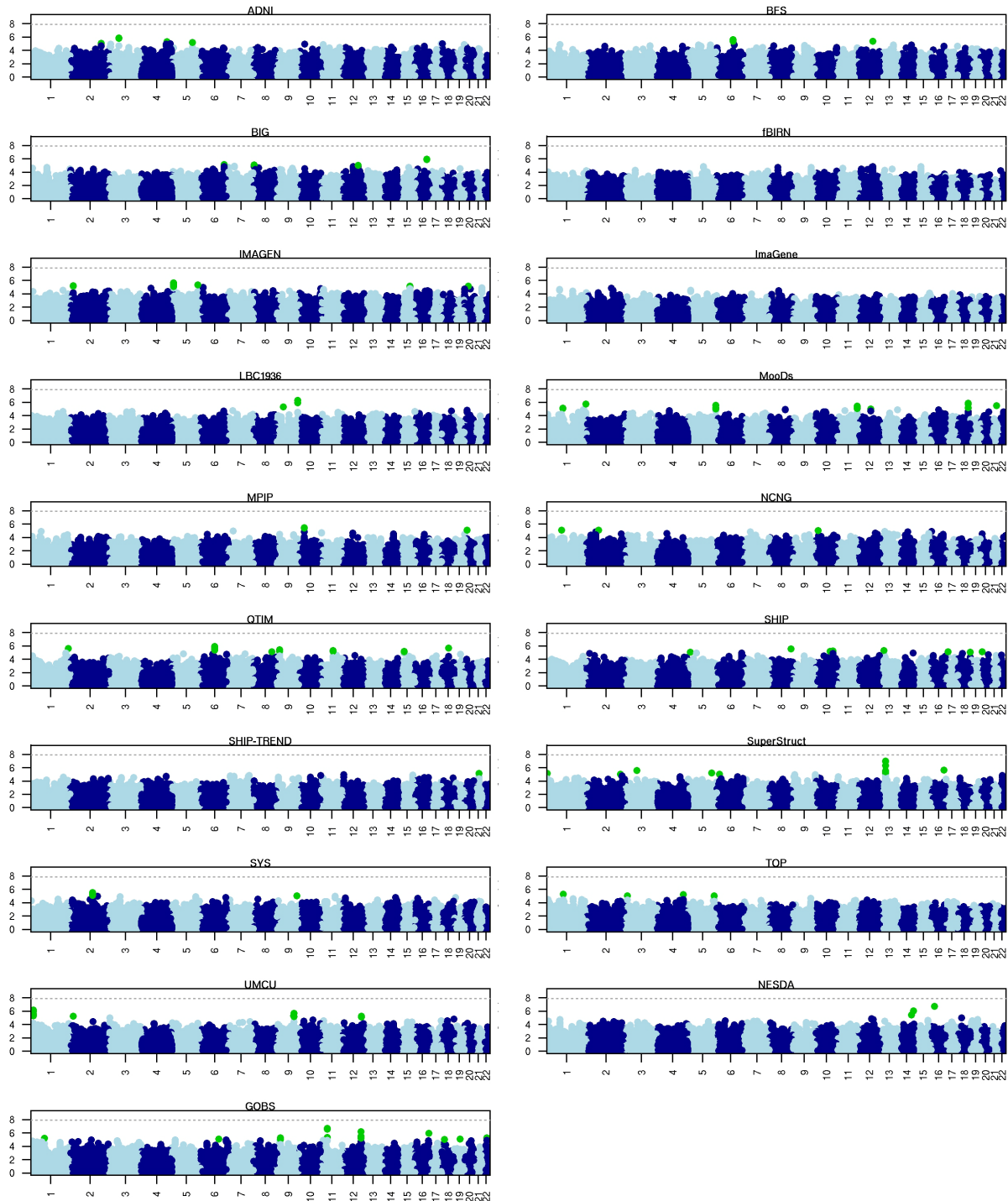
Supplementary Figure 15: Manhattan plots show genome-wide association results from each cohort using average bilateral hippocampal volume as a phenotype in all subjects (regardless of diagnosis).

Association models statistically controlled for the effects of **brain volume**, age, sex, age^2 , $age \times sex$ interaction, $age^2 \times sex$ interaction, 4 MDS components, and dummy variables for different scanner or acquisition sequence (when needed). Note the genome-wide significant effect at the **APOE** locus in the ADNI sample, as described in Supplementary Figure 11.



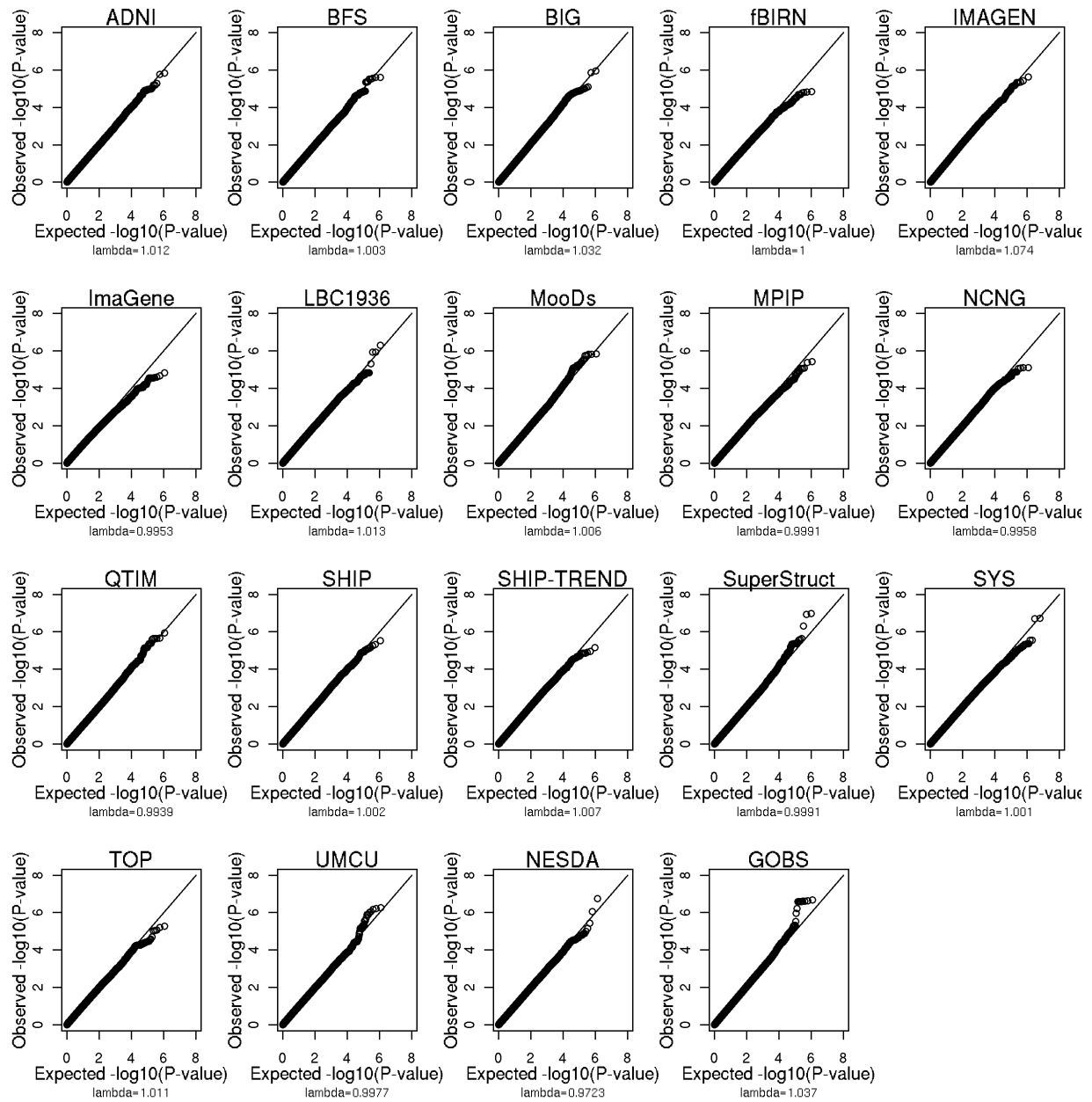
Supplementary Figure 16: QQ plots show genome-wide association results from each cohort using average bilateral hippocampal volume as the phenotype in all subjects (regardless of diagnosis).

Association models statistically controlled for the effects of **brain volume**, age, sex, age^2 , $age \times sex$ interaction, $age^2 \times sex$ interaction, 4 MDS components, and dummy variables for different scanner or acquisition sequences (when needed). Lambda values in each sample are all near 1 indicating no inflation of test-statistics.



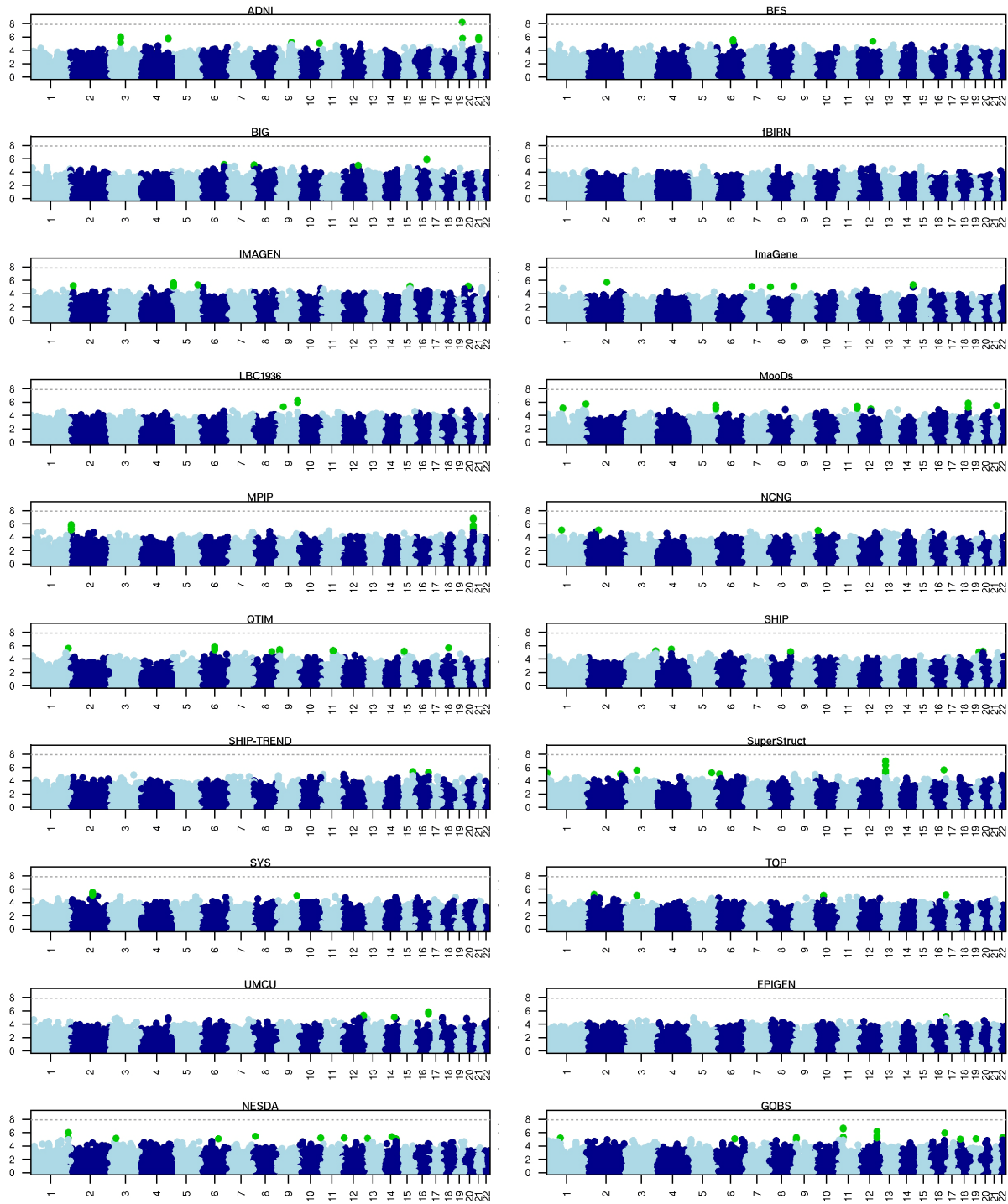
Supplementary Figure 17: Manhattan plots show genome-wide association results from each cohort using average bilateral hippocampal volume as a phenotype in healthy subjects only.

Association models statistically controlled for the effects of age, sex, age^2 , $age \times sex$ interaction, $age^2 \times sex$ interaction, 4 MDS components, and dummy variables for different scanner or acquisition sequences (when needed) without controlling for a measure of head size.



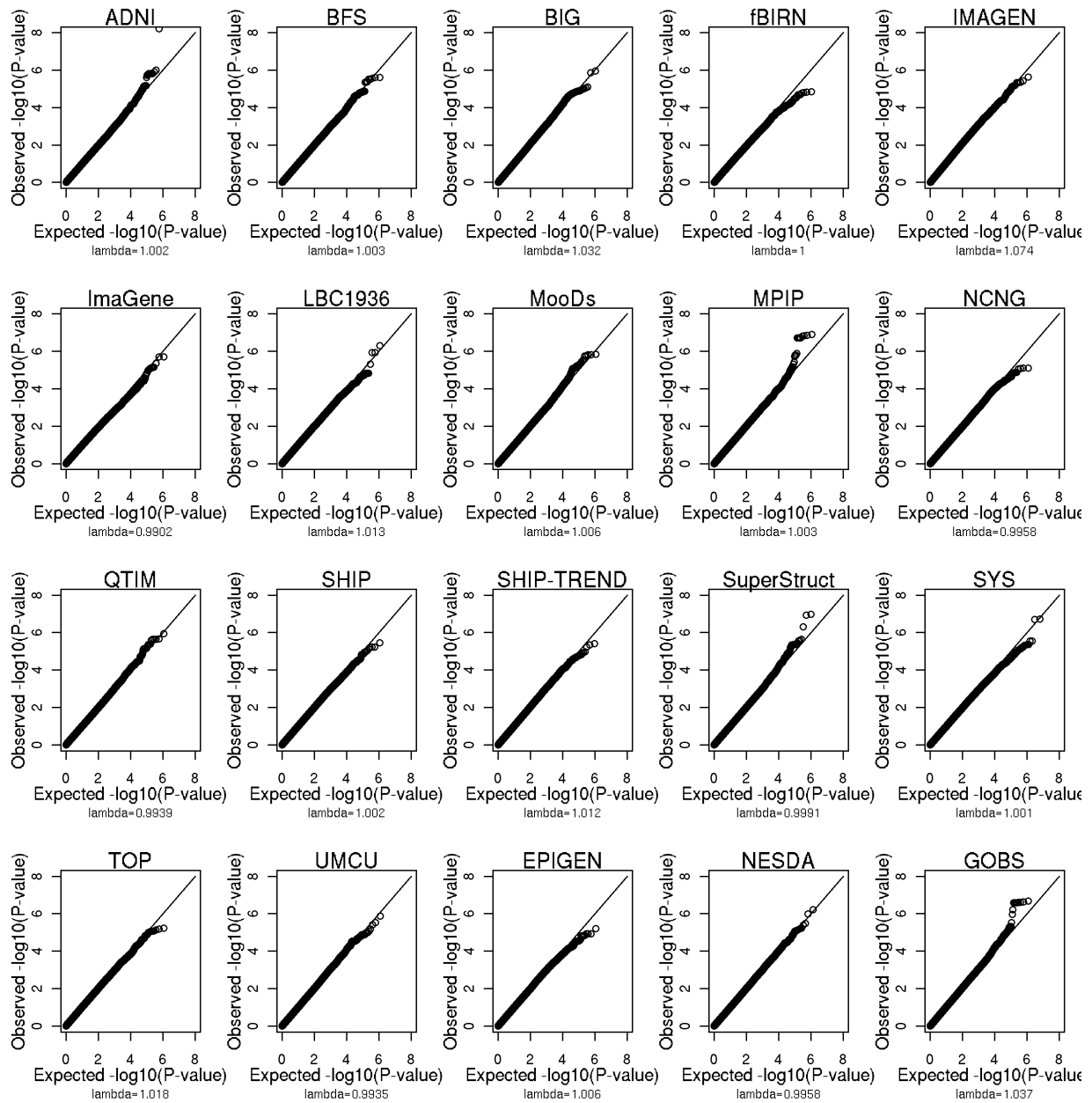
Supplementary Figure 18: QQ plots show genome-wide association results from each cohort using average bilateral hippocampal volume as a phenotype in healthy subjects only.

Associations models statistically controlled for the effects of age, sex, age^2 , $age \times sex$ interaction, $age^2 \times sex$ interaction, 4 MDS components, and dummy variables for different scanner or acquisition sequence (when needed) without controlling for a measure of head size. Lambda values in each sample are all near 1 indicating no inflation of test statistics.



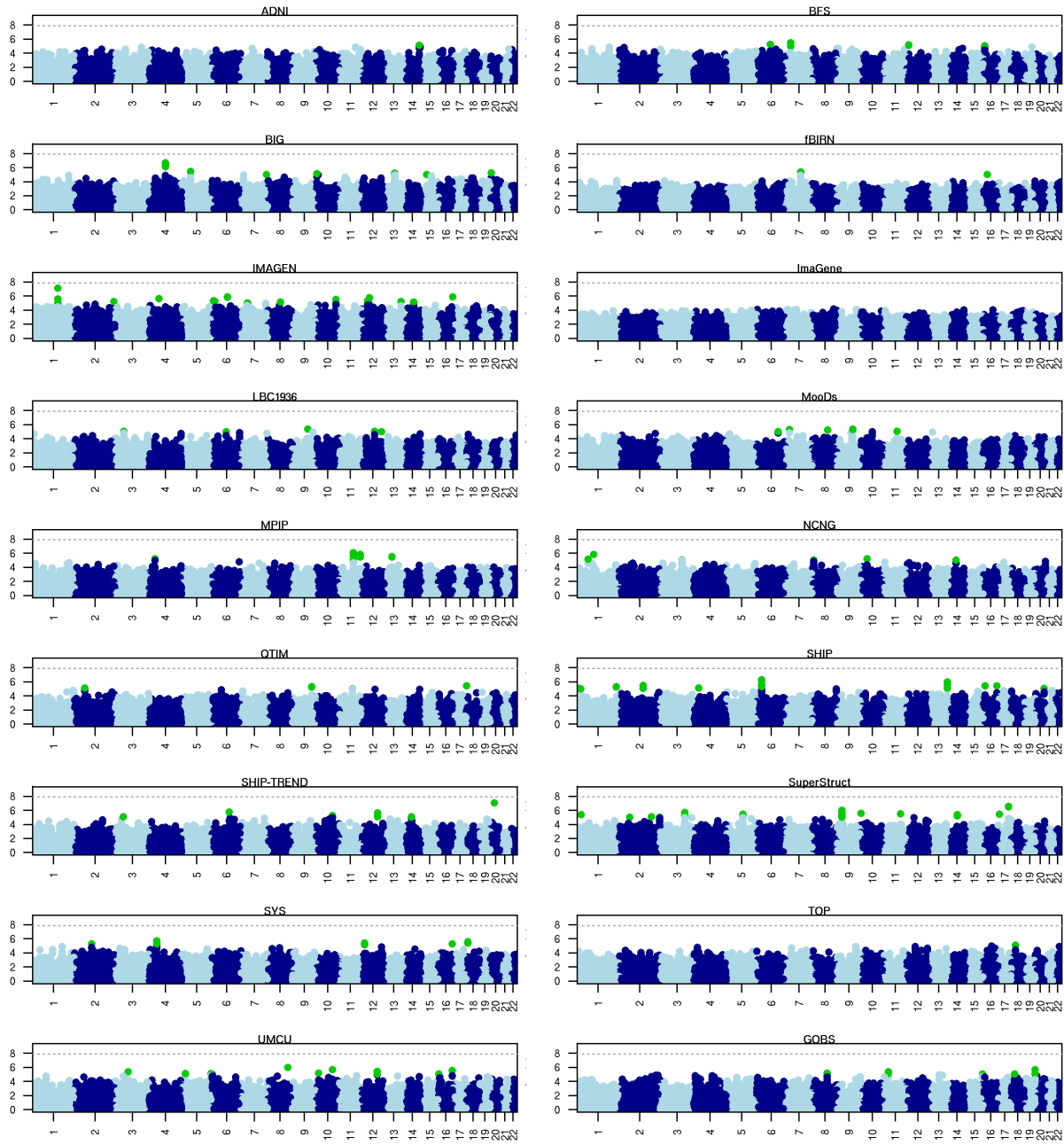
Supplementary Figure 19: Manhattan plots show genome-wide association results from each cohort using average bilateral hippocampal volume as a phenotype in all subjects (regardless of diagnosis).

Association models statistically controlled for the effects of age, sex, age^2 , $age \times sex$ interaction, $age^2 \times sex$ interaction, 4 MDS components, and dummy variables for different scanner or acquisition sequence (when needed) without controlling for a measure of head size. Note the genome-wide significant effect at the *APOE* locus in the ADNI sample, as described in Supplementary Figure 11.



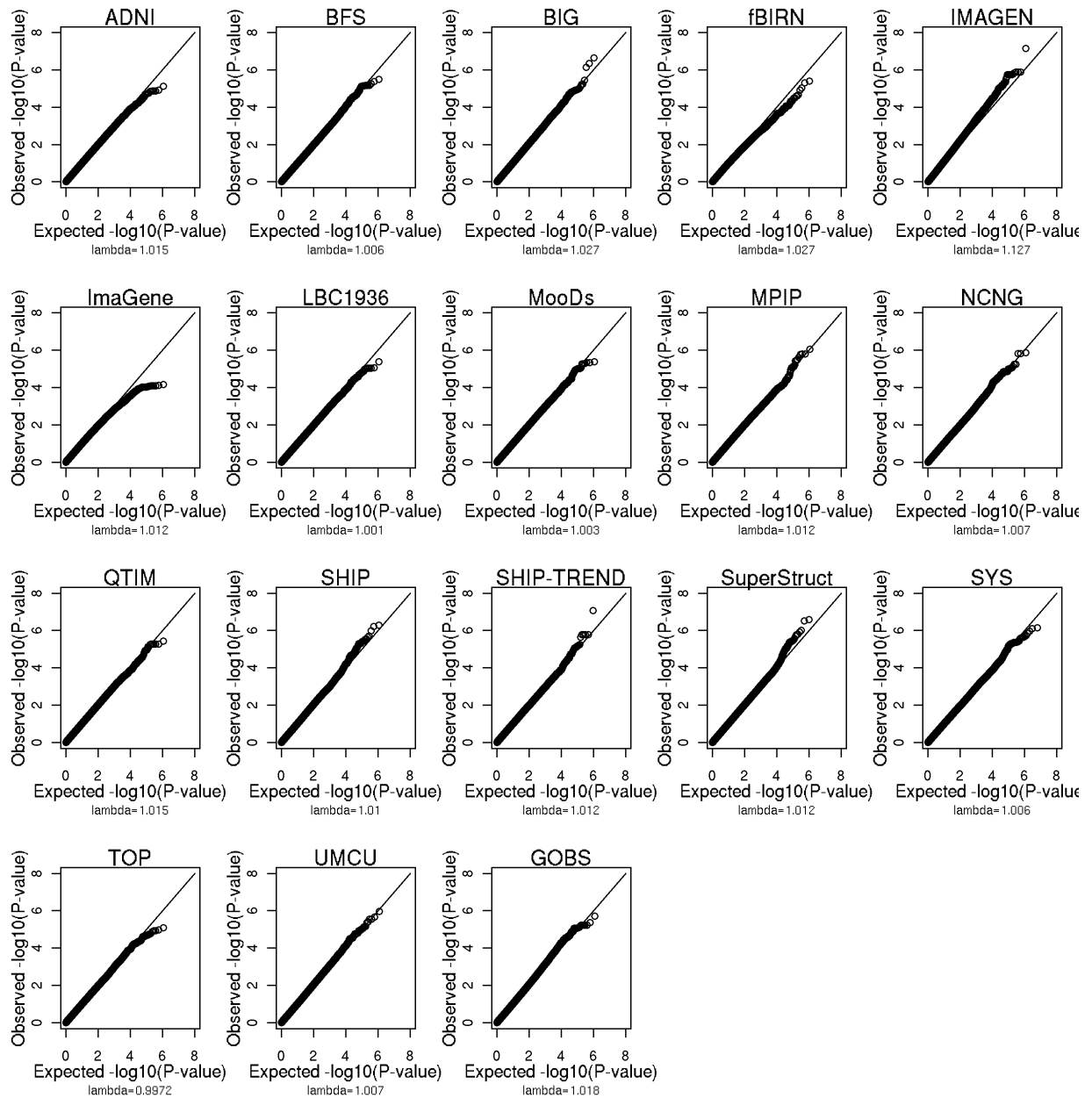
Supplementary Figure 20: QQ plots show genome-wide association results from each cohort using average bilateral hippocampal volume as a phenotype in all subjects (regardless of diagnosis).

Association models statistically controlled for the effects of age, sex, age^2 , $age \times sex$ interaction, $age^2 \times sex$ interaction, 4 MDS components, and dummy variables for different scanner or acquisition sequence (when needed) without controlling for a measure of head size. Lambda values in each sample are all near 1 indicating no inflation of test statistics.



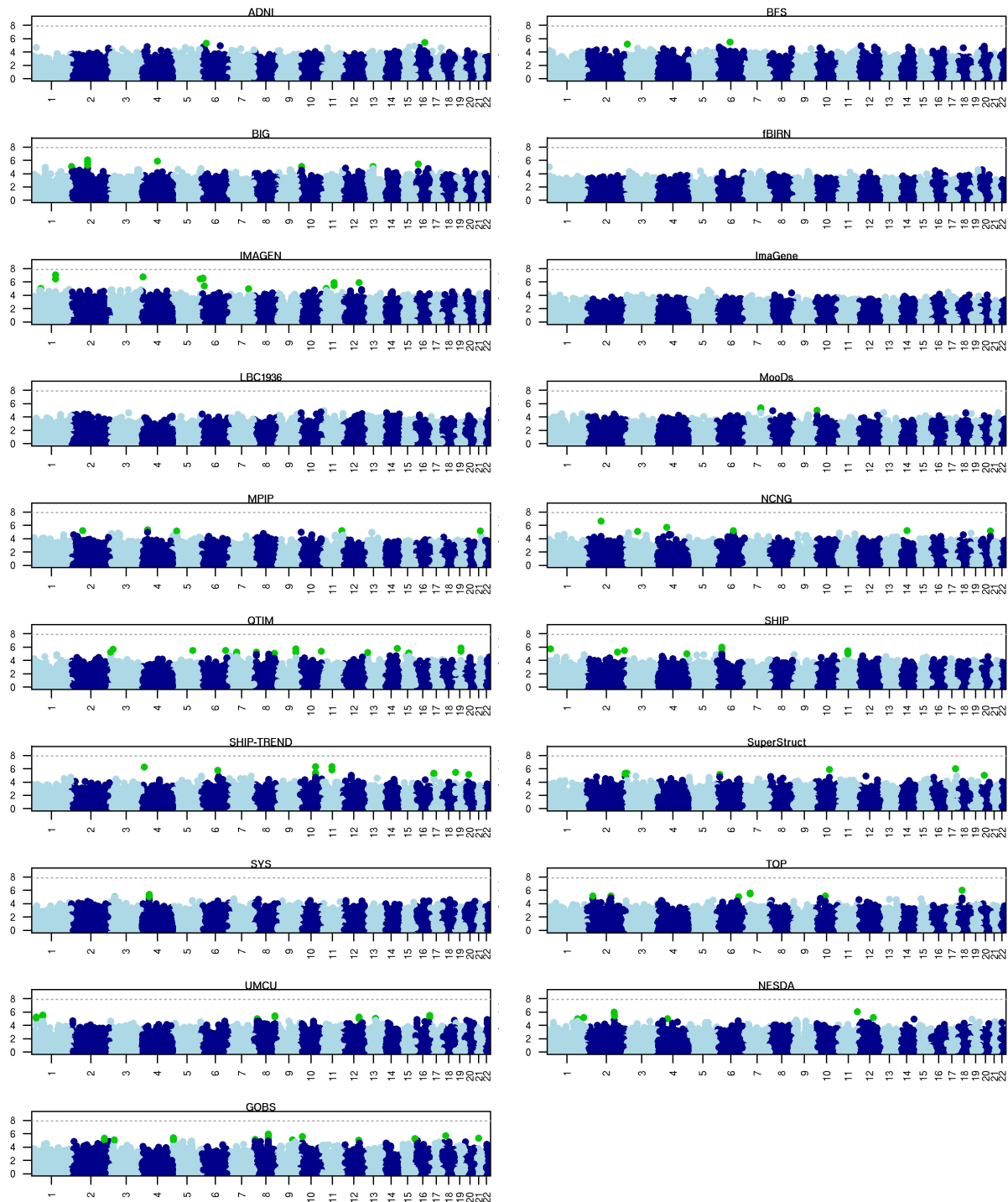
Supplementary Figure 21: Manhattan plots show genome-wide association results from each cohort for total brain volume as a phenotype in healthy subjects only.

Association models statistically controlled for the effects of age, sex, age^2 , $age \times sex$ interaction, $age^2 \times sex$ interaction, 4 MDS components, and dummy variables for different scanner or acquisition sequence (when needed).



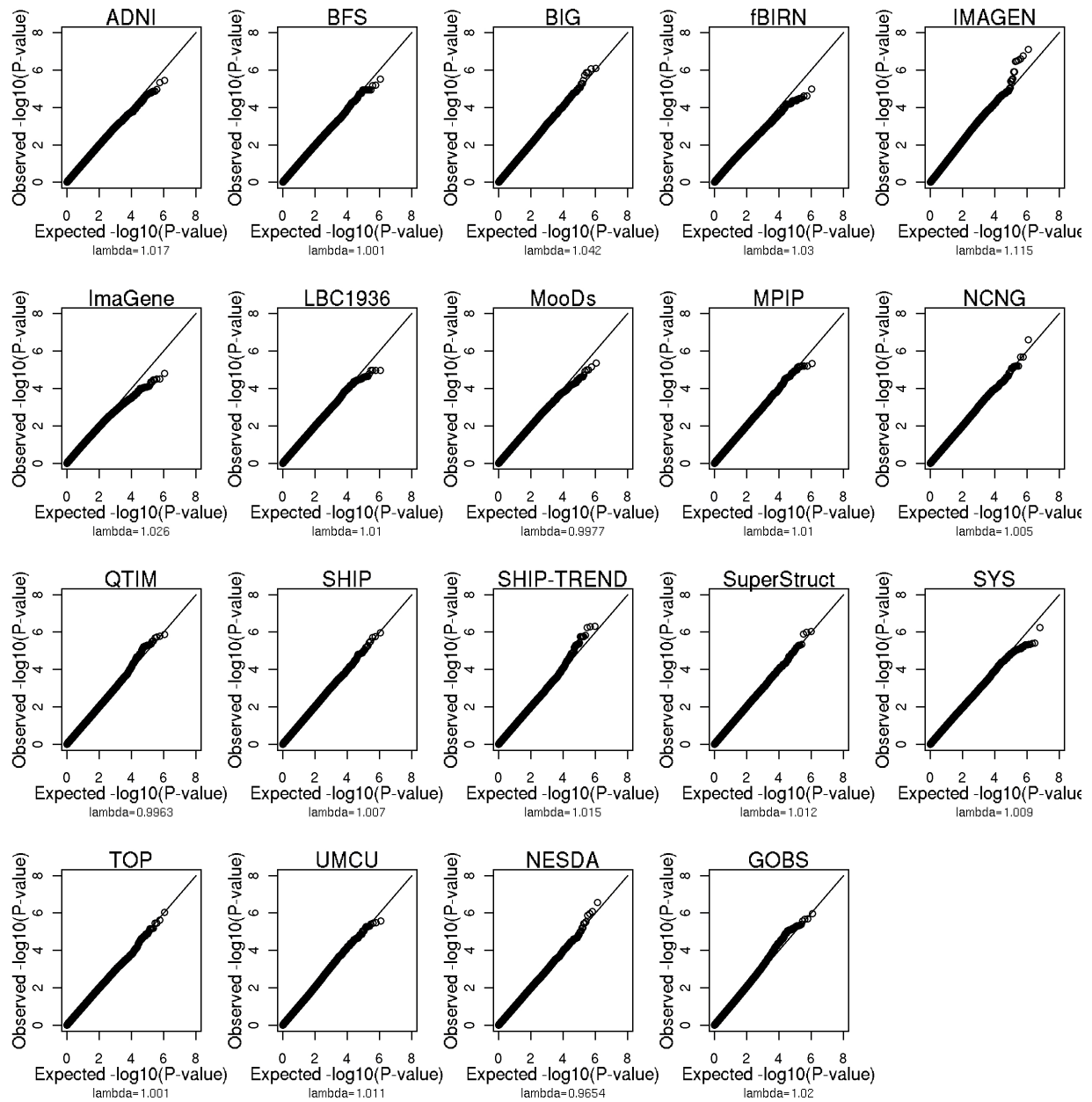
Supplementary Figure 22: QQ plots showing genome-wide association results from each cohort for total brain volume as a phenotype in healthy subjects only.

Association models statistically controlled for the effects of age, sex, age^2 , age \times sex interaction, $age^2\times$ sex interaction, 4 MDS components, and dummy variables for different scanner or acquisition sequence (when needed). Lambda values in each sample are all near 1 indicating no inflation of test statistics.



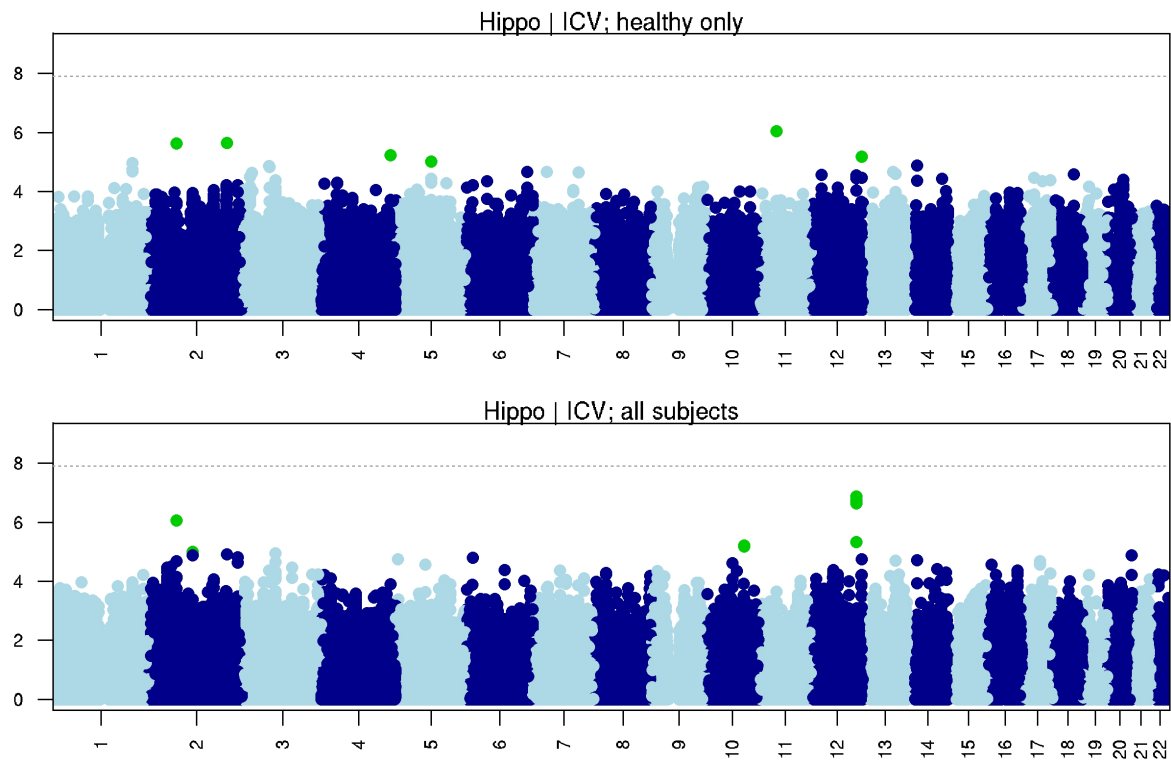
Supplementary Figure 23: Manhattan plots show genome-wide association results from each cohort using estimated total intracranial volume (ICV) as a phenotype in healthy subjects only.

Association models statistically controlled for the effects of age, sex, age^2 , $age \times sex$ interaction, $age^2 \times sex$ interaction, 4 MDS components, and dummy variables for different scanner or acquisition sequence (when needed).

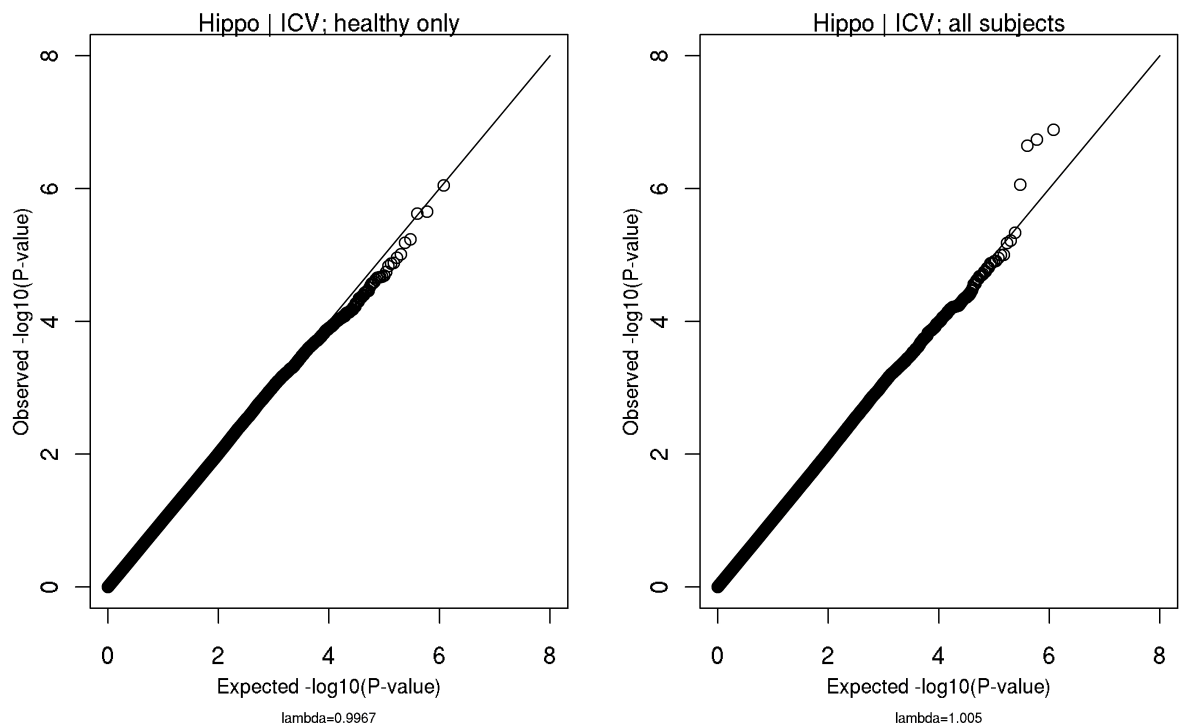


Supplementary Figure 24: QQ plots show genome-wide association results from each cohort using estimated total intracranial volume (ICV) as a phenotype in healthy subjects only.

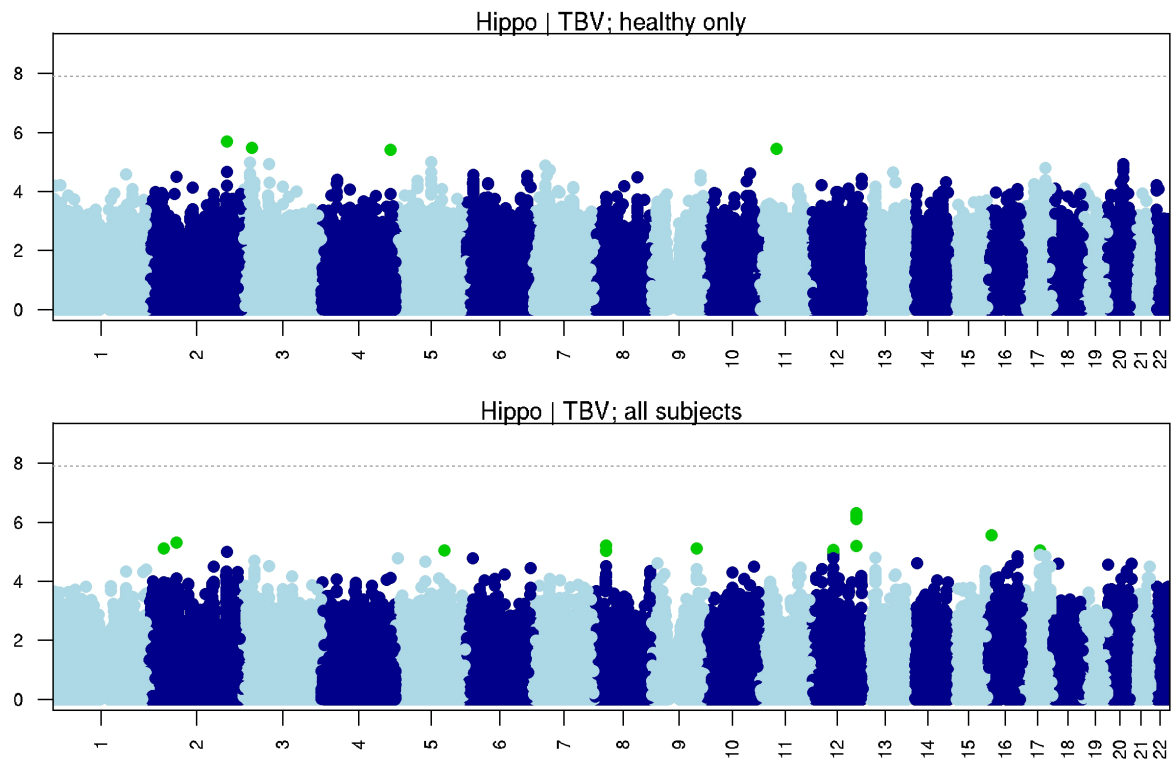
Association models statistically controlled for the effects of age, sex, age^2 , age \times sex interaction, $age^2\times$ sex interaction, 4 MDS components, and dummy variables for different scanner or acquisition sequence (when needed). Lambda values in each sample are all near 1 indicating no inflation of test-statistics.



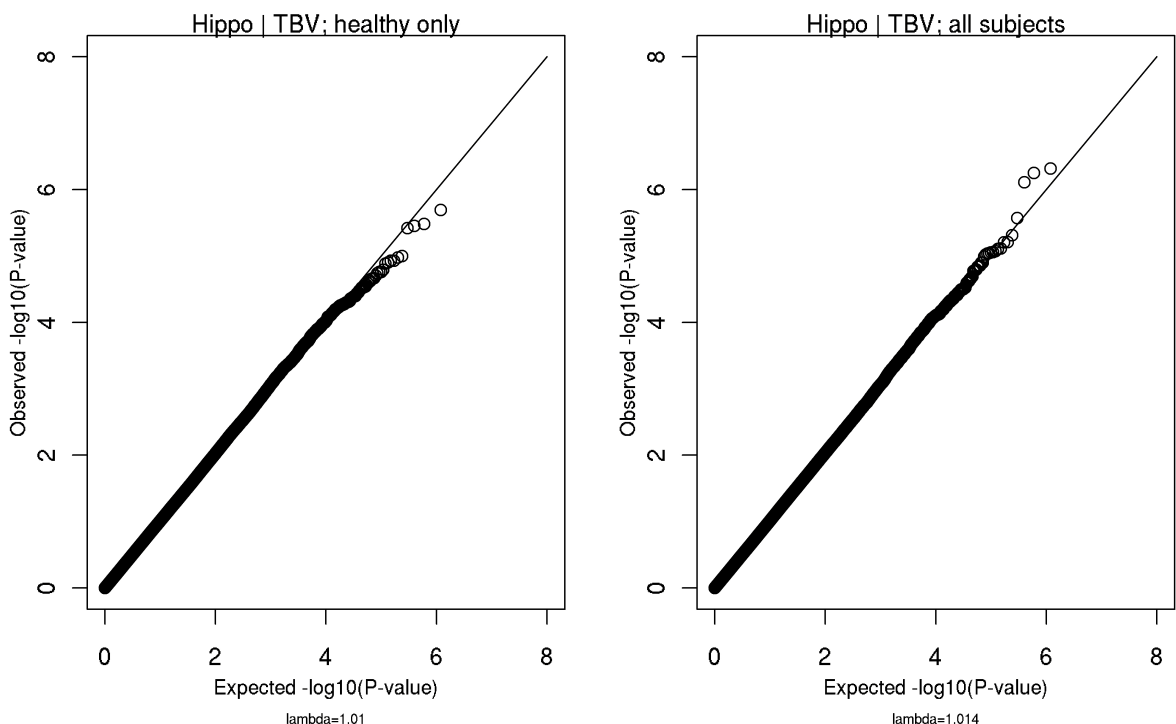
Supplementary Figure 25: Fixed effects meta-analysis of hippocampal volume controlling for estimated intracranial volume and other covariates in healthy subjects only (N=5,776) and in all subjects (N=7,795).



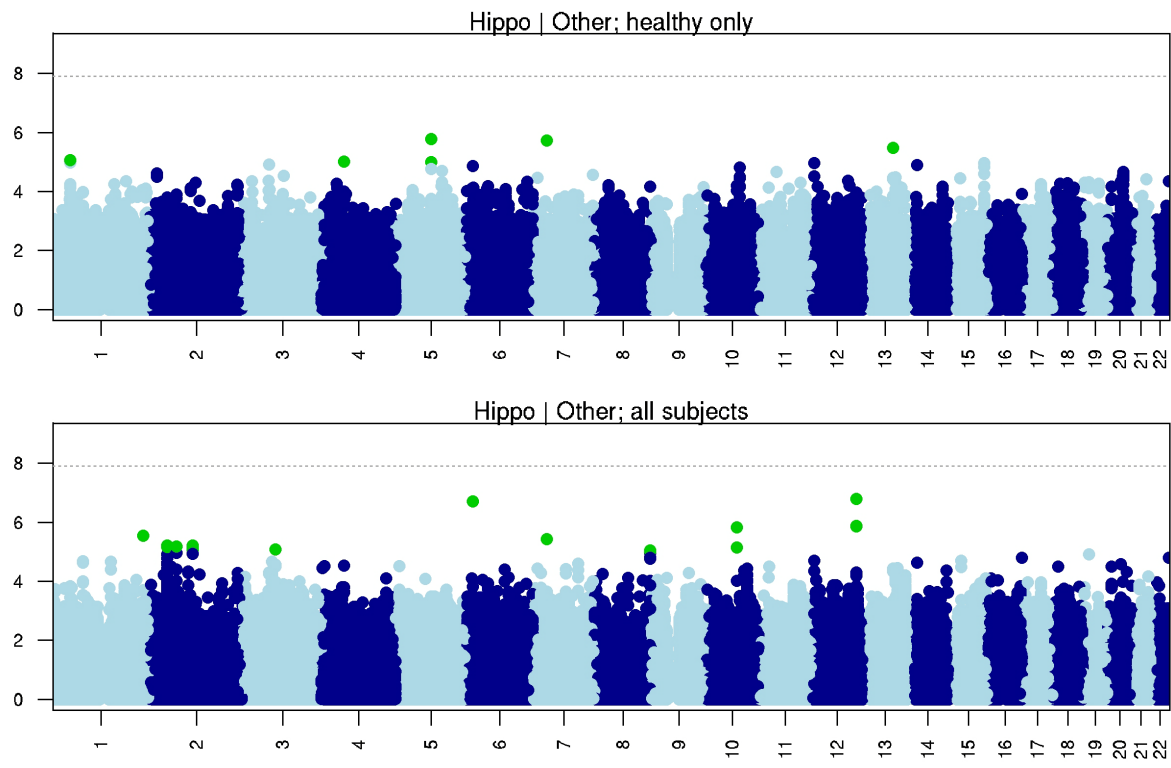
Supplementary Figure 26: QQ plots of fixed effects meta-analysis of average bilateral hippocampal volume controlling for ICV and other covariates in healthy subjects only (N=5,776) and all subjects (N=7,795).



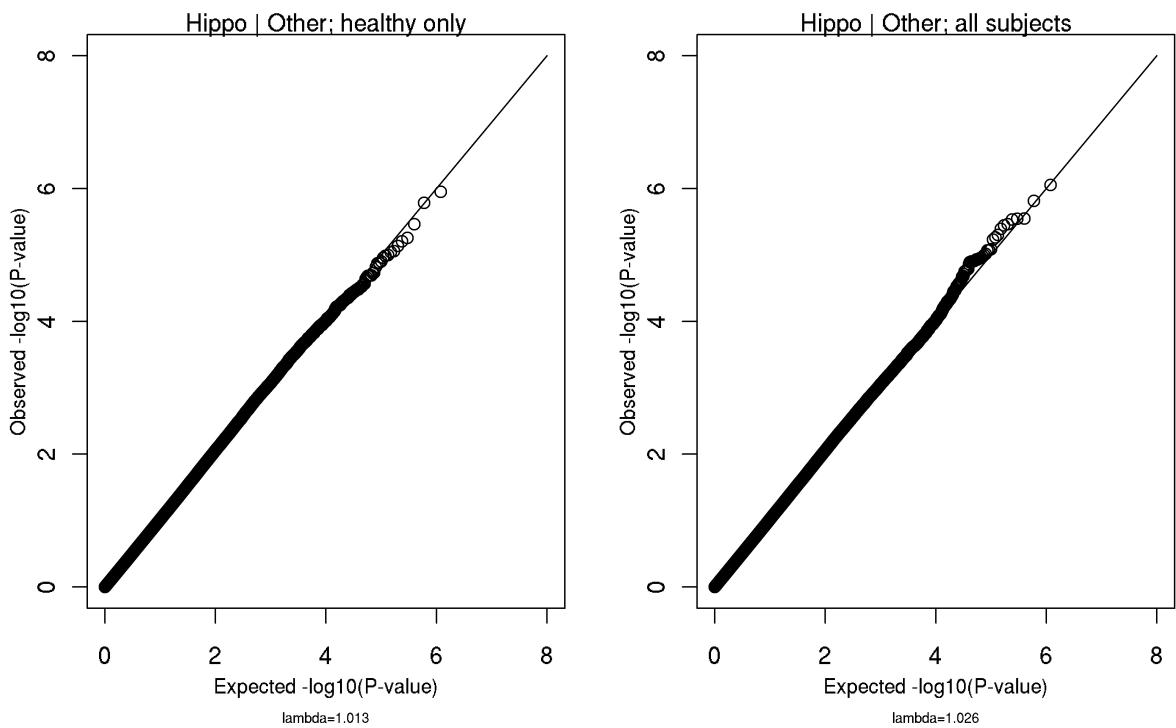
Supplementary Figure 27: Fixed effects meta-analysis of hippocampal volume controlling for brain volume and other covariates in healthy subjects only (N=5,776) and in all subjects (N=7,795).



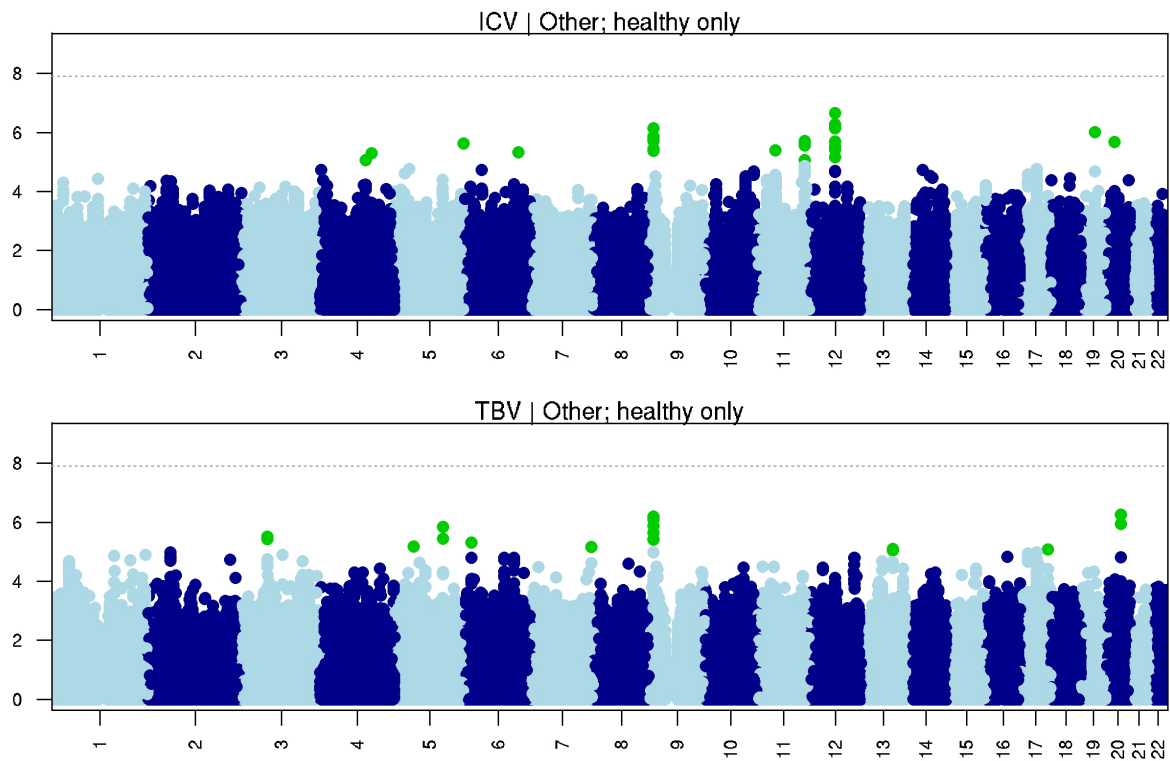
Supplementary Figure 28: QQ plots of the fixed effects meta-analysis of average bilateral hippocampal volume controlling for brain volume and other covariates in healthy subjects only (N=5,776) and in all subjects (N=7,795).



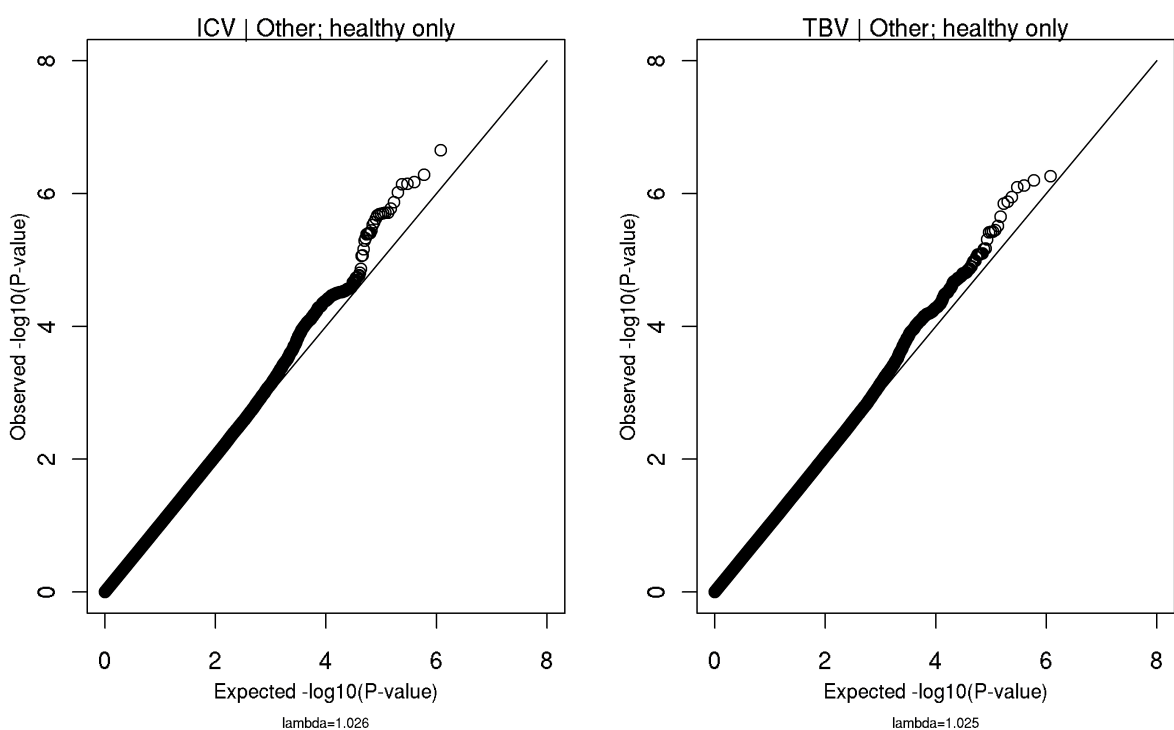
Supplementary Figure 29: Fixed effects meta-analysis of hippocampal volume controlling for other covariates in healthy subjects only (N=5,775) and in all subjects (N=7,794).



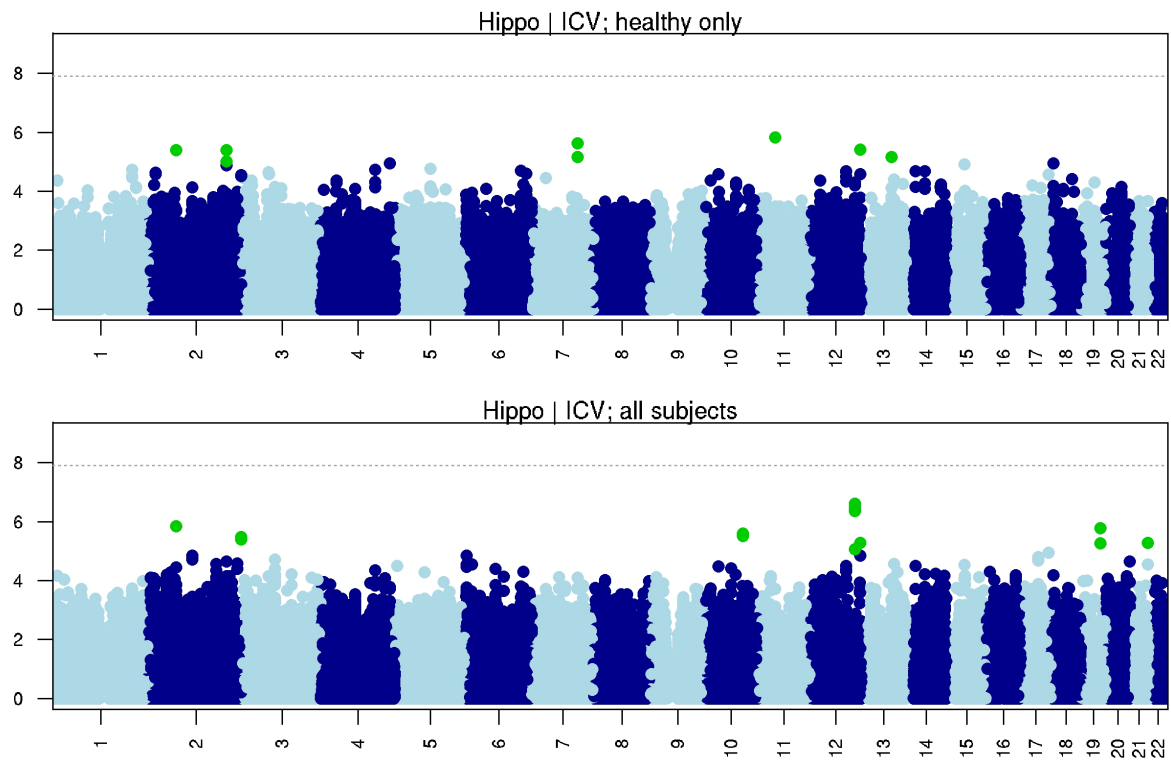
Supplementary Figure 30: QQ plots of fixed effects meta-analysis of average bilateral hippocampal volume controlling for other covariates in healthy subjects only (N=5,775) and in all subjects (N=7,794).



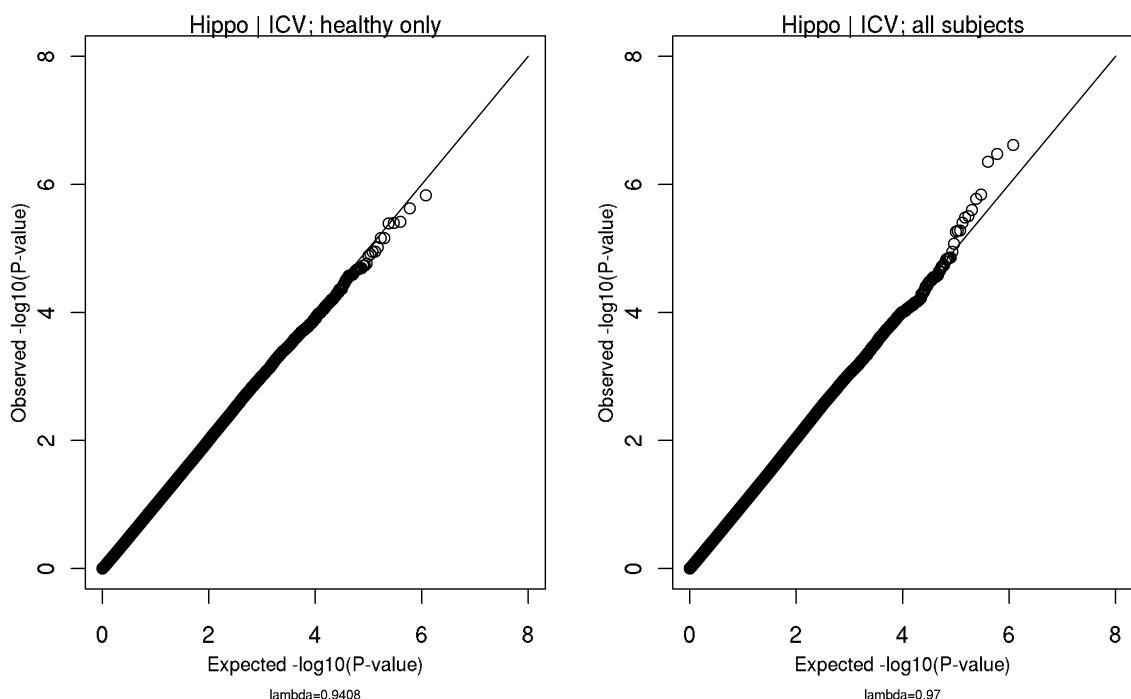
Supplementary Figure 31: Fixed effects meta-analysis of estimated intracranial volume and total brain size measures including other covariates in healthy subjects only (N=5,778).



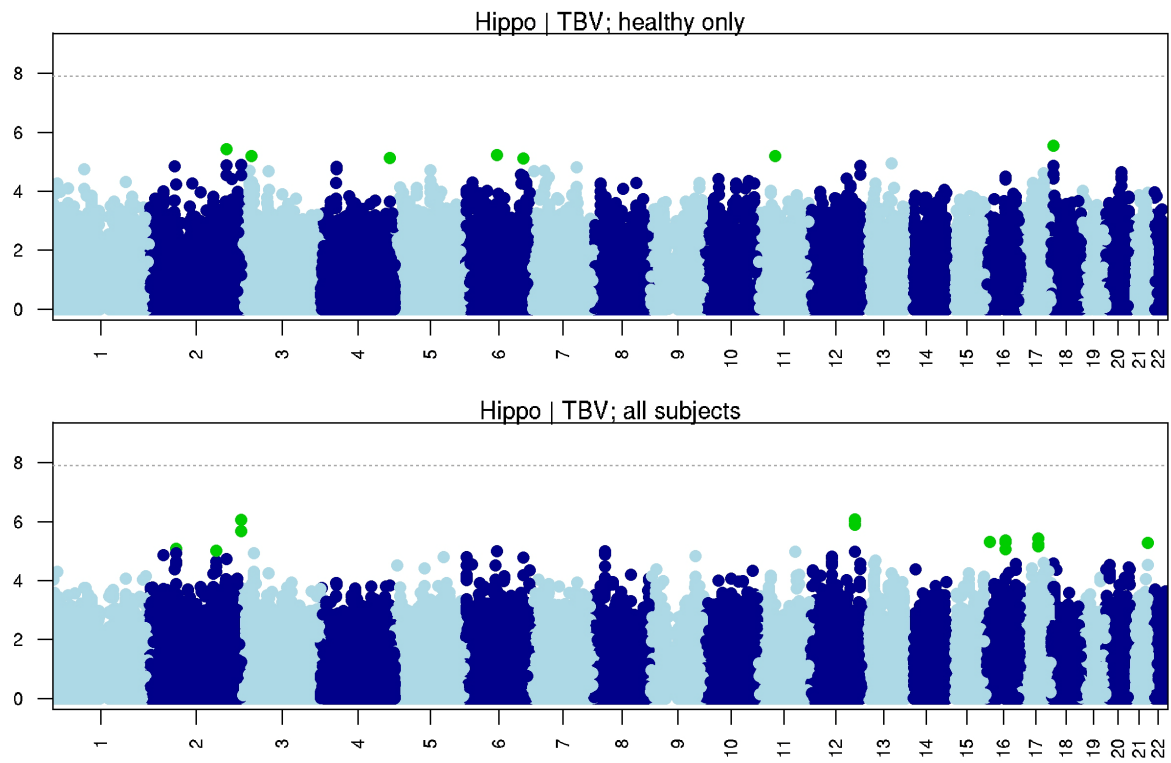
Supplementary Figure 32: QQ plots of fixed effects meta-analysis using total brain size measures as phenotypes including other covariates in healthy subjects only (N=5,778).



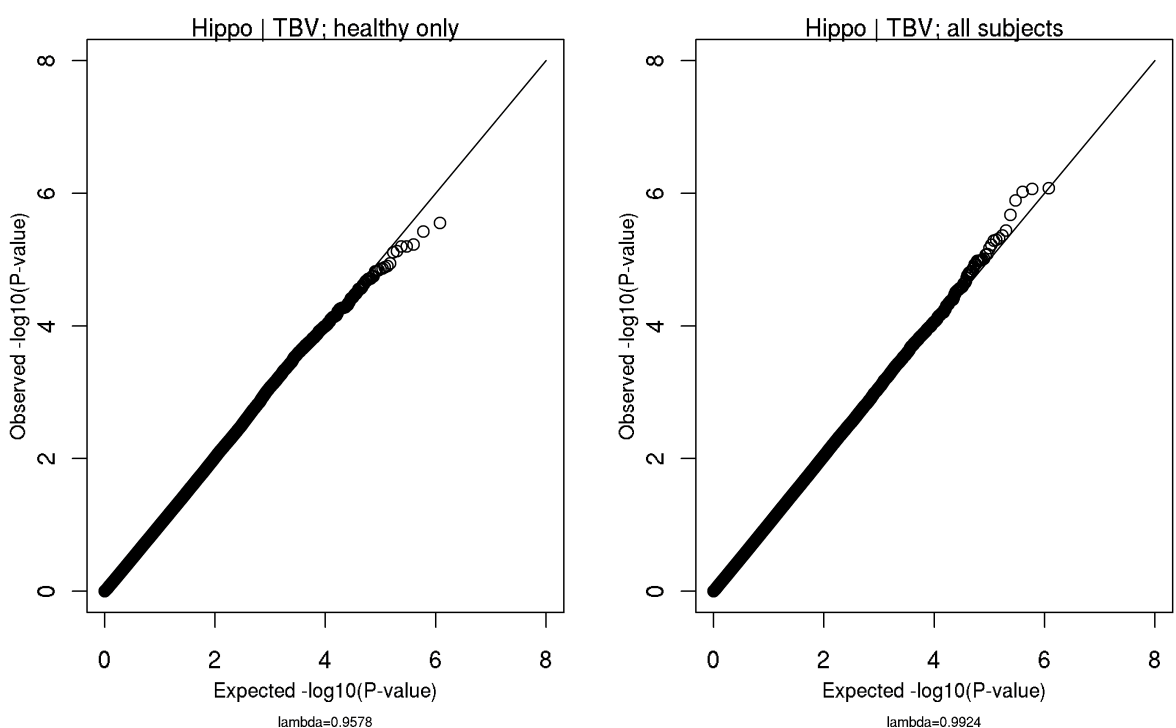
Supplementary Figure 33: Random effects meta-analysis of hippocampal volume controlling for estimated intracranial volume and other covariates in healthy subjects only (N=5,776) and in all subjects (N=7,795).



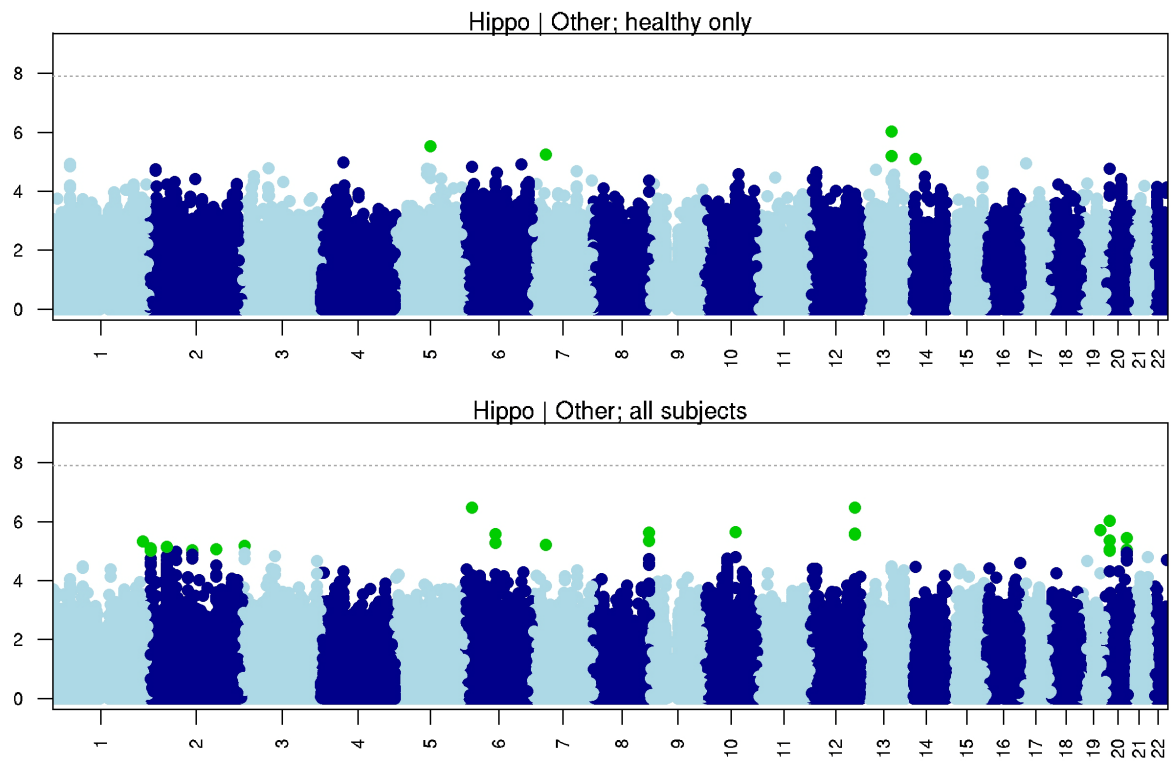
Supplementary Figure 34: QQ plots of random effects meta-analysis of hippocampal volume controlling for estimated intracranial volume and other covariates in healthy subjects only (N=5,776) and in all subjects (N=7,795).⁷



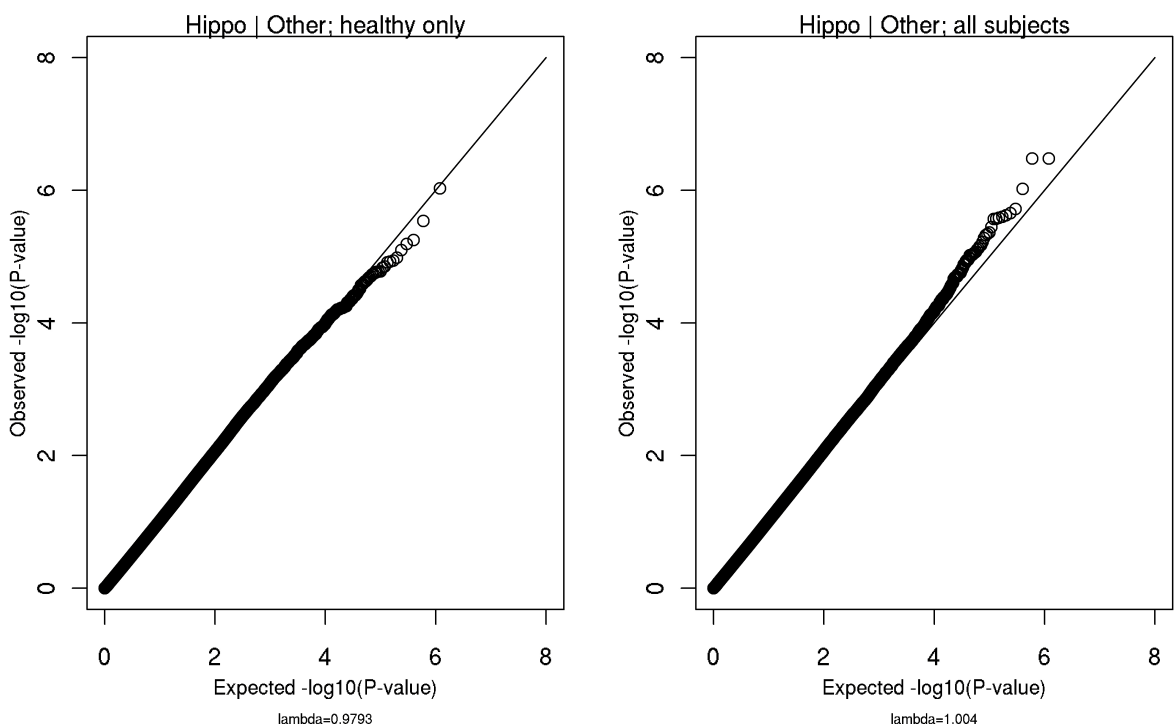
Supplementary Figure 35: Random effects meta-analysis of hippocampal volume controlling for brain volume and other covariates in healthy subjects only (N=5,776) and in all subjects (N=7,795).



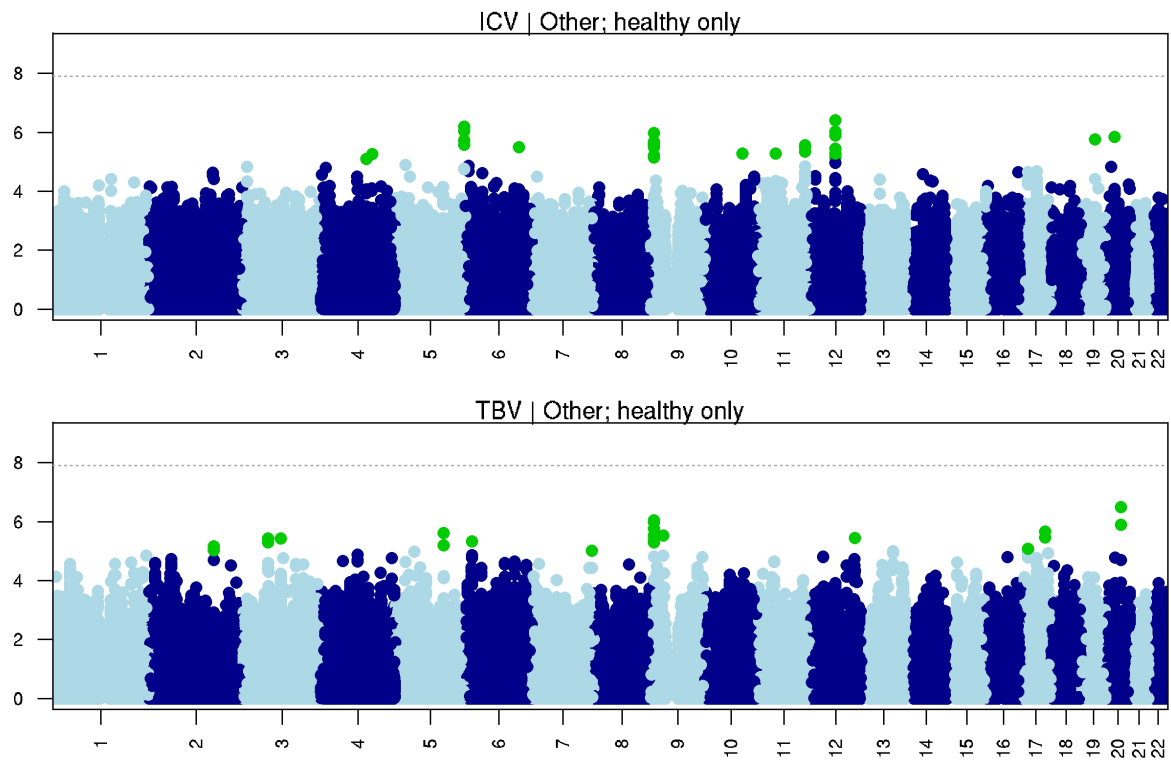
Supplementary Figure 36: QQ plots of random effects meta-analysis of hippocampal volume controlling for brain volume and other covariates in healthy subjects only (N=5,776) and in all subjects (N=7,795).



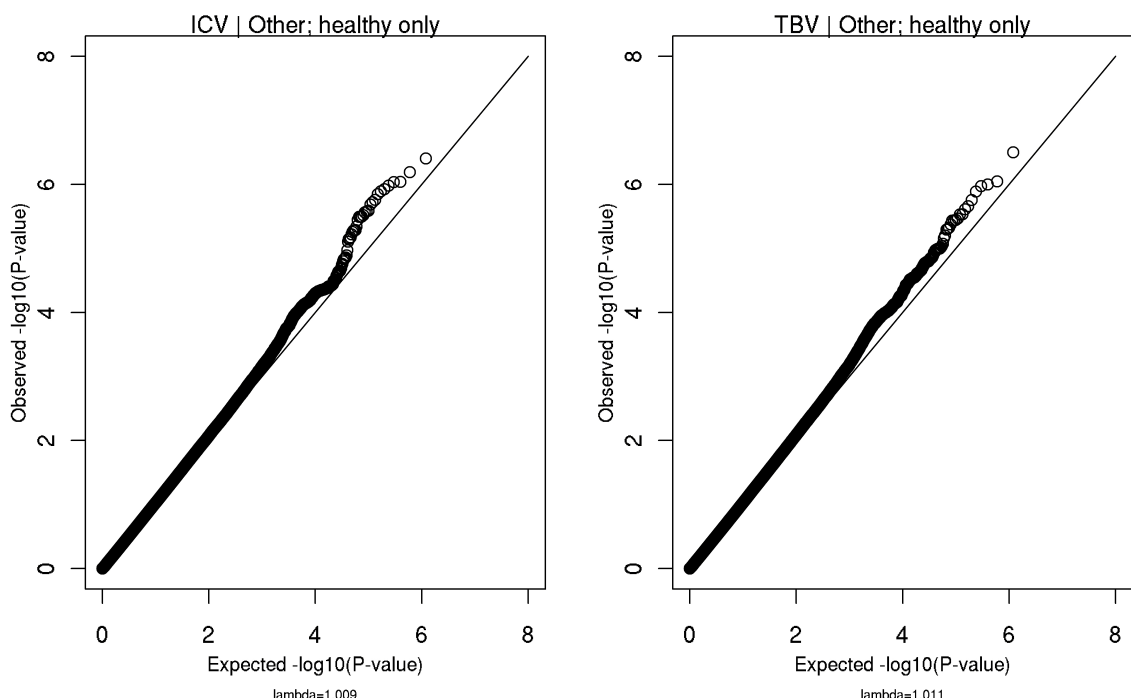
Supplementary Figure 37: Random effects meta-analysis of hippocampal volume controlling for other covariates in healthy subjects only (N=5,775) and in all subjects (N=7,794).



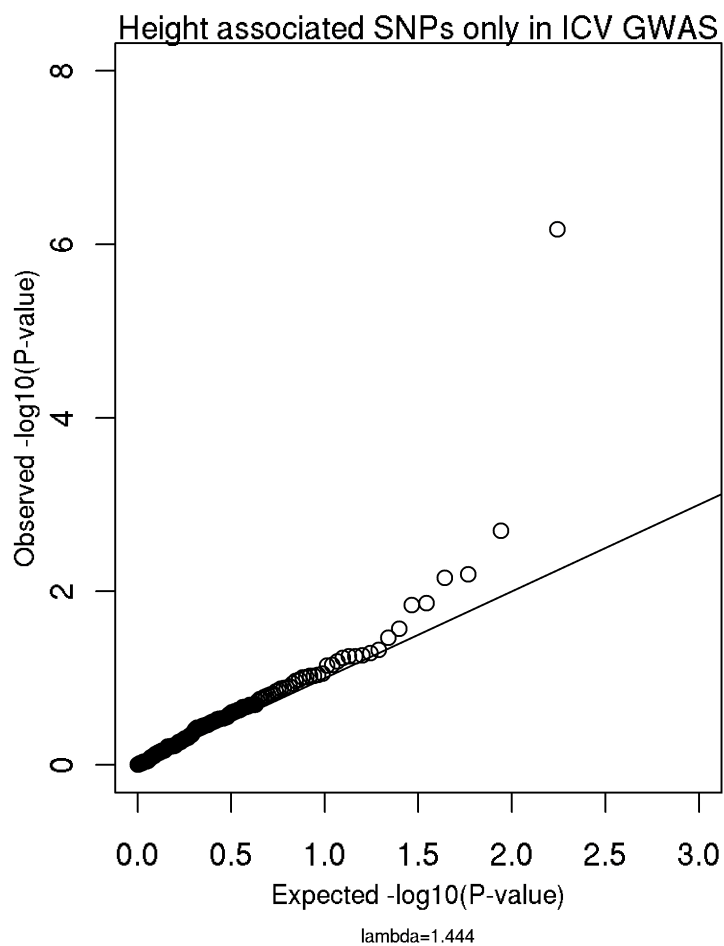
Supplementary Figure 38: QQ plots of random effects meta-analysis of hippocampal volume controlling for other covariates in healthy subjects only (N=5,775) and in all subjects (N=7,794).



Supplementary Figure 39: Random effects meta-analysis of estimated intracranial volume and total brain size measures including other covariates in healthy subjects only (N=5,778).

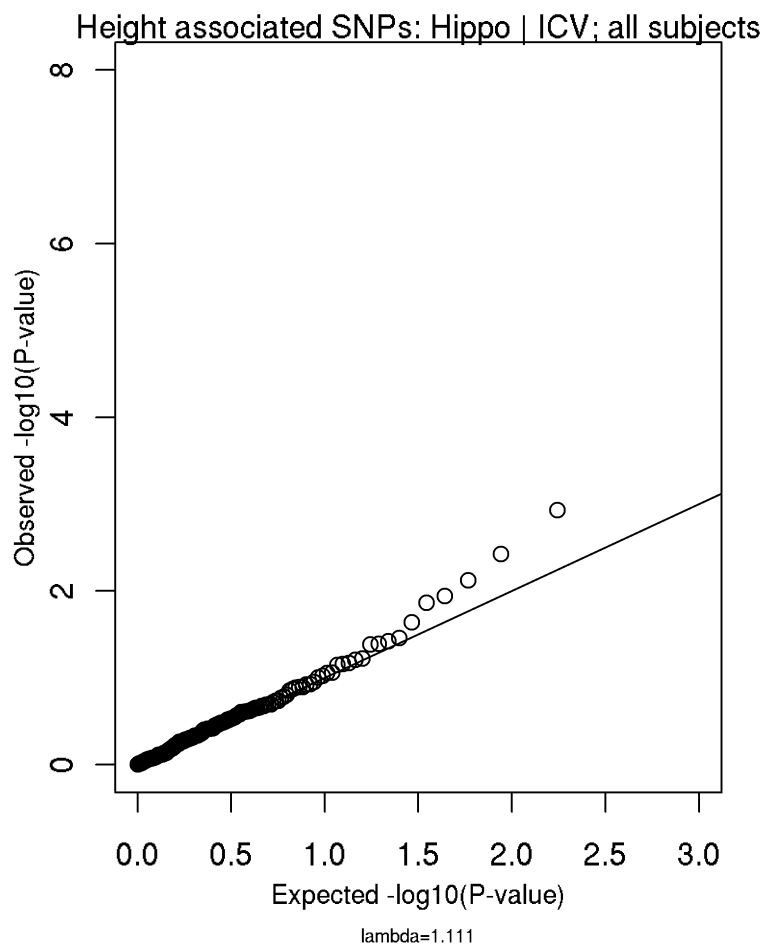


Supplementary Figure 40: QQ plots of random effects meta-analysis of total brain size measures including other covariates in healthy subjects only (N=5,778).



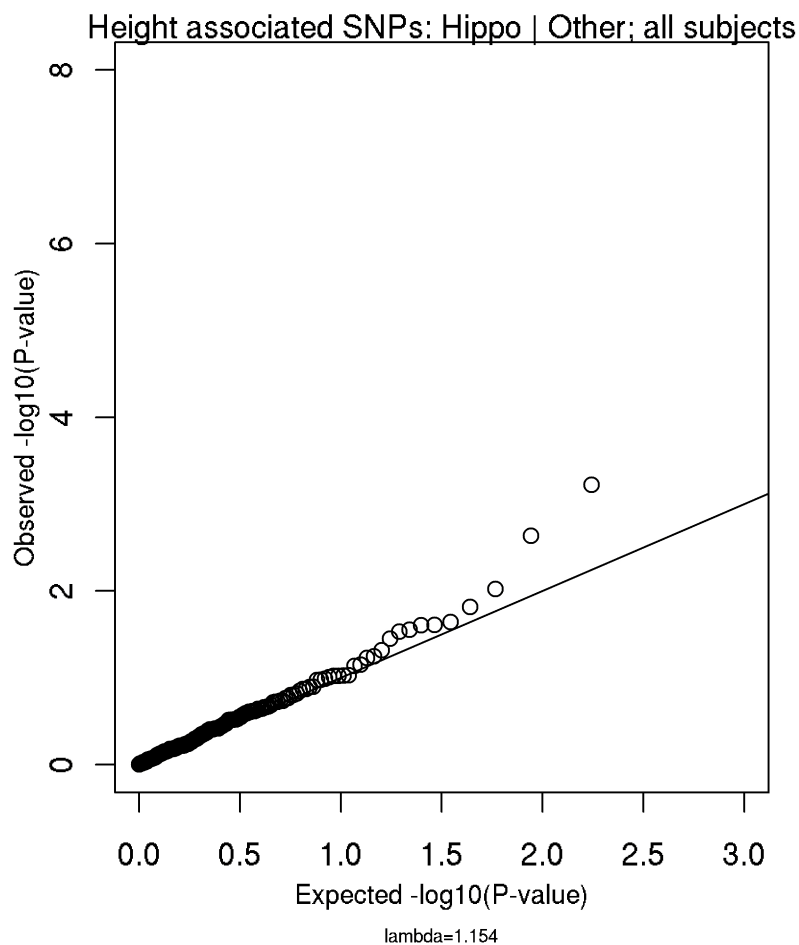
Supplementary Figure 41: QQ plot of ICV associations for 175 SNPs previously identified as strongly associated with height.

A clear statistical inflation of results above those expected by chance is seen ($\lambda = 1.444$) indicating that SNPs associated with height⁸ are also associated with ICV. As λ is calculated as the ratio of the median of the observed and expected distributions rather than the mean this result is not being driven by the single strongly associated SNP. Thus, this reflects an enrichment that is not due to a small number of large effects, but rather a systematically higher degree of association throughout the candidate SNP set. Importantly, this enhanced association is absent when considering the λ from the full GWAS analysis (1.023; **Supplementary Figures 31 and 32**) suggesting that this is unlikely to be due to a methodological artifact.



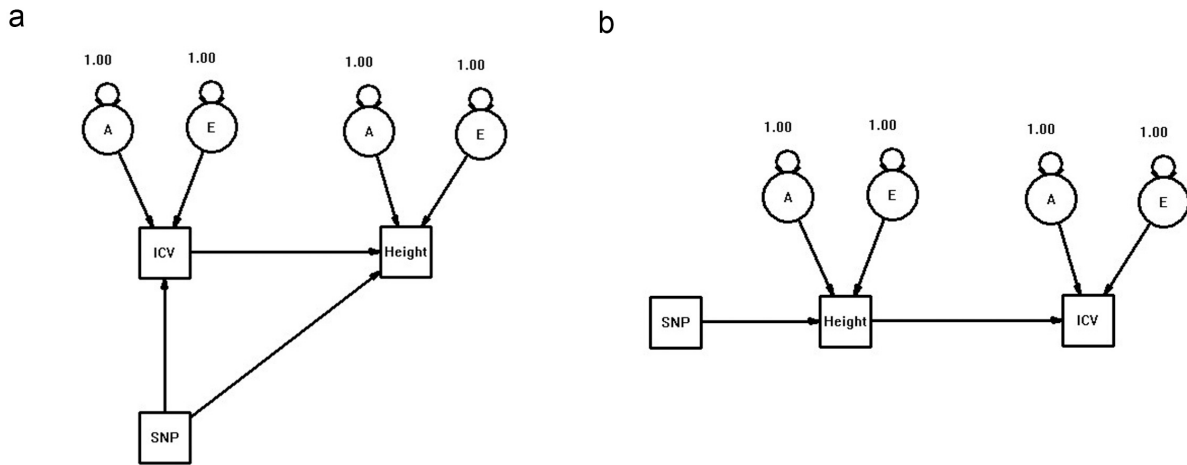
Supplementary Figure 42: QQ plot of hippocampal volume associations controlling for intracranial volume and other covariates in all subjects for 175 SNPs previously identified as strongly associated with height.

The comparatively limited inflation of results as compared to that observed for ICV ($\lambda = 1.111$) indicates there is less enrichment of SNPs associated with height⁸ in this distribution.



Supplementary Figure 43: QQ plot of hippocampal volume associations controlling for other covariates without a measure of head size in all subjects for SNPs previously identified as strongly associated with height.

Little inflation of results above that expected by chance is seen ($\lambda = 1.154$) indicating SNP associations to hippocampal volume are not highly correlated with height⁸ in the absence of ICV correction.



Supplementary Figure 44: Structural equation models of the association among rs10784502, height, and ICV.

In the QTIM sample, the association between rs10784502 and ICV ($P=0.086$) was slightly decreased when adding height as a covariate ($P=0.110$). Structural equation models were run within the OpenMx R package (<http://openmx.psyc.virginia.edu/>) and models are illustrated in the path diagrams above. “A” refers to the additive genetic component; “E” refers to the unique environmental component, and 1.00 refers to the residual error variance of these latent variables. There was no significant difference in fit between a model allowing for partial causality (panel a) as compared to a fully causal model (panel b), $\chi^2=2.8$ for 1 df, $P=0.09$. However, the partial model was slightly more parsimonious than the fully causal model (AIC 289.2 vs 290.0). This suggests that while rs10784502 is associated with both ICV and height, the effect of this variant on ICV cannot be completely accounted for by the indirect effects of this SNP on height, or by the correlation between height and ICV.

References

1. Weis, S., Haug, H., Holoubek, B. & Orun, H. The cerebral dominances: quantitative morphology of the human cerebral cortex. *The International Journal of Neuroscience* **47**, 165-8 (1989).
2. Watson, C. *et al.* Anatomic basis of amygdaloid and hippocampal volume measurement by magnetic resonance imaging. *Neurology* **42**, 1743-50 (1992).
3. Jack, C.R., Jr. *et al.* Rates of hippocampal atrophy correlate with change in clinical status in aging and AD. *Neurology* **55**, 484-89 (2000).
4. Giedd, J.N. *et al.* Quantitative MRI of the temporal lobe, amygdala, and hippocampus in normal human development: ages 4-18 years. *The Journal of Comparative Neurology* **366**, 223-30 (1996).
5. Pfluger, T. *et al.* Normative volumetric data of the developing hippocampus in children based on magnetic resonance imaging. *Epilepsia* **40**, 414-23 (1999).
6. Utsunomiya, H., Takano, K., Okazaki, M. & Mitsudome, A. Development of the temporal lobe in infants and children: analysis by MR-based volumetry. *AJNR. American Journal of Neuroradiology* **20**, 717-23 (1999).
7. Han, B. & Eskin, E. Random-effects model aimed at discovering associations in meta-analysis of genome-wide association studies. *Am. J. Hum. Genet.* **88**, 586-98 (2011).
8. Lango Allen, H. *et al.* Hundreds of variants clustered in genomic loci and biological pathways affect human height. *Nature* **467**, 832-8 (2010).

Supplementary Tables

Identification of common variants associated with human hippocampal and intracranial volumes

CONTENTS

Supplementary Table 1: Descriptions of genome-wide association study cohorts.....	52
Supplementary Table 2: Summary of brain imaging and structure segmentation methods.....	54
Supplementary Table 3: Information on genotyping methods	57
Supplementary Table 4: The correlation between FSL-derived and FreeSurfer-derived phenotypic measures.....	58
Supplementary Table 5: The pairwise correlations between average bilateral hippocampal volume, total brain volume, and ICV.....	59
Supplementary Table 6: Simulation to determine effect of QC thresholds and reference panels on imputation accuracy.....	60
Supplementary Table 7: The association of genetic variants previously identified in the literature as having relevance to the hippocampal structure.....	61
Supplementary Table 8: Affect on hippocampal volume of genetic variants associated with schizophrenia and bipolar disorder.....	62
Supplementary Table 9: SNPs with $P \leq 5 \times 10^{-5}$ for association with mean bilateral hippocampal volume in the analysis without patients correcting for Sex, Age, Age ² , Sex*Age, Sex* Age ² , MDS components, ICV.....	63
Supplementary Table 10: SNPs with $P \leq 5 \times 10^{-5}$ for association with mean bilateral hippocampal volume in the analysis including patients correcting for Sex, Age, Age ² , Sex*Age, Sex* Age ² , MDS, ICV.....	65
Supplementary Table 11: SNPs with $P \leq 5 \times 10^{-5}$ for association with mean bilateral hippocampal volume in the analysis without patients correcting for Sex, Age, Age ² , Sex*Age, Sex* Age ² , MDS.....	67
Supplementary Table 12: SNPs with $P \leq 5 \times 10^{-5}$ for association with mean bilateral hippocampal volume in the analysis including patients correcting for Sex, Age, Age ² , Sex*Age, Sex* Age ² , MDS.....	69
Supplementary Table 13: SNPs with $P \leq 5 \times 10^{-5}$ for association with mean bilateral hippocampal volume in the analysis without patients correcting for Sex, Age, Age ² , Sex*Age, Sex* Age ² , MDS, TBV.....	72
Supplementary Table 14: SNPs with $P \leq 5 \times 10^{-5}$ for association with mean bilateral hippocampal volume in the analysis including patients correcting for Sex, Age, Age ² , Sex*Age, Sex* Age ² , MDS, TBV.....	74

Supplementary Table 15: SNPs with $P \leq 5 \times 10^{-5}$ for association with estimated total intracranial volume in the analysis without patients correcting for Sex, Age, Age ² , Sex*Age, Sex* Age ² , MDS	76
Supplementary Table 16: SNPs with $P \leq 5 \times 10^{-5}$ for association with total brain volume in the analysis without patients correcting for Sex, Age, Age ² , Sex*Age, Sex* Age ² , MDS	80
Supplementary Table 17: Non-significant replications for all phenotypes	84
Supplementary Table 18: Gene-based analysis of total brain volume without patients correcting for Sex, Age, Age ² , Sex*Age, Sex* Age ² , MDS	87
Supplementary Table 19: Gene-based analysis of total intracranial volume without patients correcting for Sex, Age, Age ² , Sex*Age, Sex* Age ² , MDS	88
Supplementary Table 20: Gene-based analysis of mean bilateral hippocampal volume including patients correcting for Sex, Age, Age ² , Sex*Age, Sex* Age ² , MDS	91
Supplementary Table 21: Gene-based analysis of mean bilateral hippocampal volume without patients correcting for Sex, Age, Age ² , Sex*Age, Sex* Age ² , MDS	94
Supplementary Table 22: Gene-based analysis of mean bilateral hippocampal volume including patients correcting for Sex, Age, Age ² , Sex*Age, Sex* Age ² , MDS, ICV	95
Supplementary Table 23: Gene-based analysis of mean bilateral hippocampal volume without patients correcting for Sex, Age, Age ² , Sex*Age, Sex* Age ² , MDS, ICV	97
Supplementary Table 24: Gene-based analysis of mean bilateral hippocampal volume including patients correcting for Sex, Age, Age ² , Sex*Age, Sex* Age ² , MDS, TBV	98
Supplementary Table 25: Gene-based analysis of mean bilateral hippocampal volume without patients correcting for Sex, Age, Age ² , Sex*Age, Sex* Age ² , MDS, TBV	100
Supplementary Table 26: Correlations between brain volume and intelligence measures	101
Supplementary Table 27: Location of Manhattan and QQ plots	102

Supplementary Table 1: Descriptions of genome-wide association study cohorts.

Study Name		Study Design (Diagnosis)*	Ancestry	All Subjects				Healthy Subjects Only			
Short	Full			N	Mean Age (s.d.)	Age Range	Number Females (%)	N**	Mean Age (s.d.)	Age Range	Number Females (%)
ADNI	Alzheimer's Disease Neuroimaging Initiative ¹	Case-control (AD, MCI, healthy elderly)	European	747	75.4 (6.8)	54.6-91.0	305 (40.8)	206	76.1 (5.0)	60.0-89.7	94 (45.6)
BFS	Bipolar Family Study ^{2,3}	Population-based	European	220	24.0 (7.7)	15-60	115 (52.3)	220	24.0 (7.7)	15-60	115 (52.3)
BIG	Brain Imaging Genetics Study ⁴	Population-based	European	927	22.8 (3.3)	18-35	547 (60.4)	926	22.8 (3.3)	18-35	547 (60.4)
fBIRN	Function Biomedical Informatics Research Network ^{5,6}	Case-control (SCZ, healthy)	European	78	38.0 (12.0)	20-65	27 (34.6)	39	38.0 (13.0)	20-65	15 (38.5)
IMAGEN	IMAGEN Consortium ⁷	Population-based	European	518	14.5 (0.4)	12.9-15.7	270 (52.1)	518	14.5 (0.4)	12.9-15.7	270 (52.1)
ImaGene	ImaGene	Case-control (MCI, healthy elderly)	European	104	70.6 (8.7)	51-88	49 (47.1)	48	69.5 (7.8)	51-86	21 (43.8)
LBC1936	Lothian Birth Cohort 1936 Study ⁸	Population-based birth cohort	European	249	72.7 (0.73)	71-74	115 (46.2)	249	72.7 (0.73)	71-74	115 (46.2)
MooDS	MooDS ⁹	Population-based	European	221	33.1 (10.0)	18-51	119 (53.8)	221	33.1 (10.0)	18-51	119 (53.8)
MPIP	Max Planck Institute of Psychiatry Munich Morphometry Sample ¹⁰	Case-control (Depression, healthy)	European	550	48.3 (13.3)	17.9-87.0	318 (57.8)	177	50.1 (12.3)	23.4-78.0	105 (59.3)
NCNG	Norwegian Cognitive Neurogenetics ¹¹	Population-based	European	327	50.4 (16.6)	19-79	223 (68.2)	327	50.4 (16.6)	19-79	223 (68.2)
QTIM	Queensland Twin Imaging Measures ¹²	Population-based twin study	European	485	23.7 (2.2)	20-30	307 (63.3)	485	23.7 (2.2)	20-30	307 (63.3)
SHIP	Study of Health in Pomerania ¹³	Population-based (Depression, bipolar disorder, anxiety and somatoform disorders, alcohol addiction, stroke, healthy)	European	800	56.9 (12.7)	30-88	425 (53.1)	313	58.5 (12.9)	31-88	140 (44.7)
SHIP-TREND	Study of Health in Pomerania - TREND ¹³	Population-based (Depression, alcohol addiction, stroke, healthy)	European	871	50.4 (13.6)	21-81	484 (55.6)	761	50.9 (13.8)	22-81	427 (56.1)
Super-Struct	Genomic SuperStructure	Population-based	European	442	21.4 (3.2)	18-35	251 (56.8)	442	21.4 (3.2)	18.0-35.0	251 (56.8)
SYS	Saguenay Youth Study ¹⁴	Founder population	European	558	14.6 (1.9)	11-18	298 (53.4)	558	14.6 (1.9)	11-18	298 (53.4)
TOP	Thematically Organized Psychosis Study ^{15,16}	Case-control (schizophrenia and bipolar spectrum disorder, healthy)	European	419	34.7 (10.0)	16-72	204 (48.7)	168	36.0 (9.8)	19-58	80 (47.6)
UMCU	UMC Utrecht	Case-control (SCZ, healthy)	European	279	31.9 (11.7)	17-68	73 (26.2)	117	32.9 (12.8)	17-65	44 (37.6)
Discovery Total				7795	39.9 (9.24)	11-91	4130 (53.0)	5775	34.8 (8.51)	11-90	3171 (54.9)

^{*}(AD-Alzheimer's; MCI-Mild Cognitive Impairment; SCZ-Schizophrenia)

Replication Cohorts											
BIG Replication	Brain Imaging Genetics Study ⁴ Replication sample	Population-based	European	911	28.9 (14.0)	18-82	479 (52.6)	911	28.9 (14.0)	18-82	479 (52.6)
CHARGE	Cohorts for Heart and Aging Research in Genomic Epidemiology ¹⁷	Population-based	European	10,779	67.9 (6.4)	Not available	6016 (55.8)	10,779	67.9 (6.4)	Not available	6016 (55.8)
EPIGEN	Epilepsy Genetics Consortium ¹⁸	Epilepsy patients	European	233	38.5 (12.7)	14-85	138 (59.2)	N/A	N/A	N/A	N/A
NESDA	Netherlands Study of Depression and Anxiety ^{19,20}	Case-control (Depression, Anxiety, healthy)	European	216	37.7 (9.9)	18-57	145 (67.1)	59	39.6 (9.3)	21-54	38 (64.4)
GOBS	Genetics of Brain Structure ²¹	Population-based extended pedigree	Mexican American	605	47.1 (13.4)	18-85	371 (61.3)	605	47.1 (13.4)	18-85	371 (61.3)
NIMH-IRP	National Institute of Mental Health Intramural Research Program ²²	Case-control (Depression, Anxiety, healthy)	European, African American	237	34.4 (10.4)	18-61	172 (66.7)	94	33.0 (9.8)	20-60	67 (69.1)
TCD/NUIG	Neuropsychiatric Genetics Group, Trinity College Dublin & Clinical Neuroimaging Laboratory, National University of Ireland – Galway	Case-control (schizophrenia, schizoaffective disorder, bipolar disorder, healthy)	European	375	36.6 (12.4)	18-75	167 (44.5)	166	33.4 (13.6)	18-75	90 (54.2)
Discovery + Replication Total				21,151				18,389			

** ICV and TBV were available for 2 participants in MPIP and 1 participant in the BIG cohort who did not have HV measures.

Supplementary Table 2: Summary of brain imaging and structure segmentation methods.

Study Name	Scanner	Scan Acquisition Protocol	Hippo Seg Software	Brain Vol Seg Software	ICV Software	All Subjects		
						Mean bilateral hippocampal volume (mm ³ ; s.d.)	Mean Brain Volume (mm ³ ; s.d.)	Mean ICV (mm ³ ; s.d.)
ADNI	57 1.5T scanners used	T ₁ -weighted MP-RAGE (details at http://adni.loni.ucla.edu/research/protocols/mri-protocols/)	FreeSurfer	FreeSurfer	FreeSurfer	3167.4 (583.7)	1,008,858 (110,372)	1,564,744 (172,466)
BFS	1.5T GE Signa Scanner	Coronal gradient echo sequence with magnetization preparation with 128 coronal high-resolution T ₁ -weighted images (TI=600 ms; TE=3.4 ms; flip angle=15°; FOV=22 cm; slice thickness=1.7 mm, matrix=256x192)	FSL FIRST	FSL FAST	FSL FLIRT	4016.1 (414.2)	1,283,340 (106,890)	1,561,470 (88,470)
BIG	1.5T and 3.0T Siemens	T ₁ -weighted MPRAGE with 3D magnetization prepared rapid acquisition gradient-echo, covering the entire brain; voxel size: 1x1x1 mm ³	FSL FIRST	SPM5	FSL FLIRT	3995.6 (392.7)	1,313,642 (118,331)	1,497,625 (150,143)
fBIRN	6 3.0T GE and Siemens	T ₁ -weighted MPRAGE sequence (image dimensions=256x256x176; voxel size=0.9375x0.9375x1.2 mm ³ sagittal; TR=2300ms; TE=2.31 ms; TI=800 ms; flip angle=9°; NEX=1)	FSL FIRST	FreeSurfer	FreeSurfer	4066.1 (506.3)	1,184,498 (179,924)	1,503,735 (260,985)
IMAGEN	3.0T Siemens, Philips, GE, and Bruker	T ₁ -weighted MPRAGE sequence based on the ADNI protocol (http://adni.loni.ucla.edu/research/protocols/mri-protocols/)	FreeSurfer	FreeSurfer	FreeSurfer	4396.4 (408.5)	1,256,392 (117,930)	1,521,065 (148,423)
ImaGene	1.5T Siemens Avanto	3D fast low-angle shot (FLASH) T ₁ magnetization prepared rapid acquisition gradient echo (MPRAGE) acquisition (TR=28 ms; TE=4.5 ms; FOV=22 cm; matrix=256x192; slice thickness=1.5 mm; no gap)	AdaBoost ²³	FSL FAST	MincTracc ²⁴	3418.7 (395.1)	1,103,614 (119,136)	1,485,844 (147,235)
LBC1936	1.5 T GE Signa Horizon HDX	T ₁ -weighted IR-Prep FSPGR coronal 3D volume (160 slices, voxel size=1x1x1.3 mm ³ , TR/TE/TI=10/4/500ms)	FSL FIRST w/ FSL SUSAN ²⁵	In-house software ²⁶	Analyze 9.0 Object Extraction Tool with hand editing	3768.8 (430.9)	1,127,018 (110,793)	1,453,137 (147,100)
MooDS	3T Siemens Trio at 3 sites	T ₁ -weighted MPRAGE fast field echo 3D sequence (TR=1570 ms; TE=2.75 ms; NEX=1; flip angle=15°; matrix size=256x256; FOV=256x256 mm ² ; slice thickness=1 mm) providing an isotropic voxel of volume=1 mm ³ . Sequences were identical for scanners in Bonn, Berlin and Mannheim. Three MPRAGE images were acquired and combined to create an average image using FreeSurfer.	FreeSurfer	FreeSurfer	FreeSurfer	4649.2 (426.0)	1,332,020 (139,295)	1,622,296 (177,161.9)
MPIP	1.5T GE Signa & 1.5T Siemens	#1: T ₁ -weighted SPGR sagittal 3D volume (TR=10.3 s; TE=3.4 ms; 124 slices, matrix size=256x256, FOV=23.0x23.0 cm ² , voxel size=0.8975x0.8975x[1.2-1.4] mm ³ , flip angle=90°, birdcage resonator) #2: same scanner as #1, platform update Signa Excite, sagittal T1-weighted (spin echo sequence, TR=9.7 ms, TE=2.1 ms, FOV=25.0x25.0 cm ² , voxel size=0.875x0.875x1.2 mm ³ , 124-132 slices, flip angle=90°) #3: Siemens 1.5 Tesla, Vario, 3D MPRAGE, TR=11.6 ms, TE=4.9 ms, FOV=23x23 cm ² , matrix=512x512, 126 axial slices, voxel size 0.45x0.45x1.5 mm ³). (only N=2 subjects)	FSL FIRST	FSL FAST	FSL FLIRT	3856.0 (385.8)	1,123,632 (117,975)	1,462,477 (146,702)

NCNG	1.5T Siemens Sonata and 1.5T Siemens Avanto	#1: A Siemens Sonata 1.5 Tesla scanner (Siemens, Erlangen, Germany) with a conventional head coil was used. Two 3D MP-RAGE T ₁ -weighted sequences (duration: 8 min 46 s) were run for all participants. Each volume consisted of 128 sagittal slices (1.33x1x1 mm ³), with an in-plane voxel size of 1 mm ³ (TR=2730 ms; TE=3.43 ms; TI=1000 ms; flip angle=7°; and 256x256 matrix). #2: A Siemens Avanto scanner was used to acquire two 3D MP-RAGE T ₁ -weighted sequences (TR/TE/TI/FA=2400 ms/3.61 ms/1000 ms/8°; matrix=192x192; duration 7 min and 42 s per volume). Each volume consisted of 160 sagittal slices (1.25x1.25x1.20 mm ³).	FreeSurfer	FreeSurfer	FreeSurfer	3627.5 (427.7)	1,083,142 (135,915)	1,553,755 (173,079)
QTIM	Bruker Medspec 4T	T ₁ -weighted images of the brain were acquired with an inversion recovery rapid gradient echo sequence on a 4 Tesla MRI scanner (Bruker Medspec; with acquisition parameters: TI/TR/TE=700/1500/3.35 ms; flip angle=8°; slice thickness=0.9 mm; matrix=256x256x256).	FSL FIRST	FSL FAST	FSL FLIRT	3554.5 (387.1)	1,231,509 (113,518)	1,616,246 (124,193)
SHIP	1.5T Siemens Avanto	3D T ₁ -weighted (MP-RAGE/ axial plane, TR=1900 ms, TE=3.4 ms, Flip angle=15°) brain MRI sequence was used to acquire images at an original resolution of 1.0 x 1.0 x 1.0 mm ³	FSL FIRST	FSL FAST	FSL FLIRT	3658.2 (435.2)	1,186,411 (117,404)	1,520,244 (154,126)
SHIP-TREND	1.5T Siemens Avanto	3D T ₁ -weighted (MP-RAGE/ axial plane, TR=1900 ms, TE=3.4 ms, Flip angle=15°) brain MRI sequence was used to acquire images at an original resolution of 1.0 x 1.0 x 1.0 mm ³	FSL FIRST	FSL FAST	FSL FLIRT	3713.3 (425.3)	1,199,986 (118,298)	1,522,781 (149,251)
Super-Struct	Siemens Magnetom TrioTim syngo MR B17	T ₁ -weighted MP-RAGE sequence (TR=2200 ms; TI=1100 ms; TE=1.54 ms for image 1 to 7.01 ms for image 4; flip angle=7°; voxel size=1.2x1.2x1.2 mm ³ and FOV=230 cm ² . This multi-echo MPRAGE allows increased contrast through weighted-averaging of the four derived images ²⁷	FreeSurfer	FreeSurfer	FreeSurfer	4519.4 (400.8)	1,248,001 (122,127)	1,575,464 (196,726)
SYS	Philips 1.0T Scanner	For each participant, T ₁ -weighted MR images of the brain were acquired on a Phillips 1.0T superconducting magnet using the following parameters (3D RF-SPGR with 140–160 slices, voxel size=1x1x1 mm ³ , TR=25 ms; TE=5 ms; flip angle=30°)	FreeSurfer	FreeSurfer	FreeSurfer	4298.0 (388.7)	1,294,084 (117,703)	1,608,457 (153,961)
TOP	1.5T Siemens Magnetom Sonata	All participants underwent MRI scanning on a 1.5T Siemens Magnetom Sonata scanner (Siemens Medical Solutions, Erlangen, Germany) equipped with a standard head coil. After a conventional three-plane localizer, two sagittal T ₁ -weighted MP-RAGE volumes were acquired with the Siemens tf3d1_ns pulse sequence (TE=3.93 ms; TR=2730 ms; TI=1000 ms; flip angle=7°; FOV=24 cm ² , voxel size=1.33x0.94x1 mm ³ , number of partitions=160). Acquisition parameters were optimized for increased gray-white matter image contrast. Patients and control subjects were scanned continuously throughout the 6-year period during which the data were collected, thus ensuring that there was no confounding effect of time. There was no scanner upgrade in this period.	FreeSurfer	FreeSurfer	FreeSurfer	4116.9 (387.4)	1,163,179 (132,391)	1,562,126 (179,017)
UMCU	1.5T Philips Gyroscan NT and Achieva	3D T ₁ -weighted coronal spoiled gradient echo scan (3D-FFE) (TE=4.6 ms, TR=30 ms, flip angle=30°; 170 contiguous 1.2 mm slices, in-plane voxel size=1x1 mm ²) and T ₂ -weighted turbo-spin-echo scan (DE-TSE) (TE1=14 ms, TE2=80 ms, TR=6350 ms, flip angle=90°, in-plane voxel size=.98x.98 mm ²).	FSL FIRST	In-house software ^{28,29}	Freesurfer	4852.4 (683.9)	1,282,064 (127,299)	1,635,440 (164,160)
BIG replication	1.5T and 3.0T Siemens	T ₁ -weighted MPRAGE with 3D magnetization prepared rapid acquisition gradient-echo, covering the entire brain; voxel size: 1x1x1 mm ³	FSL FIRST	SPM5	N/A	3964.8 (394.3)	1,288,900 (125,500)	N/A
CHARGE		See accompanying paper						

EPIGEN	GE Signa 1.5T and GE Signa 3.0T	UK: 3T GE Excite HDx scanner. All data were acquired using a body coil for transmission, and 8-channel phased array coil for reception. The protocol included a whole-brain T ₁ -weighted IR-prepared FSPGR scan with the following parameters: TR=8 ms, TE=3 ms, TI=450 ms, NEX=1; flip angle =20°; matrix 256×256, FOV=18×24 cm, thickness=1.1mm, providing a voxel resolution of 0.9375×0.9375×1.1 mm ³ . Ireland: 1.5T GE Signa scanner. A 3-D SPGR sequence was acquired from a sagittal localizer in the coronal plane. The following imaging parameters were used: TR=10.1 ms, TE=4.2 ms, TI=450 ms; NEX=1; flip angle=20.0°; FOV= 24×24 cm; matrix= 256×256, resulting in 124×1.5-mm-thick image slices. Belgium: 3D T ₁ -weighted images were acquired at Hôpital Erasme, Université Libre de Bruxelles, Brussels and University Hospital Leuven using 3.0T Philips scanners with the following parameters: Université Libre de Bruxelles (TR=9.84 ms; TE=4.6 ms; flip angle=8.0, 160 contiguous slices); University Hospital Leuven (TR=1950 ms; TE=3.93 ms; TI=800 ms; flip angle= 12; 144 contiguous slices).	FreeSurfer	FreeSurfer	FreeSurfer	4099.6 (728.4)	1,222,020 (146,290)	1,470,161 (211,520)
NESDA	3.0T Philips and 1.5T Siemens	Imaging data were acquired at the LUMC, AMC, VU, and UMCG, equipped with a SENSE-8 (LUMC and UMCG), SENSE-6 (AMC) and standard RF (VU) channel head coil. For each subject, anatomical images were obtained using a sagittal 3D gradient-echo T ₁ -weighted sequence for the Philips 3T scans (TR=9 ms; TE=3.5ms; matrix=256x256; voxel size=1x1x1mm ³ , 170 slices; duration=4.5min), for the 1.5T scans (matrix=256×256; TI=300 ms; TR=15 ms; TE=7 ms; flip angle=8°; voxel size=1x1x1.5 mm ³ , 160 slices).	FSL FIRST	FSL FAST	FSL FLIRT	3477.4 (405.8)	1,233,728 (126,813)	1,436,093 (204,117)
GOBS	3.0T Siemens Magnetom Trio	High-resolution, T ₁ -weighted, 3D Turbo-flash sequence with an adiabatic inversion contrast pulse with the following scan parameters: TR/TI/TE=2100/785/3.04 ms, flip angle=13°, voxel size (isotropic)=0.8 mm. Each subject was scanned 7 (seven) times, consecutively, using the same protocol, and a single image was obtained by linearly coregistering these images and computing the average, allowing improvement over the signal-to-noise ratio and reducing motion artifacts ³⁰	FreeSurfer	FreeSurfer	FreeSurfer	4117.1 (428.7)	1,124,001 (114,630)	1,425,401 (140,790)
NIMH-IRP	3.0T GE scanners	Three hardware combinations were used: #1: Images were acquired on one of two long-bore GE 3T MRI scanners maintained to be identical. A single channel head coil was used. Images were acquired using an MP-RAGE sequence optimized for gray/white matter contrast. #2: Images were acquired on one of two identical long-bore GE 3TMRI scanners maintained to be identical An 8 channel head coil was used, and an MPRAGE sequence (TE=2.7ms; TR=7.3ms; prep time=725 ms) #3: Images were acquired on a short bore GE 3T MRI scanner, using an 8 channel head coil and an IR prepared fSPGR sequence (TE=2.6 ms, TR=5.9 ms, TI=450 ms) For all images, reconstructed resolution was 256×256×124, with an image voxel size of 0.85×0.85×1.2mm ³ , with axial slices. Some images may vary slightly in values for TE and TR in both cases, the parameter was set by requesting the “minimum” allowable interval; images were acquired over 8 years and software upgrades may have altered these parameters slightly. Prep time or inversion time remained constant. Additional preprocessing steps: All images were processed with the MNI tool N3 intensity inhomogeneity correction using the following parameters: -stop 0.001 –iterations 100 –distance 50	FSL FIRST	N/A†	FSL FLIRT	3713.9 (401.9)	N/A†	1,449,390 (150,004)
TCD/NUIG	1.5T Siemens Magnetom & 3.0T Philips Intera	1.5T: T ₁ -weighted MP-RAGE (TE=4.38 ms, TR=1140 ms, Flip angle=15°, FOV=230 cm ² , Matrix=512×512 (k-space interpolation from 256×256), 160 slices; slice thickness=0.9 mm, Voxel-size=0.45×0.45×0.9 mm ³ . 3.0T: T ₁ -weighted TFE gradient echo (TE=3.8 ms, TR=8.4 ms, Flip angle=8°, FOV=230 cm ² , Matrix=256×256, 180 slices; slice thickness=0.9 mm; Voxel-size=0.9×0.9×0.9 mm ³ .	FSL FIRST	FSL FAST	FSL FLIRT	3813.9 (407.62)	1,120,763 (102,216)	1,465,059 (133,467)

† NIMH-IRP: Brain volume was not measured due to the large number of images in the set missing either the superior aspect of the brain, or part of the cerebellum, which would invalidate this measurement.

Supplementary Table 3: Information on genotyping methods.

Study Name	Genotyping				Imputation		Association	
	Platform	SNPs removed			Imputation Software	Reference Panel	Software	Total SNPs after exclusion
		HWE threshold (P -value)	MAF threshold	Call rate threshold				
ADNI	Illumina Human610-Quad BeadChip	1×10^{-6}	0.01	95%	MACH	CEU+TSI	mach2qt1	1,181,919
BFS	Illumina OmniExpress	1×10^{-6}	0.01	95%	MACH	CEU	mach2qt1	1,174,126
BIG	Affymetrix Genome-Wide Human SNP Array 6.0	1×10^{-6}	0.05	95%	MINIMAC	CEU	mach2qt1	1,093,138
fBIRN	Illumina Infinium HumanHap370 Bead Arrays	1×10^{-6}	0.01	95%	MACH	CEU+TSI	mach2qt1	1,093,524
IMAGEN	Illumina Human660W	1×10^{-6}	0.01	95%	MACH	CEU	mach2qt1	1,181,258
ImaGene	Illumina Human Omni1-Quad	1×10^{-6}	0.01	95%	MINIMAC	CEU	mach2qt1	1,159,848
LBC1936	Illumina Human 610 Quadv1	1×10^{-6}	0.01	98%	MACH	CEU	mach2qt1	1,176,584
MooDS	Illumina Human610-Quad, Illumina Human660W-Quad	1×10^{-6}	0.01	95%	MACH	CEU+TSI	mach2qt1	1,166,431
MPIP	Illumina 100K, Illumina 300K, Illumina 550K, Illumina 610K, Illumina 660K	1×10^{-6}	0.01	95%	MACH	CEU	mach2qt1	1,162,033
NCNG	Illumina 610K	1×10^{-6}	0.01	95%	MACH	CEU	mach2qt1	1,174,060
QTIM	Illumina 610K	1×10^{-6}	0.01	95%	MACH	CEU+TSI	Merlin-offline	1,176,729
SHIP	Affymetrix Human SNP Array 6.0	1×10^{-6}	0.01	80%	IMPUTE	CEU (1000G)*	QUICKTEST	1,136,631
SHIP-TREND	Illumina Human Omni 2.5M	1×10^{-6}	0.01	95%	IMPUTE	CEU (HM II)*	QUICKTEST	968,478
Super-Struct	Illumina HumanOmni1-Quad	1×10^{-6}	0.01	95%	BEAGLE	CEU	Plink	1,030,698
SYS	Human610W-Quad Illumina BeadChip	1×10^{-6}	0.01	95%	IMPUTE	CEU (1000G)*	ProbABEL	1,187,650
TOP	Affymetrix Genome-Wide SNP Array 6.0	1×10^{-6}	0.01	95%	MACH	CEU	mach2qt1	1,168,320
UMCU	Illumina 550K	1×10^{-6}	0.05	95%	BEAGLE	CEU	Plink	1,222,157
BIG Replication	TaqMan Assay	N/A	N/A	N/A	N/A	N/A	N/A	2
CHARGE	See accompanying paper							
EPIGEN	Illumina 610quad; Illumina550kv3	1×10^{-6}	0.01	95%	MINIMAC	CEU	mach2qt1	1,169,186
NESDA	Affymetrix Human SNP Array 5.0 / Perlegen 600K/ Affymetrix Human SNP Array 6.0 907K	1×10^{-6}	0.01	95%	IMPUTE	CEU	Plink	1,342,269
GOBS	Illumina 550K combined with 510S, Illumina Human1M, and Illumina Huan1M-Duo	1×10^{-6}	0.01	95%	MACH	MEX	SOLAR	1,211,482
NIMH-IRP	Illumina 610K	1×10^{-6}	0.01	95%	BEAGLE	CEU+YRI	mach2qt1	1,201,577
TCD/NUIG	TaqMan Assay	N/A	N/A	N/A	N/A	N/A	N/A	6

*Note: SHIP-TREND imputed to HapMap I+II r22b36 CEU reference panel. SYS imputed to the CEU panel of the June 2010 b36 release of the 1000 Genomes Project using the CEU reference panel. Only SNPs that passed quality control and were present in HapMap III and enumerated in the “Total SNPs after exclusion” column.

Supplementary Table 4: The correlation between FSL-derived and FreeSurfer-derived phenotypic measures.

Select sites compared phenotypic measures derived from the two software packages, FSL and FreeSurfer, on the same subjects. These were generally computed on a subset of the full sample, and some added additional images from subjects who lacked genotyping but had been scanned in the same way. This allowed correlations between software packages to be computed in a sample of unprecedented size. The overall correlation achieved across sites was computed using a weighted average of Z scores, after Fisher transformation. The correlation between software programs is comparable to human inter-rater variability (ICC=0.73-0.85^{31,32}) which is arguably a reasonable upper bound on the accuracy of automated segmentation.

Study Name	Hippocampus		Brain Volume		ICV	
	r	N	r	N	r	N
ADNI	0.87	657	0.67	657	0.94	657
BFS	0.84	215	0.84	215	0.82	215
BIG	0.72	2180	0.97	927	0.72	927
fBIRN	0.70	78	0.75	78	0.87	78
IMAGEN	0.72	518	0.93	518	0.91	518
MooDS	0.72	137	N/A	N/A	N/A	N/A
NCNG	0.63	327	0.96	327	0.97	327
QTIM	0.71	386	0.93	386	0.73	386
SHIP	0.86	24	0.96	24	0.93	24
SHIP-TREND	0.68	24	0.98	24	0.91	24
TOP	0.71	419	0.97	419	0.94	419
UMCU	0.61	181	N/A	N/A	N/A	N/A
EPIGEN	0.78	203	N/A	N/A	N/A	N/A
GOBS	0.76	724	0.99	726	0.94	726
NIMH-IRP	0.53	20	0.91	20	0.94	20
COMBINED	0.75	6093	0.95	4321	0.90	4321

Supplementary Table 5: The pairwise correlations between average bilateral hippocampal volume, total brain volume, and ICV.

Phenotypes were segmented using the software defined in **Supplementary Table 2**.

Study Name	Hippocampus-ICV	Hippocampus-TBV	ICV -TBV	N
ADNI	0.32	0.59	0.81	747
BFS	0.38	0.19	0.76	220
BIG	0.60	0.56	0.78	927
fBIRN	0.59	0.59	0.83	78
IMAGEN	0.61	0.70	0.88	518
ImaGene	0.44	0.52	0.77	104
LBC1936	0.48	0.45	0.87	249
MooDS	0.11	0.07	0.89	137
MPIP	0.65	0.68	0.91	550
NCNG	0.48	0.77	0.79	327
QTIM	0.39	0.41	0.74	485
SHIP	0.49	0.57	0.90	800
SHIP-TREND	0.47	0.53	0.91	871
SuperStruct	0.67	0.74	0.88	442
SYS	0.43	0.49	0.88	558
TOP	0.58	0.68	0.86	419
UMCU	0.31	0.19	0.82	279
EPIGEN	0.48	0.61	0.77	233
NESDA	0.12	N/A	N/A	216
TCD/NUIG	0.54	N/A	N/A	375
GOBS	0.60	0.72	0.85	724
NIMH-IRP	0.54	N/A	N/A	237
COMBINED	0.50	0.58	0.85	9496

Supplementary Table 6: Simulation to determine effect of QC thresholds and reference panels on imputation accuracy.

To examine potential effects of differences in QC thresholds and imputation reference sets, we performed a series of simulations. Using the chromosome 1 data from 250 unrelated QTIM participants, we randomly excluded 2,500 genotyped SNPs, which were present in the HapMap 2 and 3 reference sets and the Illumina 610 quad chip. We then applied 5 different combinations of call rate and MAF QC thresholds. These 5 cleaned data sets were then phased using Mach and imputed using Minimac using 3 different reference sets (HapMap2 CEU, HapMap3 CEU and HapMap3 CEU+TSI). Following imputation, SNPs were cleaned using a MAF threshold of 0.01 and an imputation accuracy (Rsq) threshold of 0.3, with 2,444 SNPs surviving QC. The imputed genotypes were binned to create hard-call genotypes, which were then compared with the original typed genotypes to calculate concordance. As may be expected, concordance rate showed a linear relationship with Rsq. However, there was no relationship between MAF and concordance, nor the inter-marker distance surrounding the excluded SNP and concordance. In addition, there were only minor fluctuations in concordance across QC thresholds or choice of reference set suggesting that the minor variation in protocols between sites would not have resulted in meaningful differences in imputation accuracy.

Concordance (%) between imputed and typed genotypes by MAF, Rsq and inter-marker distance, by QC thresholds and imputation reference sets.

	MAF				Rsq				Inter-marker Distance (BP)			
	0-05	.05-.1	.1-.2	.2-.5	.3-.4	.4-.6	.6-.8	.8-1	0-5462	5462-10465	10465-18538	18538-385363
N (SNPs)	78	190	565	1611	7	81	204	2152	612	611	610	611
<i>Call Rate 90% & MAF .01</i>												
HapMap2 CEU	99.0	98.0	96.7	95.3	68.9	77.1	88.5	97.5	95.9	96.0	95.9	96.1
HapMap3 CEU	99.3	98.4	97.6	94.5	69.7	78.6	90.0	96.9	96.0	95.5	95.4	95.6
HapMap3 CEU TSI	99.3	98.5	97.8	94.0	69.7	78.7	89.8	96.6	95.1	95.3	95.6	95.5
<i>Call Rate 95% & MAF .01</i>												
HapMap2 CEU	99.0	98.0	96.7	95.2	69.1	77.0	88.2	97.4	95.8	96.0	95.8	96.0
HapMap3 CEU	99.3	98.4	97.6	94.4	70.0	78.5	89.9	96.9	96.0	95.5	95.4	95.6
HapMap3 CEU TSI	99.3	98.5	97.8	93.9	69.6	78.4	89.8	96.6	95.0	95.3	95.6	95.6
<i>Call Rate 99% & MAF .01</i>												
HapMap2 CEU	99.0	98.0	96.7	95.2	68.8	76.8	88.3	97.4	95.8	95.9	95.8	95.9
HapMap3 CEU	99.2	98.5	97.5	94.4	69.4	78.4	89.8	96.9	95.9	95.5	95.3	95.6
HapMap3 CEU TSI	99.3	98.5	97.7	93.9	69.8	78.5	89.5	96.6	94.9	95.3	95.6	95.5
<i>Call Rate 95% & MAF .05</i>												
HapMap2 CEU	98.7	98.0	96.7	95.3	69.5	77.0	88.2	97.4	95.9	96.0	95.8	96.0
HapMap3 CEU	99.2	98.4	97.6	94.4	69.1	78.5	89.9	96.9	96.0	95.5	95.4	95.6
HapMap3 CEU TSI	99.2	98.5	97.8	94.0	69.4	78.6	89.8	96.6	95.0	95.3	95.7	95.5
<i>Call Rate 95% & MAF .1</i>												
HapMap2 CEU	98.4	97.1	96.4	95.0	68.6	75.3	87.2	97.2	95.5	95.6	95.5	95.7
HapMap3 CEU	98.9	97.8	97.3	94.2	69.2	77.0	89.0	96.7	95.7	95.1	95.1	95.3
HapMap3 CEU TSI	98.9	97.9	97.5	93.7	70.8	76.9	88.8	96.4	94.8	95.0	95.4	95.2

Supplementary Table 7: The association of genetic variants previously identified in the literature as having relevance to the hippocampal structure.

Summary statistics are shown for the average bilateral hippocampal volume controlling for estimated intracranial volume including (N=7795) and excluding patient samples (N=5776). *P*-values are double genome controlled. Strong heterogeneity *P*-values are observed for the TOMM40 locus largely due to the significance of this SNP in the ADNI sample (see **Supplementary Figure 11**). A SNP within PICALM which is associated with Alzheimer's disease has a nominally significant association to hippocampal volume. If the direct candidate SNP was not found in HapMap3, a proxy was used with r^2 from the 1000 Genomes Project Pilot 1 CEU sample.

Gene	SNP (proxy)	A1	A2	Freq	Beta	SE	P-value	Het. P-value
Full Discovery sample – including patients								
BDNF	rs6265	T	C	0.191	-0.280	7.193	0.969	0.375
TOMM40	rs2075650	A	G	0.832	17.657	8.348	0.034	2.31×10^{-5}
CLU	rs11136000	T	C	0.399	6.173	5.791	0.287	0.186
PICALM	rs3851179	T	C	0.361	10.192	5.803	0.079	0.035
ZNF804A	rs1344706	A	C	0.584	5.555	5.639	0.325	0.908
COMT	rs4680	A	G	0.532	-7.045	5.637	0.211	0.827
	rs821616							
DISC1	(rs1754606 $r^2=1.00$)	T	C	0.718	0.465	6.204	0.940	0.240
	rs35753505							
NRG1	(rs12681411 $r^2=0.835$)	C	G	0.638	-2.870	6.065	0.636	0.116
DTNBP1	rs1011313	T	C	0.093	-7.900	9.703	0.416	0.832
	rs1018381							
DTNBP1	(rs875463 $r^2=1.00$)	A	C	0.080	-1.491	10.054	0.882	0.431
Excluding patients								
BDNF	rs6265	T	C	0.192	1.129	7.948	0.887	0.435
TOMM40	rs2075650	A	G	0.835	-4.075	9.338	0.663	0.358
CLU	rs11136000	T	C	0.401	3.033	6.414	0.636	0.218
PICALM	rs3851179	T	C	0.362	14.019	6.454	0.030	0.234
ZNF804A	rs1344706	A	C	0.585	4.055	6.272	0.518	0.568
COMT	rs4680	A	G	0.531	-8.094	6.309	0.200	0.089
	rs821616							
DISC1	(rs1754606 $r^2=1.00$)	T	C	0.722	6.137	6.877	0.372	0.546
	rs35753505							
NRG1	(rs12681411 $r^2=0.835$)	C	G	0.635	-4.569	6.755	0.499	0.378
DTNBP1	rs1011313	T	C	0.093	-2.044	10.700	0.849	0.547
	rs1018381							
DTNBP1	(rs875463 $r^2=1.00$)	A	C	0.081	-3.266	11.000	0.767	0.226

Supplementary Table 8: Affect on hippocampal volume of genetic variants associated with schizophrenia and bipolar disorder.

SNPs here were chosen based on two recent genome-wide association studies^{33,34}. Summary statistics are shown for the average bilateral hippocampal volume controlling for estimated intracranial volume including (N=7795) and excluding patient samples (N=5776). P-values are double genome controlled.

Disease	Gene	SNP	A1	A2	Freq	Beta	SE	P-value	Het. P-value
Full Discovery sample – including patients									
SCZ	MIR137	rs1625579	T	G	0.8127	-5.1455	7.0213	0.4636	0.8456
SCZ	PCGEM1	rs17662626	A	G	0.9143	4.7751	11.0873	0.6667	0.8981
SCZ	TRIM26	rs2021722	T	C	0.201	-8.6729	6.7959	0.2019	0.7051
SCZ	CSMD1	rs10503253	A	C	0.2033	-4.4359	6.6635	0.5056	0.2557
SCZ	MMP16	rs7004633	A	G	0.8108	8.5453	6.8828	0.2144	0.5218
SCZ	CNNM2	rs7914558	A	G	0.4013	-0.8133	5.4035	0.8804	0.8755
SCZ	NT5C2	rs11191580	T	C	0.9064	-5.6573	10.0856	0.5748	0.2173
SCZ	STT3A	rs548181	A	G	0.12	-3.149	8.3354	0.7056	0.5198
SCZ	CCDC68	rs12966547	A	G	0.4141	-1.45	5.3787	0.7875	0.4639
SCZ	TCF4	rs17512836	T	C	0.974	8.929	18.2013	0.6237	0.7804
BPD	ANK3	rs10994397	T	C	0.0735	0.6532	10.5971	0.9509	0.9229
BPD	SYNE1	rs9371601	T	G	0.3553	1.5089	5.6564	0.7897	0.8723
BPD	Many	rs7296288	A	C	0.5197	-1.656	5.7325	0.7727	0.02708
BPD	ODZ4	rs12576775	A	G	0.8354	-14.1551	7.1784	0.04862	0.4596
Excluding patients									
SCZ	MIR137	rs1625579	T	G	0.8165	-4.3001	7.8458	0.5836	0.6714
SCZ	PCGEM1	rs17662626	A	G	0.9143	9.9163	12.2411	0.4179	0.7109
SCZ	TRIM26	rs2021722	T	C	0.2008	-12.5489	7.5836	0.09798	0.5419
SCZ	CSMD1	rs10503253	A	C	0.2028	-4.2484	7.4504	0.5685	0.01018
SCZ	MMP16	rs7004633	A	G	0.8106	8.092	7.6541	0.2904	0.4023
SCZ	CNNM2	rs7914558	A	G	0.3973	-1.6252	6.039	0.7878	0.7901
SCZ	NT5C2	rs11191580	T	C	0.9074	-4.7374	11.4429	0.6789	0.3203
SCZ	STT3A	rs548181	A	G	0.1205	-7.8208	9.2638	0.3985	0.8351
SCZ	CCDC68	rs12966547	A	G	0.4162	-3.6666	5.9964	0.5409	0.1119
SCZ	TCF4	rs17512836	T	C	0.9739	14.8832	20.4109	0.4659	0.7819
BPD	ANK3	rs10994397	T	C	0.0718	-0.3523	11.7805	0.9761	0.7299
BPD	SYNE1	rs9371601	T	G	0.3547	5.0674	6.3257	0.4231	0.8089
BPD	Many	rs7296288	A	C	0.5201	5.4522	6.2282	0.3814	0.4013
BPD	ODZ4	rs12576775	A	G	0.8341	-12.5538	7.9696	0.1152	0.3706

Supplementary Table 9: SNPs with $P \leq 5 \times 10^{-5}$ for association with mean bilateral hippocampal volume in the analysis without patients correcting for Sex, Age, Age², Sex*Age, Sex* Age², MDS components, ICV.

SNP	Chr	Position	Effect Allele	Non-Effect Allele	Freq. Effect Allele	Effect	SE	P*	Gene	Feature**	Cons Score ***	Selection Score****		
												CHB/JPT	CEU	YRI
rs2564447	11	44530550	A	C	0.6522	36.27	7.382	8.96×10^{-7}	-	-	0.002	-	-	-
rs1456520	2	199772591	T	C	0.9517	-78.7464	16.6398	2.22×10^{-6}	-	-	0.14	-	-	0.283
rs13394815	2	70564002	A	C	0.2763	-36.8237	7.805	2.38×10^{-6}	BRD7P6	-	0.001	-	-	-
rs1495716	4	176728576	T	C	0.6235	29.475	6.5037	5.84×10^{-6}	GPM6A	intron	0.543	-	1.277	0.755
rs10848088	12	130849993	A	G	0.3505	30.6581	6.8003	6.53×10^{-6}	PIWIL1	-	0.002	-	-	0.274
rs16869805	5	90817701	T	C	0.3094	-32.7967	7.4165	9.77×10^{-6}	-	-	0.031	-	-	-
rs12569261	1	206727260	A	G	0.7736	32.1024	7.3024	1.10×10^{-5}	RASSF5	intron	0.022	1.407	1.446	-
rs4617771	14	25529773	A	G	0.1501	-38.6209	8.8643	1.32×10^{-5}	STXBP6	-	0.099	-	-	-
rs4557104	3	65232772	A	G	0.4834	27.8709	6.4036	1.35×10^{-5}	-	-	0.063	-	-	-
rs6445523	3	65966296	T	G	0.1316	-39.8694	9.1996	1.47×10^{-5}	MAGI1	intron	0.001	0.647	0.721	0.264
rs11811181	1	206724737	A	G	0.2437	-32.1416	7.4965	1.81×10^{-5}	RASSF5	intron	0	0.958	1.157	-
rs2210517	1	206729593	A	G	0.2452	-33.2043	7.7939	2.04×10^{-5}	RASSF5	intron	0.053	-	-	-
rs4870409	6	156300315	A	C	0.7886	35.2256	8.285	2.12×10^{-5}	-	-	0.012	-	-	-
rs9318486	13	78067058	T	G	0.1838	38.1275	8.974	2.15×10^{-5}	-	-	0.155	-	-	-
rs10951458	7	36170199	A	G	0.4727	26.5755	6.2595	2.18×10^{-5}	LOC100421531	-	0.021	-	0.847	1.811
rs6466626	7	117482870	A	C	0.4965	-30.1249	7.1012	2.21×10^{-5}	CTTNBP2	intron	0.777	-	0.788	-
rs13316093	3	21654425	T	C	0.5478	27.0033	6.3852	2.35×10^{-5}	ZNF385D	intron	0.114	0.684	0.96	2.93
rs17078679	13	85456392	A	G	0.9411	-55.9645	13.2854	2.53×10^{-5}	-	-	0.024	0.576	1.88	0.675
rs7237436	18	55425144	A	G	0.2737	-33.2782	7.9191	2.64×10^{-5}	ATP8B1	intron	0.133	-	-	-
rs3782291	12	26555558	T	C	0.0862	53.9209	12.8435	2.69×10^{-5}	ITPR2	intron near-gene-5	0.019	-	-	-
rs7315280	12	117320938	A	G	0.8807	-40.5934	9.6989	2.85×10^{-5}	HRK	-	0.756	-	-	-
rs1378168	3	16024923	A	G	0.7054	29.1422	6.997	3.11×10^{-5}	-	-	0.004	-	-	-
rs1874521	12	130839645	A	C	0.3829	27.337	6.6017	3.46×10^{-5}	PIWIL1	-	0.022	1.726	0.724	-
rs2622524	17	33595842	T	G	0.4354	-26.2375	6.3368	3.47×10^{-5}	SLFN5	-	0.093	0.229	0.536	-
rs7132910	12	117320658	T	C	0.8733	-39.6359	9.5804	3.52×10^{-5}	HRK	near-gene-5	0.035	-	-	-
rs394499	14	90002148	A	G	0.6222	27.2972	6.6106	3.64×10^{-5}	FOXN3	intron	0.86	-	-	0.432
rs10038508	5	90797244	A	G	0.2717	-31.9773	7.7519	3.71×10^{-5}	-	-	0.015	0.004	-	-

SNP	Chr	Position	Effect Allele	Non-Effect Allele	Freq. Effect Allele	Effect	SE	P*	Gene	Feature**	Cons Score ***	Selection Score****		
												CHB/JPT	CEU	YRI
rs6030453	20	41369963	T	C	0.7129	29.8941	7.2778	4.00x10 ⁻⁵	PTPRT	intron	0.001	-	-	0.851
rs820144	17	73611823	T	C	0.6449	-30.7489	7.4946	4.08x10 ⁻⁵	MYO15B	-	0.113	-	-	1.605
rs7614137	3	81283747	A	T	0.633	28.2445	6.8895	4.14x10 ⁻⁵	-	-	0.004	0.763	-	-
rs4444253	14	25576986	T	C	0.149	-39.0812	9.5617	4.37x10 ⁻⁵	-	-	0.068	-	-	-
rs9895813	17	53743722	C	G	0.9687	-85.3262	20.8981	4.45x10 ⁻⁵	-	-	0.009	1.526	-	1.418
rs6923338	6	52549322	T	C	0.6102	-32.1684	7.8848	4.51x10 ⁻⁵	LOC730101	-	0.185	-	-	-
rs7630516	3	81297288	A	T	0.3194	-30.2926	7.4254	4.51x10 ⁻⁵	-	-	0	1.276	0.458	0.067

* P-values are double genome controlled. **SNP features from dbSNP (<http://www.ncbi.nlm.nih.gov/SNP/>); ***PhastCons Conservation score from UCSC Genome Browser: probability that each nucleotide belongs to a conserved element (<http://hgdownload.cse.ucsc.edu/>) ; ****Positive selection scores of SNPs from <http://haplotter.uchicago.edu/>.

Supplementary Table 10: SNPs with $P \leq 5 \times 10^{-5}$ for association with mean bilateral hippocampal volume in the analysis including patients correcting for Sex, Age, Age², Sex*Age, Sex* Age², MDS, ICV.

SNP	Chr	Position	Effect Allele	Non-Effect Allele	Freq. Effect Allele	Effect	SE	P*	Gene	Feature**	Cons Score ***	Selection Score****		
												CHB/JPT	CEU	YRI
rs7315280	12	117320938	A	G	0.8793	-46.1103	8.7564	1.40×10^{-7}	HRK	near-gene-5 near-gene-5	0.756	-	-	-
rs7132910	12	117320658	T	C	0.8718	-44.96	8.6394	1.95×10^{-7}	HRK	-	0.035	-	-	-
rs7294919	12	117327592	T	C	0.8958	-50.2715	9.7355	2.42×10^{-7}	HRK	-	0.01	0.065	1.167	0.227
rs13394815	2	70564002	A	C	0.2755	-34.4158	7.0143	9.27×10^{-7}	BRD7P6	-	0.001	-	-	-
rs7132339	12	117335912	A	G	0.1071	46.4996	10.1745	4.87×10^{-6}	HRK	-	0	0.718	-	0.493
rs4110517	10	96650328	A	G	0.2278	31.2259	6.9177	6.37×10^{-6}	RPL7AP52	-	0.035	-	-	-
rs9888067	10	96648224	T	G	0.2171	30.8767	6.869	6.96×10^{-6}	RPL7AP52	-	0.004	-	-	-
rs752834	2	111798658	A	G	0.1923	-31.7784	7.2097	1.05×10^{-5}	ACOXL	intron	0.004	-	-	-
rs17549227	2	111796195	T	C	0.8013	31.4259	7.1335	1.06×10^{-5}	ACOXL	intron	0.116	-	-	-
rs7614137	3	81283747	A	T	0.6449	26.989	6.1559	1.16×10^{-5}	-	-	0.004	0.763	-	-
rs1456520	2	199772591	T	C	0.9536	-67.1596	15.3969	1.29×10^{-5}	-	-	0.14	-	-	0.283
rs17483466	2	111797458	A	G	0.8016	31.1168	7.1399	1.31×10^{-5}	ACOXL	intron	0.009	-	-	-
rs1052826	20	61576777	A	G	0.7758	-29.2323	6.7239	1.38×10^{-5}	C20orf11	utr-3	0.005	-	-	-
rs754352	2	111797920	A	G	0.8104	31.1587	7.1725	1.40×10^{-5}	ACOXL	intron	0.021	-	-	-
rs11898094	2	227924774	T	C	0.132	38.7868	8.995	1.62×10^{-5}	COL4A4	intron	0.001	-	-	-
rs17580572	6	16153962	A	G	0.1925	32.7619	7.6038	1.64×10^{-5}	MYLIP	-	0.164	0.411	1.172	0.739
rs16875511	5	5385388	T	C	0.9533	69.5733	16.2468	1.85×10^{-5}	LOC442131	-	0.695	0.231	-	-
rs10848088	12	130849993	A	G	0.3454	26.2829	6.141	1.87×10^{-5}	PIWIL1	-	0.002	-	-	0.274
rs4617771	14	25529773	A	G	0.1478	-34.4344	8.0802	2.03×10^{-5}	STXBP6	-	0.099	-	-	-
rs17078679	13	85456392	A	G	0.9419	-51.4026	12.0862	2.11×10^{-5}	-	-	0.024	0.576	1.88	0.675
rs6751950	2	70560939	T	C	0.1977	-30.9014	7.2753	2.16×10^{-5}	BRD7P6	-	0.087	2.038	0.705	1.91
rs271646	17	48000146	T	G	0.2048	-30.5146	7.1896	2.19×10^{-5}	LOC124865	-	0.182	0.673	0.564	1.867
rs1487111	3	81296550	A	G	0.6289	26.2888	6.2211	2.38×10^{-5}	-	-	0.025	0.699	-	-
rs7574757	2	227943480	T	C	0.1192	37.9088	8.9798	2.43×10^{-5}	COL4A4	intron	0.01	-	-	0.384
rs10762029	10	67974293	T	C	0.4963	25.1324	5.9664	2.53×10^{-5}	CTNNA3	intron	0.006	-	-	1.224
rs619140	16	9399292	T	C	0.1918	-29.5604	7.0589	2.82×10^{-5}	-	-	0	-	-	-
rs468648	5	75996865	A	G	0.9242	45.2614	10.8101	2.83×10^{-5}	IQGAP2	intron	0.054	-	-	0.027

SNP	Chr	Position	Effect Allele	Non-Effect Allele	Freq. Effect Allele	Effect	SE	P*	Gene	Feature**	Cons Score ***	Selection Score****		
												CHB/JPT	CEU	YRI
rs271653	17	48005880	T	C	0.2001	-29.4851	7.0481	2.87x10 ⁻⁵	LOC124865	-	0.017	0.295	0.729	1.612
rs17697039	2	57022855	T	C	0.9567	67.2698	16.1914	3.26x10 ⁻⁵	-	-	0.015	-	-	-
rs2276775	3	122646734	T	C	0.1035	37.8523	9.1564	3.57x10 ⁻⁵	SEMA5B	Coding-synonymous intron; miRNA binding site	0.306	0.288	-	-
rs4953342	2	46552047	A	G	0.7047	26.8574	6.5018	3.62x10 ⁻⁵	EPAS1	-	0.467	-	-	0.282
rs7556828	2	46663172	A	G	0.4424	23.1544	5.6284	3.89x10 ⁻⁵	-	-	0.006	-	-	-
rs10147732	14	76949292	T	C	0.0773	46.3262	11.288	4.06x10 ⁻⁵	ESRRB	Intron	0.002	-	-	-
rs9398455	6	98015352	A	G	0.0893	41.0003	10.0132	4.23x10 ⁻⁵	-	-	0.992	-	1.409	-
rs4759277	12	57533690	A	C	0.3588	-24.6121	6.0145	4.27x10 ⁻⁵	LRP1	Intron	0.028	-	1.538	0.364
rs4557104	3	65232772	A	G	0.4883	23.3827	5.723	4.39x10 ⁻⁵	-	-	0.063	-	-	-
rs1839259	16	77650847	C	G	0.458	23.0264	5.6435	4.50x10 ⁻⁵	-	-	0	2.837	1.843	0.414
rs12698902	7	69837319	A	G	0.7234	-25.8243	6.3321	4.54x10 ⁻⁵	AUTS2	Intron	0.006	-	-	-
rs7850989	9	14541236	T	C	0.8322	31.4844	7.7237	4.58x10 ⁻⁵	-	-	0.001	-	0.609	0.657
rs7922133	10	78784075	T	C	0.6809	-24.7588	6.0747	4.59x10 ⁻⁵	KCNMA1	intron	0.313	-	-	-
rs703817	12	57489828	T	C	0.4932	-22.9287	5.6359	4.74x10 ⁻⁵	STAT6	utr-3	0.026	0.489	-	0.429
rs7630516	3	81297288	A	T	0.3003	-27.1277	6.6694	4.75x10 ⁻⁵	-	-	0	1.276	0.458	0.067
rs7628478	3	81293381	A	C	0.6377	26.758	6.5841	4.82x10 ⁻⁵	-	-	0.003	0.62	-	-
rs1530628	2	46670941	T	C	0.5511	-23.0828	5.6899	4.98x10 ⁻⁵	-	-	0.011	0.226	0.56	1.146

* P-values are double genome controlled. **SNP features from dbSNP (<http://www.ncbi.nlm.nih.gov/SNP/>); ***PhastCons Conservation score from UCSC Genome Browser: probability that each nucleotide belongs to a conserved element (<http://hgdownload.cse.ucsc.edu/>) ; ****Positive selection scores of SNPs from <http://haplotter.uchicago.edu/>.

Supplementary Table 11: SNPs with $P \leq 5 \times 10^{-5}$ for association with mean bilateral hippocampal volume in the analysis without patients correcting for Sex, Age, Age², Sex*Age, Sex* Age², MDS.

SNP	Chr	Position	Effect Allele	Non-Effect Allele	Freq. Effect Allele	Effect	SE	P*	Gene	Feature**	Cons Score***	Selection Score****		
												CHB/JPT	CEU	YRI
rs16869805	5	90817701	T	C	0.3073	-38.6551	8.1171	1.92×10^{-6}	-	-	0.031	-	-	-
rs10951458	7	36170199	A	G	0.4724	32.8475	6.9392	2.21×10^{-6}	LOC100421531	-	0.021	-	0.847	1.811
rs9318486	13	78067058	T	G	0.1908	45.9235	9.9316	3.77×10^{-6}	-	-	0.155	-	-	-
rs2906457	1	44338575	A	C	0.262	-34.8558	7.8849	9.84×10^{-6}	ST3GAL3	intron	0.003	-	-	-
rs1917330	4	58186260	A	G	0.043	-84.903	19.3113	1.10×10^{-5}	-	-	0.014	-	-	-
rs10038508	5	90797244	A	G	0.2761	-37.0422	8.4359	1.13×10^{-5}	-	-	0.015	0.004	-	-
rs2527776	1	44345292	A	G	0.7456	34.544	7.8818	1.17×10^{-5}	ST3GAL3	intron	0.109	-	-	-
rs4984338	15	92645371	A	G	0.8185	40.8586	9.3397	1.22×10^{-5}	SLCO3A1	intron	0.611	-	1.485	1.198
rs7970575	12	6858971	T	C	0.1525	-44.5581	10.2000	1.25×10^{-5}	MLF2	intron	0.001	0.306	-	-
rs4557104	3	65232772	A	G	0.4837	30.5803	7.0382	1.39×10^{-5}	-	-	0.063	-	-	-
rs4617771	14	25529773	A	G	0.1636	-42.4622	9.7944	1.46×10^{-5}	STXBP6	-	0.099	-	-	-
rs17580572	6	16153962	A	G	0.2006	40.271	9.3268	1.58×10^{-5}	MYLIP	-	0.164	0.411	1.172	0.739
rs207964	15	92652173	T	C	0.1771	-42.2038	9.8043	1.67×10^{-5}	SLCO3A1	intron	0.023	-	-	-
rs11200916	10	85958126	T	C	0.0895	57.2574	13.328	1.74×10^{-5}	CDHR1	intron	0.008	-	1.293	-
rs231383	5	90830204	C	G	0.6718	34.0133	7.9605	1.93×10^{-5}	-	-	0.004	-	-	-
rs4895361	5	118474205	A	G	0.1465	-41.4275	9.7753	2.26×10^{-5}	DMXL1	intron	0.04	-	-	-
rs6030453	20	41369963	T	C	0.705	33.9483	8.0402	2.42×10^{-5}	PTPRT	intron	0.001	-	-	0.851
rs2564447	11	44530550	A	C	0.6538	34.5883	8.1974	2.45×10^{-5}	-	-	0.002	-	-	-
rs343155	2	20592798	A	G	0.2646	32.9802	7.8592	2.71×10^{-5}	LOC100289450	-	0	-	1.146	1.311
rs12437502	15	92660866	T	C	0.2234	-43.8339	10.4776	2.87×10^{-5}	SLCO3A1	intron	0.005	0.848	0.877	-
rs1022819	20	41369589	A	G	0.7063	31.4561	7.5374	3.00×10^{-5}	PTPRT	intron	0.016	2.114	1.035	1.189
rs3807230	7	154476554	T	C	0.3057	35.7571	8.5751	3.05×10^{-5}	DPP6	-	0.002	0.302	0.365	0.376
rs4812639	20	41364512	T	C	0.706	32.0913	7.7082	3.14×10^{-5}	PTPRT	intron	0.022	-	-	0.04
rs1375513	3	100771291	T	G	0.8031	-39.3009	9.4747	3.35×10^{-5}	-	-	0.003	-	-	0.259
rs16985186	20	39055032	A	G	0.9315	75.0466	18.0963	3.37×10^{-5}	-	-	0.004	0.321	-	-
									Coding-synonymous					
rs2302371	12	6858126	A	G	0.1511	-42.2182	10.1854	3.40×10^{-5}	MLF2		0.006	0.343	0.686	-
rs6016884	20	41363243	A	G	0.2943	-31.5291	7.6115	3.44×10^{-5}	PTPRT	intron	0.003	1.535	1.029	0.351

SNP	Chr	Position	Effect Allele	Non-Effect Allele	Freq. Effect Allele	Effect	SE	P*	Gene	Feature**	Cons Score***	Selection Score****		
												CHB/JPT	CEU	YRI
rs16987610	2	20605249	A	G	0.9497	-74.7779	18.0784	3.53×10^{-5}	LOC100289450	-	0.304	-	-	0.697
rs11200925	10	85984323	A	G	0.2329	34.0008	8.2203	3.53×10^{-5}	LRIT2	missense	0.991	0.943	-	-
rs17078679	13	85456392	A	G	0.9315	-60.6571	14.7067	3.72×10^{-5}	-	-	0.024	0.576	1.88	0.675
rs10262052	7	11485527	T	C	0.4965	28.5079	6.9261	3.86×10^{-5}	THSD7A	intron near-gene-5	0	1.364	-	2.195
rs4933984	10	85985508	A	G	0.7778	-34.014	8.2689	3.90×10^{-5}	LRIT2	introm	0.097	1.88	-	-
rs10507873	13	78217691	A	G	0.166	38.7915	9.4312	3.90×10^{-5}	SCEL	introm	0.131	-	-	-
rs7181743	15	31809253	A	G	0.9047	-57.4148	13.9632	3.93×10^{-5}	OTUD7A	introm	0.002	-	-	0.017
rs11817531	10	85981351	A	G	0.222	33.9242	8.2524	3.94×10^{-5}	LRIT2	utr-3	0	2.015	-	-
rs9544561	13	78225526	A	G	0.1747	38.8566	9.4544	3.96×10^{-5}	SCEL	-	0.213	-	-	-
rs2250702	21	38103630	T	C	0.2811	40.6984	9.9393	4.23×10^{-5}	SIM2	intron near-gene-3	0.003	0.218	-	1.307
rs3903828	13	78219649	T	C	0.834	-38.5886	9.4395	4.35×10^{-5}	SCEL	introm	0.017	-	-	-
rs6030450	20	41365250	A	G	0.7071	31.1286	7.6316	4.52×10^{-5}	PTPRT	introm	0.022	0.201	-	1.074
rs6808752	3	64024529	A	G	0.2737	31.6577	7.7872	4.80×10^{-5}	PSMD6	-	0.02	-	-	1.29
rs11107789	12	95313261	T	C	0.9378	73.6483	18.1265	4.84×10^{-5}	LOC100505569	-	0.002	-	-	0.318
rs10920654	1	190131750	T	C	0.1502	40.4579	9.969	4.94×10^{-5}	FAM5C	Intron	0.392	0.338	1.26	-
rs8138283	22	49841479	A	G	0.6637	-34.1202	8.4123	4.99×10^{-5}	-	-	0.006	-	-	1.028

* P-values are double genome controlled. **SNP features from dbSNP (<http://www.ncbi.nlm.nih.gov/SNP/>); ***PhastCons Conservation score from UCSC Genome Browser: probability that each nucleotide belongs to a conserved element (<http://hgdownload.cse.ucsc.edu/>) ; ****Positive selection scores of SNPs from <http://haplotter.uchicago.edu/>.

Supplementary Table 12: SNPs with $P \leq 5 \times 10^{-5}$ for association with mean bilateral hippocampal volume in the analysis including patients correcting for Sex, Age, Age², Sex*Age, Sex* Age², MDS.

SNP	Chr	Position	Effect Allele	Non-Effect Allele	Freq. Effect Allele	Effect	SE	P*	Gene	Feature**	Cons Score***	Selection Score****		
												CHB/JPT	CEU	YRI
rs7294919	12	117327592	T	C	0.8954	-56.0905	10.8277	2.22×10^{-7}	-	-	0.01	0.065	1.167	0.227
rs17580572	6	16153962	A	G	0.1931	43.3904	8.442	2.75×10^{-7}	-	-	0.164	0.411	1.172	0.739
rs7315280	12	117320938	A	G	0.8789	-46.5572	9.7393	1.75×10^{-6}	HRK	near-gene-5	0.756	-	-	-
rs7132910	12	117320658	T	C	0.8713	-45.7692	9.5871	1.81×10^{-6}	HRK	near-gene-5	0.035	-	-	-
rs7132339	12	117335912	A	G	0.1076	53.8409	11.2846	1.83×10^{-6}	-	-	0	0.718	-	0.493
rs7922133	10	78784075	T	C	0.6787	-32.0435	6.7341	1.95×10^{-6}	KCNMA1	intron	0.313	-	-	-
rs1294338	1	233438952	T	G	0.7897	36.5302	7.8935	3.69×10^{-6}	-	-	0.019	-	-	0.126
rs10951458	7	36170199	A	G	0.4698	28.7638	6.2908	4.82×10^{-6}	-	-	0.021	-	0.847	1.811
rs7556828	2	46663172	A	G	0.4421	28.1186	6.2864	7.72×10^{-6}	-	-	0.006	-	-	-
rs17549227	2	111796195	T	C	0.8028	35.5007	7.9482	7.95×10^{-6}	ACOXL	intron	0.116	-	-	-
rs6751950	2	70560939	T	C	0.1986	-35.8013	8.0362	8.39×10^{-6}	-	-	0.087	2.038	0.705	1.91
rs1530628	2	46670941	T	C	0.5515	-28.1154	6.3227	8.72×10^{-6}	-	-	0.011	0.226	0.56	1.146
rs4980123	10	78788660	T	G	0.8012	-35.0879	7.9116	9.21×10^{-6}	KCNMA1	intron	0.003	-	-	-
rs17483466	2	111797458	A	G	0.8031	35.239	7.955	9.43×10^{-6}	ACOXL	intron	0.009	-	-	-
rs7612339	3	81270797	T	C	0.4995	29.7326	6.7521	1.07×10^{-5}	-	-	0	-	-	-
rs752834	2	111798658	A	G	0.1919	-35.4179	8.056	1.10×10^{-5}	ACOXL	intron	0.004	-	-	-
rs3639	8	141684170	T	C	0.6883	-30.9949	7.0679	1.16×10^{-5}	PTK2	intron	0.041	0.416	0.985	-
rs4961287	8	141706320	A	G	0.3478	28.4474	6.5104	1.25×10^{-5}	PTK2	intron	0.04	0.857	0.877	-
rs11997161	8	141738587	T	C	0.4855	27.254	6.2669	1.37×10^{-5}	PTK2	intron	0.419	0.828	-	-
rs4852161	2	70562650	T	C	0.6693	31.594	7.2719	1.40×10^{-5}	-	-	0.233	-	-	0.278
rs754352	2	111797920	A	G	0.811	34.7211	8.0125	1.47×10^{-5}	ACOXL	intron	0.021	-	-	-
rs7249167	19	16037359	A	G	0.1293	-40.7877	9.4288	1.52×10^{-5}	CYP4F11	intron	0.009	-	-	-
rs12986899	2	46660752	A	C	0.6018	-27.5186	6.3705	1.56×10^{-5}	-	-	0.38	0.6	0.159	-
rs13257090	8	141729463	T	C	0.491	-26.7653	6.2572	1.89×10^{-5}	PTK2	intron	0.006	0.455	-	-
rs8138283	22	49841479	A	G	0.6641	-33.4429	7.8371	1.98×10^{-5}	-	-	0.006	-	-	1.028
rs550269	16	88881635	T	C	0.1431	44.6501	10.4683	2.00×10^{-5}	GALNS	intron	0.001	-	-	0.648
rs6993266	8	141762659	A	G	0.5114	26.653	6.2527	2.02×10^{-5}	PTK2	intron	0	0.513	-	-
rs13003074	2	46671420	A	T	0.3997	26.9047	6.3212	2.08×10^{-5}	-	-	0.136	0.531	0.09	-

SNP	Chr	Position	Effect Allele	Non-Effect Allele	Freq. Effect Allele	Effect	SE	P*	Gene	Feature**	Cons Score***	Selection Score****		
												CHB/JPT	CEU	YRI
rs6994744	8	141740868	A	C	0.5106	-26.5908	6.256	2.13x10 ⁻⁵	PTK2	intron	0.254	0.828	-	-
rs16967388	15	33535342	A	G	0.9145	56.1561	13.3129	2.46x10 ⁻⁵	-	-	0.014	-	-	-
rs7970575	12	6858971	T	C	0.14	-39.3749	9.3381	2.48x10 ⁻⁵	MLF2	intron	0.001	0.306	-	-
rs11806197	1	77964855	A	G	0.8295	-34.4947	8.1943	2.56x10 ⁻⁵	AK5	intron	0.004	-	-	-
rs12042881	1	77968443	A	G	0.1705	34.4687	8.205	2.66x10 ⁻⁵	AK5	intron	0.005	-	-	-
rs7616034	3	71951781	T	C	0.7555	30.7034	7.3137	2.69x10 ⁻⁵	-	-	0.345	-	1.591	0.204
rs2769264	1	151344741	T	G	0.8128	35.2744	8.4053	2.71x10 ⁻⁵	SELENBP1	intron	0.013	-	-	-
rs1530621	2	46688688	T	C	0.5832	-26.4832	6.3312	2.88x10 ⁻⁵	-	-	0.875	-	-	-
rs7565770	2	46683683	A	C	0.5504	-26.499	6.3362	2.89x10 ⁻⁵	-	-	0.008	0.729	0.389	-
rs4617771	14	25529773	A	G	0.1473	-37.6098	8.9963	2.91x10 ⁻⁵	-	-	0.099	-	-	-
rs12049202	1	77967523	T	C	0.1814	35.7762	8.5642	2.95x10 ⁻⁵	AK5	intron	0.155	-	1.935	0.387
rs6975771	7	116122845	A	G	0.1659	35.2235	8.4656	3.17x10 ⁻⁵	-	-	0.005	-	-	-
rs6119628	20	34170174	A	C	0.698	-28.5251	6.8671	3.27x10 ⁻⁵	FER1L4	-	0.003	-	-	-
rs2121698	2	46709571	T	C	0.4141	26.3235	6.3435	3.33x10 ⁻⁵	LOC388946	intron	0.503	-	0.033	-
rs763855	3	81331298	T	C	0.4881	27.3317	6.5907	3.37x10 ⁻⁵	-	-	0.024	-	-	-
rs1917330	4	58186260	A	G	0.037	-72.4734	17.5455	3.62x10 ⁻⁵	-	-	0.014	-	-	-
rs2388344	5	8833852	T	C	0.5317	29.9806	7.2719	3.74x10 ⁻⁵	-	-	0.014	-	-	-
rs4689705	4	7325002	T	C	0.2943	30.3719	7.3754	3.82x10 ⁻⁵	SORCS2	intron	0.001	-	-	-
rs17697039	2	57022855	T	C	0.9563	73.8709	17.9471	3.85x10 ⁻⁵	-	-	0.015	-	-	-
rs8090471	18	12926924	A	G	0.6961	28.6469	6.9615	3.87x10 ⁻⁵	-	-	0.002	-	0.703	-
rs2423477	20	9791900	A	G	0.3977	26.6077	6.469	3.90x10 ⁻⁵	PAK7	intron	0.001	0.789	0.817	-
rs7630516	3	81297288	A	T	0.287	-30.6181	7.446	3.92x10 ⁻⁵	-	-	0	1.276	0.458	0.067
rs16915019	11	26016331	A	C	0.9666	74.7447	18.1926	3.98x10 ⁻⁵	-	-	0.233	-	-	1.654
rs8043175	15	33554336	A	G	0.0756	-49.9717	12.1769	4.06x10 ⁻⁵	-	-	0.037	0.145	0.042	-
rs9588748	13	90408366	A	G	0.5792	-26.7795	6.5478	4.32x10 ⁻⁵	-	-	0.06	0.464	0.045	-
rs17132392	4	2277731	T	G	0.0142	-188.881	46.2123	4.37x10 ⁻⁵	ZFYVE28	intron	0.001	0.859	-	-
rs10507873	13	78217691	A	G	0.1562	35.1101	8.6023	4.48x10 ⁻⁵	SCEL	intron	0.131	-	-	-
rs7559484	2	46660445	T	C	0.5453	-25.6874	6.2944	4.48x10 ⁻⁵	-	-	0.012	0.202	0.937	-
rs10883869	10	105211432	T	G	0.579	-26.1765	6.4156	4.50x10 ⁻⁵	CALHM2	intron	0.534	-	-	-
rs10262052	7	11485527	T	C	0.5001	25.5471	6.2676	4.58x10 ⁻⁵	THSD7A	intron	0	1.364	-	2.195

SNP	Chr	Position	Effect Allele	Non-Effect Allele	Freq. Effect Allele	Effect	SE	P*	Gene	Feature**	Cons Score***	Selection Score****		
												CHB/JPT	CEU	YRI
rs2808825	13	89489268	T	C	0.1865	36.2119	8.8908	4.64x10 ⁻⁵	-	-	0.186	0.085	0.222	-
rs1074312	7	85056750	C	G	0.1914	-34.9208	8.5884	4.78x10 ⁻⁵	-	-	0.406	-	-	-
rs2769265	1	151344150	A	C	0.1888	-34.0604	8.3819	4.83x10 ⁻⁵	SELENBP1	intron	0.303	-	-	-
rs13394815	2	70564002	A	C	0.2765	-31.7709	7.8218	4.87x10 ⁻⁵	-	-	0.001	-	-	-
rs7571742	2	46660306	A	G	0.5449	-25.6507	6.3168	4.89x10 ⁻⁵	-	-	0.043	0.728	-	-
rs9398455	6	98015352	A	G	0.0895	45.2014	11.1371	4.94x10 ⁻⁵	-	-	0.992	-	1.409	-

* P-values are double genome controlled. **SNP features from dbSNP (<http://www.ncbi.nlm.nih.gov/SNP/>) ; ***PhastCons Conservation score from UCSC Genome Browser: probability that each nucleotide belongs to a conserved element (<http://hgdownload.cse.ucsc.edu/>) ; ****Positive selection scores of SNPs from <http://haplotter.uchicago.edu/>.

Supplementary Table 13: SNPs with $P \leq 5 \times 10^{-5}$ for association with mean bilateral hippocampal volume in the analysis without patients correcting for Sex, Age, Age², Sex*Age, Sex* Age², MDS, TBV.

SNP	Chr	Position	Effect Allele	Non-Effect Allele	Freq. Effect Allele	Effect	SE	P*	Gene	Feature**	Cons Score ***	Selection Score***		
												CHB/JPT	CEU	YRI
rs1456520	2	199772591	T	C	0.9513	-74.107	15.6784	2.28×10^{-6}	-	-	0.14	-	-	0.283
rs13316093	3	21654425	T	C	0.5482	28.4239	6.1415	3.69×10^{-6}	ZNF385D	intron	0.114	0.684	0.96	2.93
rs2564447	11	44530550	A	C	0.652	32.4347	7.0295	3.95×10^{-6}	-	-	0.002	-	-	-
rs1495716	4	176728576	T	C	0.6236	28.7344	6.2479	4.24×10^{-6}	GPM6A	intron	0.543	-	1.277	0.755
rs16869805	5	90817701	T	C	0.3038	-31.0351	7.0628	1.11×10^{-5}	-	-	0.031	-	-	-
rs1378168	3	16024923	A	G	0.7043	29.3699	6.701	1.17×10^{-5}	-	-	0.004	-	-	-
rs4557104	3	65232772	A	G	0.4849	26.6506	6.1128	1.30×10^{-5}	-	-	0.063	-	-	-
rs6030453	20	41369963	T	C	0.7127	30.2575	6.9421	1.31×10^{-5}	PTPRT	intron	0.001	-	-	0.851
rs4812639	20	41364512	T	C	0.7136	29.0259	6.6773	1.38×10^{-5}	PTPRT	intron	0.022	-	-	0.04
rs17160130	7	31445815	T	C	0.1411	-37.7168	8.6946	1.44×10^{-5}	-	-	0.003	0.195	-	0.811
rs9913027	17	61241107	T	C	0.5058	-27.5745	6.4267	1.78×10^{-5}	TANC2	intron	0.027	-	-	-
rs6016884	20	41363243	A	G	0.2866	-28.3037	6.6223	1.92×10^{-5}	PTPRT	intron	0.003	1.535	1.029	0.351
rs1022819	20	41369589	A	G	0.7133	27.9192	6.5326	1.92×10^{-5}	PTPRT	intron	0.016	2.114	1.035	1.189
rs17172125	7	42885952	C	G	0.8939	-46.223	10.8403	2.01×10^{-5}	-	-	0	-	0.717	-
rs6030450	20	41365250	A	G	0.7147	28.0682	6.6108	2.18×10^{-5}	PTPRT	intron	0.022	0.201	-	1.074
rs6650780	2	199797322	A	G	0.0389	89.9669	21.2882	2.38×10^{-5}	-	-	0.028	-	-	0.295
rs9318486	13	78067058	T	G	0.1833	36.3561	8.6109	2.42×10^{-5}	-	-	0.155	-	-	-
rs10038508	5	90797244	A	G	0.2701	-31.038	7.3522	2.43×10^{-5}	-	-	0.015	0.004	-	-
rs10885090	10	112890917	C	G	0.4221	25.914	6.1633	2.62×10^{-5}	-	-	0.02	-	-	-
rs1454765	3	16110666	T	G	0.7236	27.947	6.6547	2.67×10^{-5}	-	-	0.006	-	0.716	0.992
rs10920654	1	190131750	T	C	0.1413	36.2792	8.6653	2.83×10^{-5}	FAM5C	intron	0.392	0.338	1.26	-
rs9477420	6	17411585	T	C	0.3131	26.7206	6.3987	2.97×10^{-5}	CAP2	intron	0.141	-	0.499	1.381
rs10986190	9	126818818	A	G	0.6723	26.8309	6.4458	3.15×10^{-5}	LOC10042	-	0.004	-	-	-
rs10951458	7	36170199	A	G	0.4731	24.9342	5.9979	3.22×10^{-5}		1531	-	0.021	-	0.847
rs11156073	6	156319889	T	G	0.5456	-26.3779	6.3479	3.25×10^{-5}	-	-	0.019	-	-	-
rs6770617	3	16036830	A	G	0.6995	27.5308	6.6271	3.26×10^{-5}	-	-	0.125	-	-	0.194
rs7625628	3	16035590	T	C	0.299	-27.5686	6.6403	3.30×10^{-5}	-	-	0.123	-	-	-
rs13394815	2	70564002	A	C	0.2771	-30.9446	7.4751	3.48×10^{-5}	BRD7P6	-	0.001	-	-	-

SNP	Chr	Position	Effect Allele	Non-Effect Allele	Freq. Effect Allele	Effect	SE	P*	Gene	Feature**	Cons Score ***	Selection Score****		
												CHB/JPT	CEU	YRI
rs1378169	3	16010612	C	G	0.296	-27.5611	6.6649	3.55x10 ⁻⁵	-	-	0.566	-	-	-
rs1893889	8	109437949	A	G	0.6844	-27.0302	6.546	3.64x10 ⁻⁵	TTC35	-	0.171	0.137	-	-
rs1022818	20	41365700	A	G	0.7155	26.9826	6.5555	3.86x10 ⁻⁵	PTPRT	intron	0.001	-	-	-
rs10848088	12	130849993	A	G	0.3511	26.8499	6.5353	3.98x10 ⁻⁵	PIWIL1	-	0.002	-	-	0.274
rs231383	5	90830204	C	G	0.6741	28.4265	6.9245	4.04x10 ⁻⁵	-	-	0.004	-	-	-
rs10043890	5	90867639	A	T	0.7102	26.6959	6.5161	4.19x10 ⁻⁵	-	-	0.001	-	-	-
rs17379883	6	17416064	A	G	0.31	26.156	6.4013	4.39x10 ⁻⁵	CAP2	intron	0.084	1.504	0.289	-
rs2341571	4	40710831	A	G	0.6101	-26.1018	6.3898	4.41x10 ⁻⁵	-	-	0.266	-	-	0.239
rs9465032	6	17405178	A	T	0.2835	26.9202	6.5912	4.42x10 ⁻⁵	CAP2	intron	0.006	2.158	0.163	2.17
rs7040016	9	126858551	A	T	0.2412	30.7617	7.5406	4.51x10 ⁻⁵	-	-	0.003	0.9	0.135	-
rs239368	17	61129121	T	C	0.5037	-25.7588	6.3184	4.57x10 ⁻⁵	TANC2	intron	0.018	-	-	-
rs6876474	5	55471740	C	G	0.8034	61.7976	15.1679	4.62x10 ⁻⁵	ANKRD55	intron	0.153	-	-	0.581
rs16884951	5	55460756	C	G	0.208	-63.5825	15.6306	4.75x10 ⁻⁵	ANKRD55	intron	0.007	-	-	0.741
rs4919611	10	103894939	A	C	0.8707	39.4388	9.7049	4.83x10 ⁻⁵	PPRC1	intron	0.054	-	-	-
rs4870409	6	156300315	A	C	0.7888	32.1827	7.9195	4.83x10 ⁻⁵	-	-	0.012	-	-	-

* P-values are double genome controlled. **SNP features from dbSNP (<http://www.ncbi.nlm.nih.gov/SNP/>); ***PhastCons Conservation score from UCSC Genome Browser: probability that each nucleotide belongs to a conserved element (<http://hgdownload.cse.ucsc.edu/>) ; ****Positive selection scores of SNPs from <http://haplotter.uchicago.edu/>.

Supplementary Table 14: SNPs with $P \leq 5 \times 10^{-5}$ for association with mean bilateral hippocampal volume in the analysis including patients correcting for Sex, Age, Age², Sex*Age, Sex* Age², MDS, TBV.

SNP	Chr	Position	Effect Allele	Non-Effect Allele	Freq. Effect Allele	Effect	SE	P*	Gene	Feature**	Cons Score ***	Selection Score****	CHB/JPT	CEU	YRI
rs7294919	12	117327592	T	C	0.8962	-47.0571	9.4142	5.78×10^{-7}	HRK	-	0.01	0.065	1.167	0.227	
rs7315280	12	117320938	A	G	0.8796	-41.9594	8.446	6.77×10^{-7}	HRK	near-gene-5	0.756	-	-	-	
rs7132910	12	117320658	T	C	0.872	-40.8873	8.3331	9.27×10^{-7}	HRK	near-gene-5	0.035	-	-	-	
rs619140	16	9399292	T	C	0.1908	-31.8352	6.8316	3.16×10^{-6}	-	-	0	-	-	-	
rs13394815	2	70564002	A	C	0.2763	-30.5322	6.727	5.66×10^{-6}	BRD7P6	-	0.001	-	-	-	
rs12056676	8	28451539	A	C	0.6292	-31.2399	6.9609	7.19×10^{-6}	-	-	0.004	0.336	-	0.749	
rs7132339	12	117335912	A	G	0.1069	44.2154	9.8562	7.26×10^{-6}	HRK	-	0	0.718	-	0.493	
rs6716296	2	38174964	A	G	0.343	25.7871	5.8045	8.89×10^{-6}	FAM82A1	intron	0.043	1.075	-	-	
rs2636859	9	117029422	C	G	0.386	26.0713	5.8736	9.05×10^{-6}	COL27A1	intron	0.544	0.32	1.116	0.125	
rs4759277	12	57533690	A	C	0.3603	-25.5372	5.7759	9.81×10^{-6}	LRP1	intron	0.028	-	1.538	0.364	
rs17440025	8	28442098	A	G	0.706	-28.5313	6.4642	1.02×10^{-5}	-	-	0.27	-	-	0.257	
rs17465113	5	124734492	T	C	0.0785	47.9672	10.8719	1.02×10^{-5}	-	-	0.006	-	-	-	
rs271646	17	48000146	T	G	0.2061	-30.3709	6.8922	1.05×10^{-5}	LOC124865	-	0.182	0.673	0.564	1.867	
rs164658	8	28441566	A	G	0.3073	26.9401	6.1186	1.07×10^{-5}	FZD3	-	0.042	0.339	1.211	0.369	
rs4367982	12	57531632	A	G	0.6375	25.3219	5.7594	1.10×10^{-5}	LRP1	intron	0.047	-	-	-	
rs1456520	2	199772591	T	C	0.9532	-63.7304	14.5448	1.18×10^{-5}	-	-	0.14	-	-	0.283	
rs271653	17	48005880	T	C	0.2008	-29.4225	6.7858	1.45×10^{-5}	LOC124865	-	0.017	0.295	0.729	1.612	
rs1466535	12	57534470	A	G	0.3491	-25.0807	5.7847	1.45×10^{-5}	LRP1	intron	0.235	0.82	-	0.46	
rs9913027	17	61241107	T	C	0.5081	-24.8496	5.7596	1.60×10^{-5}	TANC2	intron	0.027	-	-	-	
rs1839259	16	77650847	C	G	0.4556	23.3343	5.4112	1.62×10^{-5}	-	-	0	2.837	1.843	0.414	
rs4759044	12	57530670	T	C	0.5602	24.3437	5.6547	1.67×10^{-5}	LRP1	intron	0.001	-	1.062	-	
rs743760	13	33071127	C	G	0.3492	-24.6445	5.7528	1.84×10^{-5}	N4BP2L2	intron	0.019	0.563	-	-	
rs16875511	5	5385388	T	C	0.9535	66.5101	15.544	1.88×10^{-5}	LOC442131	-	0.695	0.231	-	-	
rs17580572	6	16153962	A	G	0.1925	31.0955	7.2749	1.92×10^{-5}	MYLIP	-	0.164	0.411	1.172	0.739	
rs703817	12	57489828	T	C	0.4951	-23.2269	5.4356	1.93×10^{-5}	STAT6	utr-3	0.026	0.489	-	0.429	
rs4680886	3	28007973	A	G	0.2085	-29.3493	6.9347	2.31×10^{-5}	-	-	0.004	-	-	-	
rs1117412	16	77651113	C	G	0.5443	-22.9643	5.4362	2.40×10^{-5}	-	-	0	2.837	1.843	0.531	
rs468648	5	75996865	A	G	0.9243	43.8327	10.4012	2.51×10^{-5}	IQGAP2	intron	0.054	-	-	0.027	

SNP	Chr	Position	Effect Allele	Non-Effect Allele	Freq. Effect Allele	Effect	SE	P*	Gene	Feature**	Cons Score ***	Selection Score****		
												CHB/JPT	CEU	YRI
rs7193915	16	77647073	T	C	0.469	22.7877	5.4143	2.57x10 ⁻⁵	-	-	0.087	2.225	1.9	0.513
rs913417	9	14520611	A	G	0.7617	-26.6832	6.3602	2.72x10 ⁻⁵	-	-	0.001	0.256	0.264	-
rs4617771	14	25529773	A	G	0.1484	-32.4359	7.7335	2.74x10 ⁻⁵	STXBP6	-	0.099	-	-	-
rs1052826	20	61576777	A	G	0.7759	-27.2049	6.4981	2.83x10 ⁻⁵	C20orf11	utr-3	0.005	-	-	-
rs8090471	18	12926924	A	G	0.6954	25.1137	6.0063	2.90x10 ⁻⁵	LOC646171	-	0.002	-	0.703	-
rs530652	20	930560	T	C	0.6062	25.8326	6.2031	3.12x10 ⁻⁵	RSPO4	-	0.011	0.906	1.486	-
rs17440102	8	28444787	A	G	0.29	25.9263	6.2574	3.42x10 ⁻⁵	-	-	0.012	-	-	0.403
rs1155406	16	60376163	A	G	0.0587	-50.124	12.1095	3.49x10 ⁻⁵	LOC729159	-	0.013	-	-	-
rs4557104	3	65232772	A	G	0.4895	22.673	5.4789	3.50x10 ⁻⁵	-	-	0.063	-	-	-
rs4968767	17	61443944	A	C	0.509	-23.7045	5.7366	3.59x10 ⁻⁵	TANC2	intron	0	-	-	-
rs820144	17	73611823	T	C	0.6444	-27.386	6.6287	3.61x10 ⁻⁵	MYO15B	-	0.113	-	-	1.605
rs2838923	21	46846944	A	G	0.72	26.9813	6.5315	3.61x10 ⁻⁵	COL18A1	intron	0.003	-	-	0.751
rs17829596	2	165985503	T	C	0.8605	34.5601	8.3687	3.63x10 ⁻⁵	SCN3A	intron	0.075	0.674	-	0.082
rs7077280	10	122925371	T	C	0.9885	224.5223	54.3755	3.64x10 ⁻⁵	LOC100129699	-	0.079	-	-	-
rs1791463	11	106416708	A	G	0.7525	-26.799	6.5073	3.82x10 ⁻⁵	-	-	0.789	-	-	-
rs239368	17	61129121	T	C	0.506	-23.3524	5.6786	3.92x10 ⁻⁵	TANC2	intron	0.018	-	-	-
rs841718	12	57492996	A	G	0.5933	-22.8525	5.5629	3.99x10 ⁻⁵	STAT6	intron	0.027	0.871	0.149	1.601
rs7210972	17	61232478	A	G	0.4733	22.4969	5.4782	4.01x10 ⁻⁵	TANC2	intron	0.047	3.074	0.926	0.844
rs1106975	6	164616969	A	G	0.9121	-41.7009	10.1578	4.04x10 ⁻⁵	-	-	0.036	-	-	-
rs3087776	17	61510278	T	C	0.4901	-22.5941	5.509	4.11x10 ⁻⁵	CYB561	utr-3	0.002	-	-	0.479
rs2636860	9	117030582	A	G	0.3881	22.5748	5.5255	4.40x10 ⁻⁵	COL27A1	intron	0.258	0.185	1.077	0.009
rs6487598	12	27451600	A	T	0.9711	71.254	17.4424	4.41x10 ⁻⁵	STK38L	intron	0.019	-	-	-
rs12150107	17	61109044	A	G	0.494	23.1932	5.6784	4.42x10 ⁻⁵	TANC2	intron	0.101	-	-	-
rs12639500	3	28026396	A	G	0.7374	25.3514	6.2083	4.44x10 ⁻⁵	-	-	0.046	0.242	1.143	0.166
rs4968777	17	61530211	T	C	0.4968	24.5974	6.0344	4.58x10 ⁻⁵	CYB561	-	0.007	-	-	-
rs271645	17	47999993	A	G	0.7309	25.663	6.2958	4.58x10 ⁻⁵	LOC124865	-	0.499	0.263	0.655	-
rs4658573	1	242094314	A	C	0.2816	29.789	7.3092	4.59x10 ⁻⁵	RPL23AP20	-	0.026	0.904	0.493	-
rs9315167	13	33069188	T	C	0.3624	-22.7268	5.588	4.76x10 ⁻⁵	N4BP2L2	intron	0.015	0.667	-	0.164
rs486992	11	100984844	A	G	0.6274	-22.9628	5.6582	4.94x10 ⁻⁵	PGR	intron	0.003	0.065	0.629	-

* P-values are double genome controlled. **SNP features from dbSNP (<http://www.ncbi.nlm.nih.gov/SNP/>); ***PhastCons Conservation score from UCSC Genome Browser: probability that each nucleotide belongs to a conserved element (<http://hgdownload.cse.ucsc.edu/>) ; ****Positive selection scores of SNPs from <http://haplotter.uchicago.edu/>.

Supplementary Table 15: SNPs with $P \leq 5 \times 10^{-5}$ for association with estimated total intracranial volume in the analysis without patients correcting for Sex, Age, Age², Sex*Age, Sex* Age², MDS.

SNP	Chr	Position	Effect Allele	Non-Effect Allele	Freq. Effect Allele	Effect	SE	P*	Gene	Feature**	Cons Score ***	Selection Score****		
												CHB/J PT	CEU	YRI
rs10784502	12	66343810	T	C	0.5124	-11860.7	2319	3.14×10^{-7}	HMGA2	Intron	0.284	1.595	-	-
rs8756	12	66359752	A	C	0.5116	-11451.8	2310.946	7.22×10^{-7}	HMGA2	utr-3	0.983	1.339	-	-
rs1351394	12	66351826	T	C	0.4898	11381.25	2319.473	9.26×10^{-7}	HMGA2	Intron	0.011	1.476	-	-
rs10400419	12	66389968	T	C	0.464	11532.03	2355.648	9.81×10^{-7}	-	-	0.004	1.194	-	-
rs10125582	9	8135549	T	C	0.7362	13667.73	2793.921	9.98×10^{-7}	-	-	0.002	-	-	-
rs8110509	19	30981639	A	C	0.205	14217.68	2938.809	1.31×10^{-6}	ZNF536	Intron	0.001	0.664	-	-
rs11787770	9	8142694	A	G	0.2551	-12401	2598.944	1.83×10^{-6}	-	-	0.002	0.135	1.016	-
rs1416595	9	8148244	C	G	0.7415	12273.25	2595.954	2.27×10^{-6}	-	-	0.009	0.241	0.703	-
rs502553	11	122115386	T	C	0.8631	15708.32	3342.31	2.60×10^{-6}	LOC100507145	-	0.014	-	-	-
rs911763	9	8133859	T	G	0.7497	12305.93	2618.744	2.61×10^{-6}	-	-	0.991	-	0.523	-
rs4936679	11	122102623	T	C	0.1537	-15099.5	3214.906	2.64×10^{-6}	LOC100507145	-	0.029	1.398	0.525	0.057
rs1042725	12	66358347	T	C	0.4932	-10821.6	2306.257	2.70×10^{-6}	HMGA2	utr-3	0.034	-	1.061	1.387
rs10790490	11	122110188	T	C	0.1516	-15106.3	3222.084	2.75×10^{-6}	LOC100507145	-	0.008	1.908	0.534	-
rs2749812	20	23062927	A	G	0.1687	-15716.5	3357.399	2.85×10^{-6}	CD93	utr-3	0	-	0.497	-
rs1800197	5	177419967	T	C	0.2841	12282.3	2636.485	3.18×10^{-6}	PROP1	missense	0.026	-	-	0.528
rs622166	11	122121081	A	G	0.1351	-15570.9	3360.688	3.60×10^{-6}	LOC100507145	-	0.006	-	-	-
rs7968682	12	66371880	T	G	0.5256	-11692.5	2534.298	3.96×10^{-6}	-	-	0.016	0.965	-	-
rs1998338	9	8140651	A	G	0.2421	-12046.5	2632.424	4.74×10^{-6}	-	-	0.014	-	0.663	-
rs12298541	12	66306441	A	C	0.3732	12694.86	2785.634	5.18×10^{-6}	HMGA2	Intron Coding - synonymous	0.001	0.48	-	-
rs20542	11	46403649	T	C	0.12	-19725.5	4331.422	5.26×10^{-6}	MDK		0.53	-	-	-
rs2224580	9	8142291	A	C	0.2393	-12072.1	2651.888	5.31×10^{-6}	-	-	0.1	-	0.379	-
rs911766	9	8140904	A	G	0.7503	12821.43	2819.12	5.42×10^{-6}	-	-	0.007	-	0.66	-
rs17066180	6	137552527	A	G	0.0127	-140536	31087.75	6.17×10^{-6}	-	-	0.008	-	-	1.396
rs7692647	4	132464732	A	G	0.868	16301.16	3620.865	6.73×10^{-6}	-	-	0.001	0.792	0.014	0.905
rs1480474	12	66326943	A	G	0.5799	11199.16	2522.536	9.01×10^{-6}	HMGA2	Intron	0.004	1.285	-	-
rs489877	11	122128526	A	C	0.867	14807.45	3369.438	1.11×10^{-5}	LOC100507145	-	0.638	-	-	-
rs9997610	4	116391247	T	G	0.2544	-11202.9	2550.728	1.12×10^{-5}	-	-	0	0.387	0.372	1.25
rs520036	11	122163143	T	G	0.8727	14841.99	3454.941	1.74×10^{-5}	LOC100507145	-	0.003	-	-	-

SNP	Chr	Position	Effect Allele	Non-Effect Allele	Freq. Effect Allele	Effect	SE	P*	Gene	Feature**	Cons Score ***	Selection Score****		
												CHB/J PT	CEU	YRI
rs497879	11	122148259	A	G	0.1361	-14360.7	3367.057	2.00x10 ⁻⁵	LOC100507145	-	0.687	-	-	-
rs10214135	5	38366662	T	C	0.8181	13618.02	3206.859	2.17x10 ⁻⁵	EGFLAM	Intron	0.072	0.863	1.427	-
rs2435211	17	44063244	T	C	0.2974	11200.19	2639.105	2.20x10 ⁻⁵	MAPT	Intron	0.121	-	-	-
rs12161896	14	45066033	A	G	0.8729	15192.54	3589.644	2.31x10 ⁻⁵	-	-	0.048	-	-	-
rs2281470	4	3319553	T	C	0.0877	23074.07	5454.573	2.34x10 ⁻⁵	RGS12	Coding-synonymous	0.597	-	-	0.241
rs9462840	6	42824756	A	G	0.712	-12510	2958.934	2.36x10 ⁻⁵	KIAA0240	Intron	0.029	-	-	-
rs7966895	12	66383843	A	G	0.655	10725.38	2546.694	2.54x10 ⁻⁵	-	-	0.02	-	0.476	-
rs4246208	10	126654898	T	C	0.7541	-11787.6	2803.238	2.61x10 ⁻⁵	ZRANB1	Intron	0.001	-	-	-
rs8100439	19	30983806	A	C	0.1495	13726.16	3264.979	2.62x10 ⁻⁵	ZNF536	Intron	0.886	-	0.439	-
rs537119	11	122143668	C	G	0.8653	14165.07	3376.095	2.72x10 ⁻⁵	LOC100507145	-	0.105	-	-	-
rs7968902	12	66363070	T	G	0.4323	9967.931	2377.072	2.75x10 ⁻⁵	HMGA2	-	0.124	-	1.315	1.649
rs10461828	5	27022711	A	C	0.102	17816.03	4269.656	3.01x10 ⁻⁵	CDH9	Intron	0.005	0.183	-	-
rs17631676	17	43549526	A	G	0.8093	12484.57	2999.739	3.16x10 ⁻⁵	PLEKHM1	Intron	0.005	-	-	-
rs17651213	17	44051924	A	G	0.2219	-11121.2	2678.501	3.30x10 ⁻⁵	MAPT	Intron	0.002	-	-	-
rs763751	17	19326857	T	C	0.9846	66317.82	15975.78	3.31x10 ⁻⁵	-	-	0.003	-	-	1.221
rs4962711	10	126644482	T	C	0.2438	11621.58	2802.437	3.37x10 ⁻⁵	ZRANB1	Intron	0.052	-	-	-
rs4319486	11	46320679	A	C	0.2903	-12291	2963.898	3.37x10 ⁻⁵	CREB3L1	-	0.042	-	-	-
rs1076222	17	44109769	C	G	0.779	11145.53	2688.494	3.39x10 ⁻⁵	MAPT	-	0.002	-	0.135	-
rs17575850	17	44144387	A	C	0.2216	-11146.8	2689.547	3.41x10 ⁻⁵	KIAA1267	-	0.018	-	2.176	-
rs2141299	17	44240986	A	C	0.2214	-11153.6	2692.975	3.45x10 ⁻⁵	KIAA1267	-	0.005	-	-	-
rs1881194	17	44248814	A	G	0.2211	-11158.3	2694.143	3.45x10 ⁻⁵	KIAA1267	Coding-synonymous	0.981	-	-	-
rs17574824	17	44115107	T	C	0.2212	-11132.2	2688.944	3.47x10 ⁻⁵	KIAA1267	-	0	-	0.108	-
rs2532269	17	44250108	T	C	0.7727	11161.45	2699.817	3.56x10 ⁻⁵	KIAA1267	-	0.091	-	-	2.567
rs526977	11	122155670	T	C	0.8689	15325.64	3707.468	3.57x10 ⁻⁵	LOC100507145	-	0.003	-	-	-
rs1120557	14	63129440	A	G	0.0798	-18748.5	4539.098	3.62x10 ⁻⁵	-	-	0.179	1.946	-	-
rs12150506	17	44090536	A	G	0.2246	-11121.2	2695.171	3.69x10 ⁻⁵	MAPT	Intron	0.005	-	-	-
rs11079729	17	44115569	A	C	0.2212	-11091.7	2688.452	3.70x10 ⁻⁵	KIAA1267	-	0.008	-	0.732	-
rs17575556	17	44135827	A	G	0.2213	-11092	2688.907	3.71x10 ⁻⁵	KIAA1267	-	0.026	-	2.146	-
rs2532234	17	44272266	A	G	0.7787	11114.57	2694.608	3.71x10 ⁻⁵	KIAA1267	-	0.183	-	-	-
rs2732711	17	44350293	A	G	0.7795	11229.58	2722.865	3.72x10 ⁻⁵	LOC100132570	-	0.068	-	1.05	-

SNP	Chr	Position	Effect Allele	Non-Effect Allele	Freq. Effect Allele	Effect	SE	P*	Gene	Feature**	Cons Score ***	Selection Score****		
												CHB/J PT	CEU	YRI
rs17574604	17	44111613	A	G	0.7791	11084.45	2688.859	3.75x10 ⁻⁵	KIAA1267	Coding-synonymous	0.654	-	0.362	-
rs480700	9	14079067	T	C	0.6444	9753.47	2367.946	3.81x10 ⁻⁵	NFIB	-	0.013	-	-	1.192
rs7927724	11	46323209	A	G	0.2902	-12217.6	2966.188	3.81x10 ⁻⁵	CREB3L1	-	0.004	-	-	-
rs17652961	17	44108355	A	G	0.2212	-11077.3	2689.469	3.81x10 ⁻⁵	KIAA1267	utr-3	0.227	-	0.718	-
rs12947718	17	43493101	A	G	0.1814	-12354	3000.779	3.84x10 ⁻⁵	ARHGAP27	Intron	0	-	0.742	-
rs17659881	17	44157597	A	G	0.7786	11070.29	2689.002	3.84x10 ⁻⁵	KIAA1267	-	0	-	-	-
rs2532270	17	44249800	A	G	0.2214	-11089	2693.811	3.85x10 ⁻⁵	KIAA1267	-	0.013	-	-	-
rs12414609	10	105162141	A	G	0.5408	-9467.31	2299.999	3.85x10 ⁻⁵	PDCD11	Intron	0.011	-	-	-
rs17652449	17	44088937	C	G	0.2209	-11057.5	2686.333	3.85x10 ⁻⁵	MAPT	Intron	0.002	-	0.269	-
rs17653162	17	44111827	A	C	0.221	-11066.7	2689.295	3.87x10 ⁻⁵	KIAA1267	-	0.007	-	0.359	-
rs7350928	17	44108100	T	C	0.2209	-11061.7	2688.207	3.87x10 ⁻⁵	KIAA1267	utr-3	0.046	-	0.718	-
rs17660065	17	44162284	T	C	0.7785	11067.42	2689.868	3.88x10 ⁻⁵	KIAA1267	-	0.109	-	-	-
										utr-3; miRNA binding site				
rs17574361	17	44108202	A	G	0.7791	11056.42	2688.253	3.91x10 ⁻⁵	KIAA1267	-	0.44	-	0.718	-
rs17652502	17	44094471	A	G	0.2208	-11053.7	2688.055	3.92x10 ⁻⁵	MAPT	Intron	0.005	-	0.489	-
rs12150090	17	44115886	T	C	0.2211	-11059.9	2689.703	3.92x10 ⁻⁵	KIAA1267	-	0.003	-	0.756	-
rs2469933	17	44285531	A	G	0.2267	-11073.6	2693.237	3.93x10 ⁻⁵	KIAA1267	-	0.173	-	-	-
rs17571739	17	44032915	T	C	0.7786	11043.27	2686.812	3.95x10 ⁻⁵	MAPT	Intron	0.003	-	-	-
rs17660132	17	44165803	T	C	0.7786	11053.5	2689.691	3.96x10 ⁻⁵	KIAA1267	-	0	-	-	-
rs11191672	10	105138961	T	C	0.4609	9444.519	2298.326	3.97x10 ⁻⁵	TAF5	Intron	0.111	0.975	1.29	1.009
rs17573175	17	44071089	C	G	0.7791	10999.09	2678.761	4.03x10 ⁻⁵	MAPT	Intron	0.026	-	0.885	-
rs1117253	17	44149297	A	C	0.7787	11046.59	2690.635	4.03x10 ⁻⁵	KIAA1267	-	0	-	2.176	-
rs1052587	17	44102604	T	C	0.7793	11034.49	2688.022	4.04x10 ⁻⁵	MAPT	utr-3	0.344	-	-	-
rs8070723	17	44081064	A	G	0.7726	11005.18	2682.071	4.07x10 ⁻⁵	MAPT	Intron	0.046	-	0.325	-
rs17659953	17	44159725	T	C	0.2213	-11041.5	2691.232	4.08x10 ⁻⁵	KIAA1267	-	0.506	-	2.426	-
rs242559	17	44025888	A	C	0.7721	11050.25	2694.303	4.11x10 ⁻⁵	MAPT	Intron	0.001	0.122	1.113	0.507
rs17650860	17	44039008	A	G	0.2209	-11038.8	2692.003	4.12x10 ⁻⁵	MAPT	Intron	0.004	-	-	-
rs1078268	17	44075901	A	G	0.7789	11004.55	2684.233	4.14x10 ⁻⁵	STH	near-gene-5	0.002	-	0.321	-
rs12150447	17	44128125	A	C	0.7792	11046	2695.307	4.16x10 ⁻⁵	KIAA1267	-	0.001	-	-	-
rs17571718	17	44032768	T	C	0.7787	11014.85	2688.056	4.17x10 ⁻⁵	MAPT	Intron	0.012	-	0.9	-

SNP	Chr	Position	Effect Allele	Non-Effect Allele	Freq. Effect Allele	Effect	SE	P*	Gene	Feature**	Cons Score ***	Selection Score****		
												CHB/J PT	CEU	YRI
rs17572169	17	44045974	T	C	0.2211	-10985.1	2681.23	4.18x10 ⁻⁵	MAPT	Intron	0.351	-	-	-
rs2668692	17	44293020	A	G	0.2273	-11033.3	2693.603	4.20x10 ⁻⁵	KIAA1267	-	0.155	-	1.878	-
rs7146225	14	69421378	A	G	0.723	12387.12	3025.173	4.23x10 ⁻⁵	ACTN1	Intron	0.009	2.05	-	-
rs17571857	17	44035706	A	G	0.7788	11008.02	2688.978	4.24x10 ⁻⁵	MAPT	Intron	0.5	-	-	-
rs17650872	17	44039516	T	G	0.2215	-10988.6	2684.857	4.26x10 ⁻⁵	MAPT	Intron	0.002	-	-	-
rs2292807	10	105155645	T	C	0.5407	-9395.83	2296.343	4.28x10 ⁻⁵	PDCD11	near-gene-5	0.004	1.029	1.245	0.896
rs17572893	17	44064208	A	G	0.2206	-10953.3	2678.016	4.31x10 ⁻⁵	MAPT	Intron	0.003	-	1.392	-
rs11191676	10	105155066	A	C	0.4593	9390.884	2296.259	4.32x10 ⁻⁵	PDCD11	near-gene-5	0.008	-	-	-
rs17577094	17	44187492	A	G	0.7788	10998.49	2689.688	4.33x10 ⁻⁵	KIAA1267	-	0.029	-	-	-
rs17572851	17	44063766	A	G	0.7791	10941.1	2677.11	4.37x10 ⁻⁵	MAPT	Intron Coding-synonymous	0.018	-	-	-
rs1052553	17	44073889	A	G	0.7796	10939.95	2679.193	4.44x10 ⁻⁵	MAPT	-	0.959	-	0.678	-
rs11191666	10	105127278	A	G	0.5394	-9353.48	2290.91	4.45x10 ⁻⁵	TAF5	near-gene-5	0.001	1.04	1.342	0.898
rs6508153	18	50262963	A	C	0.2359	-10650.2	2609.025	4.46x10 ⁻⁵	DCC	Intron	0.001	0.31	0.426	-
rs17572361	17	44052009	T	C	0.7789	10935.5	2679.478	4.48x10 ⁻⁵	MAPT	Intron	0.001	-	0.937	-
rs12942666	17	43499839	A	G	0.819	12236.92	3000.49	4.54x10 ⁻⁵	ARHGAP27	Intron	0.157	-	-	-
rs7944584	11	47336320	A	T	0.7233	10531.5	2585.069	4.62x10 ⁻⁵	MADD	Intron Coding-synonymous	0.006	-	-	-
rs1052551	17	44068924	A	G	0.2201	-10915.3	2679.777	4.64x10 ⁻⁵	MAPT	-	0.426	-	-	-
rs7545737	1	119533823	A	G	0.681	10864.01	2667.413	4.64x10 ⁻⁵	TBX15	near-gene-5	0.018	-	-	-
rs10883858	10	105127708	A	G	0.4598	9330.4	2291.898	4.68x10 ⁻⁵	TAF5	near-gene-5	0.982	-	-	-
rs1468241	17	44196153	A	G	0.7788	10958.92	2692.82	4.71x10 ⁻⁵	KIAA1267	-	0.018	-	2.382	-
rs2532316	17	44213712	A	G	0.2214	-10947.7	2690.816	4.73x10 ⁻⁵	KIAA1267	-	0	-	2.293	-
rs17660464	17	44177993	A	C	0.2276	-10938	2688.672	4.74x10 ⁻⁵	KIAA1267	-	0.101	-	3.066	-
rs1981997	17	44056767	A	G	0.2273	-10885.4	2678.758	4.83x10 ⁻⁵	MAPT	Intron	0.102	-	-	-
rs17651549	17	44061278	T	C	0.2204	-10884.9	2680.158	4.88x10 ⁻⁵	MAPT	Intron	0.552	-	-	-
rs1800547	17	44051846	A	G	0.7789	10883.51	2681.166	4.92x10 ⁻⁵	MAPT	Intron	0.447	-	0.937	-
rs7905968	10	105135319	T	C	0.4895	9327.943	2298.716	4.95x10 ⁻⁵	TAF5	Intron	0.081	-	-	-
rs4327091	17	44021717	A	G	0.2221	-10908.5	2688.562	4.96x10 ⁻⁵	MAPT	Intron	0.001	-	-	-
rs6889596	5	123030802	T	C	0.2833	-10040.5	2475.574	5.00x10 ⁻⁵	-	-	0	2.245	0.582	0.089

* P-values are double genome controlled. **SNP features from dbSNP (<http://www.ncbi.nlm.nih.gov/SNP/>); ***PhastCons Conservation score from UCSC Genome Browser: probability that each nucleotide belongs to a conserved element (<http://hgdownload.cse.ucsc.edu/>) ; ****Positive selection scores of SNPs from <http://haplotter.uchicago.edu/>.

Supplementary Table 16: SNPs with $P \leq 5 \times 10^{-5}$ for association with total brain volume in the analysis without patients correcting for Sex, Age, Age², Sex*Age, Sex* Age², MDS.

SNP	Chr	Position	Effect Allele	Non-Effect Allele	Freq. Effect Allele	Effect	SE	P^*	Gene	Feature**	Cons Score***	Selection Score****		
												CHB/JPT	CEU	YRI
rs6093346	20	39066915	A	G	0.060	-18873.02	3815.81	7.58×10^{-7}	-	-	0.214	0.437	-	0.508
rs1998338	9	8140651	A	G	0.244	-10028.92	2039.06	8.73×10^{-7}	-	-	0.014	-	0.663	-
rs911763	9	8133859	T	G	0.747	9921.76	2031.22	1.04×10^{-6}	-	-	0.991	-	0.523	-
rs2224580	9	8142291	A	C	0.241	-10024.00	2057.10	1.10×10^{-6}	-	-	0.1	-	0.379	-
rs7267007	20	39068372	T	C	0.937	17723.47	3687.43	1.54×10^{-6}	-	-	0.017	0.286	-	0.954
rs11787770	9	8142694	A	G	0.257	-9579.65	2006.23	1.80×10^{-6}	-	-	0.002	0.135	1.016	-
rs10057590	5	124335247	A	C	0.467	8458.42	1776.13	1.91×10^{-6}	-	-	0.035	-	-	0.963
rs1416595	9	8148244	C	G	0.740	9342.00	1999.53	2.98×10^{-6}	-	-	0.009	0.241	0.703	-
rs6808752	3	64024529	A	G	0.266	9020.65	1957.75	4.07×10^{-6}	PSMD6	-	0.02	-	-	1.29
rs6864049	5	124330522	A	G	0.473	8010.77	1750.14	4.71×10^{-6}	-	-	0	-	-	0.741
rs6764606	3	64020447	T	C	0.429	8009.07	1753.45	4.93×10^{-6}	PSMD6	-	0.005	1.622	0.506	-
rs10125582	9	8135549	T	C	0.734	9867.60	2161.26	4.98×10^{-6}	-	-	0.002	-	-	-
rs911766	9	8140904	A	G	0.748	9989.85	2189.95	5.08×10^{-6}	-	-	0.007	-	0.66	-
rs770940	6	16838006	T	C	0.924	16910.03	3747.96	6.43×10^{-6}	-	-	0.906	0.519	-	-
rs6891163	5	49615106	A	T	0.954	-18834.44	4235.96	8.74×10^{-6}	-	-	0.015	-	-	-
rs3823518	7	154476409	T	C	0.609	-8869.83	1996.31	8.87×10^{-6}	DPP6	-	0.034	-	0.174	0.168
rs2173141	13	82641339	T	C	0.369	-7930.85	1798.31	1.03×10^{-5}	-	-	0.412	-	0.924	0.479
rs7329093	13	82641446	T	C	0.364	-7975.87	1808.89	1.04×10^{-5}	-	-	0.013	0.961	-	-
rs9545953	13	82591114	T	C	0.366	-7967.87	1809.46	1.07×10^{-5}	-	-	0.469	1.332	0.806	-
rs981915	13	82640195	T	C	0.366	-7956.61	1806.84	1.07×10^{-5}	-	-	0	0.961	-	-
rs16978020	17	72382917	A	C	0.101	-23748.35	5395.89	1.08×10^{-5}	GPR142	-	0.007	0.804	2.747	-
rs1497066	13	82627500	T	G	0.636	7942.42	1812.31	1.17×10^{-5}	-	-	0.003	0.916	0.411	-
rs12336338	9	8116662	A	C	0.248	-9233.06	2119.28	1.32×10^{-5}	-	-	0.536	-	1.223	-
rs2717039	2	58169166	T	G	0.382	7873.89	1809.01	1.35×10^{-5}	-	-	0.978	-	-	-
rs17631676	17	43549526	A	G	0.810	9832.25	2259.03	1.35×10^{-5}	PLEKHM1	intron	0.005	-	-	-
rs763751	17	19326857	T	C	0.984	52925.08	12206.04	1.45×10^{-5}	RNF112	-	0.003	-	-	1.221
rs13060756	3	100736117	A	C	0.960	-20635.63	4782.75	1.60×10^{-5}	-	-	0.99	-	-	-
rs12410712	1	242567214	T	C	0.916	-14376.55	3333.42	1.61×10^{-5}	PLD5	intron	0.009	-	-	-

SNP	Chr	Position	Effect Allele	Non-Effect Allele	Freq. Effect Allele	Effect	SE	P*	Gene	Feature**	Cons Score***	Selection Score****		
												CHB/JPT	CEU	YRI
rs7208015	17	19320879	C	G	0.984	53699.87	12493.47	1.72x10 ⁻⁵	RNF112	near-gene-3	0.435	1.441	-	-
rs10494373	1	162619362	A	C	0.918	-13693.29	3187.51	1.74x10 ⁻⁵	DDR2	intron	0.121	-	-	0.083
rs2717038	2	58168831	A	G	0.617	-7738.49	1805.03	1.81x10 ⁻⁵	-	-	0.996	-	-	1.891
rs2011186	16	56705869	T	C	0.437	-8318.67	1942.56	1.85x10 ⁻⁵	MT1B	-	0.054	0.154	0.305	0.752
rs2011186	16	56705869	T	C	0.437	-8318.67	1942.56	1.85x10 ⁻⁵	MT1B	-	0.054	0.154	0.305	0.752
rs2011186	16	56705869	T	C	0.437	-8318.67	1942.56	1.85x10 ⁻⁵	MT1B	-	0.054	0.154	0.305	0.752
rs2011186	16	56705869	T	C	0.437	-8318.67	1942.56	1.85x10 ⁻⁵	MT1B	-	0.054	0.154	0.305	0.752
rs2011186	16	56705869	T	C	0.437	-8318.67	1942.56	1.85x10 ⁻⁵	MT1B	-	0.054	0.154	0.305	0.752
rs2011186	16	56705869	T	C	0.437	-8318.67	1942.56	1.85x10 ⁻⁵	MT1B	-	0.054	0.154	0.305	0.752
rs16985186	20	39055032	A	G	0.954	19765.68	4628.45	1.95x10 ⁻⁵	-	-	0.004	0.321	-	-
rs6942123	6	16833106	T	C	0.068	-16734.23	3923.11	1.99x10 ⁻⁵	-	-	0.001	0.634	0.093	-
rs2398132	6	100981200	A	C	0.514	-8004.63	1876.68	2.00x10 ⁻⁵	ASCC3	intron	0.003	-	-	-
rs10850408	12	115380393	T	C	0.321	8026.08	1881.68	2.00x10 ⁻⁵	-	-	0.005	0.263	-	0.136
rs11068326	12	117527314	T	C	0.798	10332.75	2424.41	2.03x10 ⁻⁵	TESC	intron	0.003	0.593	-	-
rs16879290	6	16833699	T	C	0.928	14796.70	3472.48	2.03x10 ⁻⁵	-	-	0.001	0.21	1.258	2.102
rs9491352	6	125596750	A	T	0.170	9875.30	2318.19	2.05x10 ⁻⁵	HDDC2	utr-3; miRNA binding site	0.017	0.12	1.824	0.023
rs11012	17	43513441	T	C	0.187	-9574.18	2254.54	2.17x10 ⁻⁵	PLEKHM1	utr-3	0.001	-	-	-
rs12942666	17	43499839	A	G	0.820	9620.52	2266.42	2.19x10 ⁻⁵	ARHGAP27	intron	0.157	-	-	-
rs1376338	3	64031906	T	C	0.731	-9075.03	2141.00	2.25x10 ⁻⁵	-	-	0	-	1.548	-
rs11155496	6	100988939	T	C	0.515	-7946.55	1875.92	2.27x10 ⁻⁵	ASCC3	intron	0.002	-	-	-
rs4461738	6	100977940	T	C	0.515	-7932.84	1874.27	2.31x10 ⁻⁵	ASCC3	intron	0.044	-	-	-
rs12997383	2	211529850	T	C	0.119	-12372.99	2926.10	2.35x10 ⁻⁵	CPS1	intron	0.002	0.297	0.372	0.694
rs2386314	17	19314296	T	C	0.984	50818.91	12025.90	2.38x10 ⁻⁵	RNF112	near-gene-5	0	1.929	-	-
rs2717025	2	58163146	T	G	0.384	7620.36	1803.76	2.39x10 ⁻⁵	-	-	0.004	-	-	0.938
rs3820151	1	203046534	A	G	0.833	10596.92	2508.49	2.40x10 ⁻⁵	PPFIA4	utr-3	0.026	-	-	-
rs3799716	6	125618558	A	C	0.168	9722.15	2305.77	2.48x10 ⁻⁵	HDDC2	intron	0.022	-	2.065	-
rs3734645	6	125615257	T	C	0.166	9767.92	2317.41	2.50x10 ⁻⁵	HDDC2	intron	0.003	0.699	-	0.348
rs2717026	2	58163178	A	G	0.622	-7586.78	1801.52	2.54x10 ⁻⁵	-	-	0.018	-	-	0.938
rs1417700	6	125614121	A	C	0.163	9741.73	2316.01	2.60x10 ⁻⁵	HDDC2	intron	0.036	0.707	-	0.35

SNP	Chr	Position	Effect Allele	Non-Effect Allele	Freq. Effect Allele	Effect	SE	P*	Gene	Feature**	Cons Score***	Selection Score****		
												CHB/JPT	CEU	YRI
rs9563190	13	54483253	A	C	0.564	-7393.22	1757.92	2.60x10 ⁻⁵	-	-	0	0.283	1.013	-
rs10223874	6	125614421	T	C	0.834	-9734.32	2315.74	2.63x10 ⁻⁵	HDDC2	intron	0	0.707	-	0.35
rs1417701	6	125614100	A	C	0.163	9735.66	2316.18	2.63x10 ⁻⁵	HDDC2	intron	0.019	0.707	-	0.35
rs2527776	1	44345292	A	G	0.749	8316.41	1979.60	2.66x10 ⁻⁵	ST3GAL3	intron	0.109	-	-	-
rs10513432	3	152535365	T	C	0.963	20202.65	4810.57	2.67x10 ⁻⁵	LOC100287091	-	0.001	0.612	0.924	-
rs10513432	3	152535365	T	C	0.963	20202.65	4810.57	2.67x10 ⁻⁵	LOC100287091	-	0.001	0.612	0.924	-
rs2386315	17	19326702	A	G	0.016	-51573.53	12300.07	2.75x10 ⁻⁵	RNF112	-	0.001	1.441	-	-
rs6563272	13	82694749	A	G	0.372	-7530.80	1800.20	2.87x10 ⁻⁵	-	-	0.004	1.064	0.226	0.006
rs16893468	5	64467770	A	G	0.071	-14281.73	3420.46	2.98x10 ⁻⁵	ADAMTS6	intron	0.015	-	-	0.117
rs3807230	7	154476554	T	C	0.302	8995.60	2159.26	3.10x10 ⁻⁵	DPP6	-	0.002	0.302	0.365	0.376
rs311636	8	90605197	A	G	0.799	10489.95	2521.38	3.18x10 ⁻⁵	-	-	0.433	-	0.241	0.136
rs9482637	6	125607559	A	T	0.161	9647.09	2318.93	3.18x10 ⁻⁵	HDDC2	intron	0.003	-	2.304	0.082
rs11707025	3	64055501	T	G	0.730	-8187.32	1974.31	3.37x10 ⁻⁵	LOC100287879	-	0.009	-	-	0.798
rs10744835	12	115353849	A	G	0.298	7906.31	1906.66	3.37x10 ⁻⁵	-	-	0.054	0.62	-	-
rs3760401	17	48846615	A	G	0.519	7956.65	1919.57	3.40x10 ⁻⁵	LUC7L3	-	0.008	-	-	-
rs3760401	17	48846615	A	G	0.519	7956.65	1919.57	3.40x10 ⁻⁵	LUC7L3	-	0.008	-	-	-
rs9565748	13	82736934	T	G	0.632	7464.72	1801.05	3.40x10 ⁻⁵	-	-	0.001	1.171	0.578	1.002
rs7556565	1	44416090	T	C	0.796	8934.44	2157.67	3.46x10 ⁻⁵	IPO13	intron	0.212	-	-	-
rs6563275	13	82792992	A	G	0.634	7448.58	1802.46	3.59x10 ⁻⁵	-	-	0.006	1.208	0.581	0.05
rs6675620	1	44417630	T	C	0.796	8912.59	2157.16	3.60x10 ⁻⁵	IPO13	intron	0.577	1.768	2.637	0.176
rs12947718	17	43493101	A	G	0.181	-9353.11	2266.95	3.69x10 ⁻⁵	ARHGAP27	intron	0	-	0.742	-
rs1576673	13	82706929	T	C	0.633	7460.37	1810.80	3.79x10 ⁻⁵	-	-	0.003	1.037	0.558	-
rs34018943	17	43508303	A	G	0.817	10031.50	2437.88	3.87x10 ⁻⁵	SH3D20	intron	0.157	-	-	-
rs4448553	1	44411589	A	G	0.206	-8880.75	2158.99	3.90x10 ⁻⁵	IPO13	near-gene-5	0.136	-	-	-
rs2906466	1	44322220	A	G	0.246	-8382.14	2037.85	3.90x10 ⁻⁵	ST3GAL3	intron	0	-	-	-
rs10962382	9	16335469	A	C	0.667	8246.24	2004.98	3.91x10 ⁻⁵	-	-	0.01	0.302	2.807	-
rs1450985	3	64060128	A	G	0.438	7373.44	1793.00	3.92x10 ⁻⁵	LOC100287879	-	0	-	0.108	-
rs1450985	3	64060128	A	G	0.438	7373.44	1793.00	3.92x10 ⁻⁵	LOC100287879	-	0	-	0.108	-
rs11036844	11	42345388	T	C	0.038	-70977.01	17274.78	3.98x10 ⁻⁵	-	-	0.039	-	-	0.069
rs10500786	11	13583784	A	G	0.479	7134.77	1737.37	4.01x10 ⁻⁵	-	-	0.011	-	-	-

SNP	Chr	Position	Effect Allele	Non-Effect Allele	Freq. Effect Allele	Effect	SE	P*	Gene	Feature**	Cons Score***	Selection Score****		
												CHB/JPT	CEU	YRI
rs2389851	7	17796043	T	G	0.987	52974.42	12908.22	4.06x10 ⁻⁵	-	-	0.001	-	-	1.375
rs9300042	11	42349961	C	G	0.962	70991.95	17305.47	4.09x10 ⁻⁵	-	-	0.581	-	-	-
rs2301993	1	44426025	A	G	0.793	8865.57	2161.24	4.10x10 ⁻⁵	IPO13	intron	0.142	-	-	0.395
rs11036848	11	42351806	A	C	0.962	71033.89	17328.29	4.14x10 ⁻⁵	-	-	0.005	-	-	-
rs7905091	10	100046078	T	G	0.138	10986.81	2683.09	4.23x10 ⁻⁵	LOXL4	-	0.024	-	-	0.624
rs11052734	12	33663573	T	C	0.974	71208.15	17411.09	4.32x10 ⁻⁵	-	-	0.01	-	-	-
rs2329212	13	82766617	T	C	0.367	-7406.11	1812.44	4.38x10 ⁻⁵	-	-	0.005	1.234	0.807	1.108
rs11069727	13	108937833	A	G	0.750	9771.94	2396.96	4.57x10 ⁻⁵	TNFSF13B	intron	0.024	-	-	-
rs2469206	15	77247268	A	G	0.784	-8793.67	2159.50	4.66x10 ⁻⁵	RCN2	-	0.947	0.326	0.05	-
rs2469206	15	77247268	A	G	0.784	-8793.67	2159.50	4.66x10 ⁻⁵	RCN2	-	0.947	0.326	0.05	-
rs867322	4	153878480	A	G	0.564	-7461.99	1833.08	4.69x10 ⁻⁵	FHDC1	intron	0.533	0.06	0.874	0.916
rs4789658	17	72389526	A	T	0.105	-12829.84	3156.67	4.82x10 ⁻⁵	-	-	0.129	-	-	0.38

* P-values are double genome controlled. **SNP features from dbSNP (<http://www.ncbi.nlm.nih.gov/SNP/>) ; ***PhastCons Conservation score from UCSC Genome Browser: probability that each nucleotide belongs to a conserved element (<http://hgdownload.cse.ucsc.edu/>) ; ****Positive selection scores of SNPs from <http://haplotter.uchicago.edu/selection>

Supplementary Table 17: Non-significant replications for all phenotypes.

Replication was attempted for the top 5 SNPs for each analysis. Only one SNP per locus is shown. Discovery sample *P*-values are double genome controlled. The combined p-values including all replication samples is shown in bold.

Sample	N	Freq. effect allele	B	SE	P-value	Heterogeneity P-value	% Variance Explained
<u>Mean Hippocampal Volume correcting for Sex, Age, Age², Sex*Age, Sex*Age² - including Patients</u>							
rs17580572 (Chromosome 6:16261941, Effect Allele:A, Non-effect Allele:G)							
Discovery - fixed effects	7794	0.194	41.64	8.47	8.85x10 ⁻⁷	0.851	0.279
ENIGMA CEU/TSI replication	449	0.184	73.42	41.58	0.077	0.614	0.492
ENIGMA CEU+YRI or MEX replication	842	0.285	-22.31	21.38	0.297	0.143	0.115
CHARGE replication	10663	0.201	1.25	5.60	0.823	0.501	0.001
Discovery + Replications	19748	0.207	13.19	4.53	0.004	5.94x10 ⁻⁵	0.038
rs752834 (Chromosome 2:111515129, Effect Allele:A, Non-effect Allele:G)							
Discovery - fixed effects	7794	0.191	-37.50	8.09	3.60x10 ⁻⁶	0.460	0.224
ENIGMA CEU/TSI replication	449	0.193	-17.38	41.52	0.676	0.021	0.029
ENIGMA CEU+YRI or MEX replication	842	0.154	-44.80	25.25	0.076	0.151	0.295
CHARGE replication	10358	0.197	-7.20	5.75	0.201	0.774	0.016
Discovery + Replications	19443	0.194	-17.65	4.57	1.11x10⁻⁴	0.025	0.064
<u>Mean Hippocampal Volume correcting for Sex, Age, Age², Sex*Age, Sex*Age² - excluding Patients</u>							
rs1456520 (Chromosome 2:199480836, Effect Allele:T, Non-effect Allele:C)							
Discovery - fixed effects	5775	0.951	-74.11	15.59	2.04x10 ⁻⁶	0.521	0.263
ENIGMA CEU/TSI replication	216	0.962	-135.53	256.34	0.597	1.000	0.408
ENIGMA CEU+YRI or MEX replication	699	0.485	-58.63	28.04	0.037	0.548	0.969
CHARGE replication	9280	0.961	13.30	12.50	0.287	0.247	0.013
Discovery + Replications	15970	0.902	-15.30	9.65	0.112	0.005	0.027

Sample	N	Freq. effect allele	B	SE	P-value	Heterogeneity P-value	% Variance Explained
<u><i>Estimated Intracranial Volume correcting for Sex, Age, Age², Sex*Age, Sex*Age² - excluding Patients</i></u>							
rs1800197 (Chromosome 5:177352573, Effect Allele:T, Non-effect Allele:C)							
Discovery - fixed effects	5778	0.284	12282.29	2636.49	3.18x10 ⁻⁶	0.018	0.245
ENIGMA CEU/TSI replication	59	0.308	19870.67	49092.25	0.686	1.000	0.404
ENIGMA CEU+YRI or MEX replication	699	0.242	4183.00	7325.81	0.568	0.225	0.031
CHARGE replication	8175	0.300	-950.34	1898.43	0.617	NA	0.002
Discovery + Replications	14711	0.293	3609.34	1506.91	0.016	0.0008	0.021
rs10125582 (Chromosome 9:8125549, Effect Allele:T, Non-effect Allele:C)							
Discovery - fixed effects	5778	0.736	13667.74	2793.92	9.99x10 ⁻⁷	0.952	0.290
ENIGMA CEU/TSI replication	59	0.756	-25909.80	46364.90	0.576	1.000	0.594
ENIGMA CEU+YRI or MEX replication	699	0.662	-1823.38	6567.22	0.781	0.850	0.007
CHARGE replication (proxy rs1416595)	8175	0.756	-556.90	1915.38	0.771	NA	0.000
Discovery + Replications	14711	0.745	3640.51	1535.13	0.018	3.25x10 ⁻⁴	0.019
rs8110509 (Chromosome 19:35673479, Effect Allele:A, Non-effect Allele:C)							
Discovery - fixed effects	5778	0.205	14217.68	2938.81	1.31x10 ⁻⁶	0.810	0.264
ENIGMA CEU/TSI replication	59	0.249	-75976.10	44611.60	0.089	1.000	5.182
ENIGMA CEU+YRI or MEX replication	699	0.180	4404.03	7734.56	0.569	0.917	0.028
CHARGE replication	8175	0.202	1279.08	2013.59	0.525	NA	0.002
Discovery + Replications	14711	0.201	5260.55	1622.98	1.19x10⁻³	3.49x10 ⁻³	0.034

Sample	N	Freq. effect allele	B	SE	P-value	Heterogeneity P-value	% Variance Explained
<u>Total Brain Volume correcting for Sex, Age, Age², Sex*Age, Sex*Age² - excluding Patients</u>							
rs1998338 (Chromosome 9:8130651, Effect Allele:A, Non-effect Allele:G)							
Discovery - fixed effects	5778	0.243	-10028.92	2039.06	8.72x10 ⁻⁷	0.723	0.256
ENIGMA MEX replication	605	0.293	-2681.43	5604.54	0.632	NA	0.023
Discovery + Replications	6383	0.250	-9170.04	1916.18	1.71x10⁻⁶	0.218	0.220
rs911763 (Chromosome 9:8123859, Effect Allele:T, Non-effect Allele:G)							
Discovery - fixed effects	5778	0.747	9921.76	2031.22	1.04x10 ⁻⁶	0.758	0.258
ENIGMA MEX replication	605	0.686	3072.71	5627.55	0.585	NA	0.031
Discovery + Replications	6383	0.740	9132.32	1910.57	1.75x10⁻⁶	0.3466	0.225
rs2173141 (Chromosome 13:81539340, Effect Allele:T, Non-effect Allele:C)							
Discovery - fixed effects	5778	0.369	-7930.85	1798.31	1.03x10 ⁻⁵	0.354	0.203
ENIGMA MEX replication	605	0.497	6433.13	5132.70	0.211	NA	0.157
Discovery + Replications	6383	0.383	-6360.39	1697.16	1.79x10⁻³	8.26x10 ⁻³	0.134
rs4789658 (Chromosome 17:69901121, Effect Allele:A, Non-effect Allele:T)							
Discovery - fixed effects	4541	0.105	-12829.84	3156.67	4.82x10 ⁻⁵	0.049	0.215
ENIGMA MEX replication	605	0.160	-22164.96	7123.63	0.002	NA	1.005
Discovery + Replications	5146	0.114	-14362.03	2886.01	6.47x10⁻⁷	0.230	0.294
rs6093346 (Chromosome 20:38500329, Effect Allele:A, Non-effect Allele:G)							
Discovery - fixed effects	5778	0.061	-18873.02	3815.67	7.52x10 ⁻⁷	0.145	0.283
ENIGMA MEX replication	605	0.079	29023.89	10403.49	0.005	NA	0.933
Discovery + Replications	6383	0.063	-13193.56	3582.44	2.31x10⁻³	1.54x10 ⁻⁵	0.144

Supplementary Table 18: Gene-based analysis of total brain volume without patients correcting for Sex, Age, Age², Sex*Age, Sex*Age², MDS.

SNP *P*-values are double genome controlled.

Gene	Gene <i>P</i>	Chromosome	Start Position	Length	SNP	Position	Features	SNP <i>P</i>
PSMD6	3.49x10 ⁻⁵	3	63976231	52889	rs6808752	64024529	-	4.07x10 ⁻⁶
-	-	-	-	-	rs6764606	64020447	-	4.93x10 ⁻⁶
-	-	-	-	-	rs13087186	64012756	-	1.89x10 ⁻⁴
-	-	-	-	-	rs13093232	64019642	-	2.97x10 ⁻³
-	-	-	-	-	rs40610	64009508	near-gene-5	5.14x10 ⁻³
-	-	-	-	-	rs166229	64021228	-	1.27x10 ⁻²
-	-	-	-	-	rs3816157	63999322	intron	3.08x10 ⁻²
-	-	-	-	-	rs2578011	64004819	intron	3.69x10 ⁻²
-	-	-	-	-	rs35837	64013249	-	3.72x10 ⁻²
PLEKHM1	4.80x10 ⁻⁵	17	43493266	94880	rs17631676	43549526	intron	1.35x10 ⁻⁵
-	-	-	-	-	rs11012	43513441	utr-3	2.17x10 ⁻⁵
-	-	-	-	-	rs7218394	43553150	intron	2.75x10 ⁻²

Supplementary Table 19: Gene-based analysis of total intracranial volume without patients correcting for Sex, Age, Age², Sex*Age, Sex* Age², MDS.

SNP *P*-values are double genome controlled.

Gene	Gene <i>P</i>	Chromosome	Start Position	Length	SNP	Position	Features	SNP <i>P</i>
HMGA2	7.17x10 ⁻⁶	12	66213240	151831	rs10784502	66343810	intron	3.14x10 ⁻⁷
-	-	-	-	-	rs8756	66359752	utr-3	7.22x10 ⁻⁷
-	-	-	-	-	rs1351394	66351826	intron	9.26x10 ⁻⁷
-	-	-	-	-	rs1042725	66358347	utr-3	2.70x10 ⁻⁶
-	-	-	-	-	rs12298541	66306441	intron	5.18x10 ⁻⁶
-	-	-	-	-	rs1480474	66326943	intron	9.01x10 ⁻⁶
-	-	-	-	-	rs7968902	66363070	-	2.75x10 ⁻⁵
-	-	-	-	-	rs1979440	66346624	intron	8.49x10 ⁻⁵
-	-	-	-	-	rs7487625	66319996	intron	1.32x10 ⁻⁴
-	-	-	-	-	rs12422370	66363539	-	7.26x10 ⁻⁴
-	-	-	-	-	rs12424086	66364509	-	8.95x10 ⁻⁴
-	-	-	-	-	rs2272047	66236735	intron	1.02x10 ⁻³
-	-	-	-	-	rs10878346	66320873	intron	1.12x10 ⁻³
-	-	-	-	-	rs11175944	66256395	intron	1.16x10 ⁻³
-	-	-	-	-	rs1460126	66261977	intron	1.16x10 ⁻³
-	-	-	-	-	rs11834900	66247051	intron	1.25x10 ⁻³
-	-	-	-	-	rs7961706	66241898	intron	1.39x10 ⁻³
-	-	-	-	-	rs17179670	66349812	intron	1.47x10 ⁻³
-	-	-	-	-	rs10878344	66303735	intron	3.39x10 ⁻³
-	-	-	-	-	rs1563834	66298031	intron	5.89x10 ⁻³
-	-	-	-	-	rs343092	66250940	intron	8.67x10 ⁻³
-	-	-	-	-	rs17101853	66284873	intron	1.16x10 ⁻²
-	-	-	-	-	rs1460122	66231117	intron	2.08x10 ⁻²
-	-	-	-	-	rs11175947	66284336	intron	2.71x10 ⁻²
-	-	-	-	-	rs7959396	66256947	intron	2.85x10 ⁻²
-	-	-	-	-	rs17101839	66245568	intron	2.87x10 ⁻²
-	-	-	-	-	rs1480469	66346121	intron	2.90x10 ⁻²
-	-	-	-	-	rs7979673	66227257	intron	3.15x10 ⁻²

Gene	Gene P	Chromosome	Start Position	Length	SNP	Position	Features	SNP P
-	-	-	-	-	rs6581658	66217345	near-gene-5	3.44x10 ⁻²
-	-	-	-	-	rs189339	66252294	intron	3.58x10 ⁻²
-	-	-	-	-	rs7977687	66216073	-	4.70x10 ⁻²
PROP1	1.57x10 ⁻⁵	5	177414236	14007	rs1800197	177419967	missense	3.18x10 ⁻⁶
-	-	-	-	-	rs4072924	177422823	intron	1.42x10 ⁻³
-	-	-	-	-	rs6883364	177418754	near-gene-3	1.79x10 ⁻³
-	-	-	-	-	rs6601199	177418027	-	6.03x10 ⁻³
CD93	1.81x10 ⁻⁵	20	23054993	16984	rs2749812	23062927	utr-3	2.85x10 ⁻⁶
-	-	-	-	-	rs2749817	23059255	-	1.28x10 ⁻⁴
-	-	-	-	-	rs2749813	23062984	utr-3	2.15x10 ⁻⁴
-	-	-	-	-	rs1998080	23057347	-	1.17x10 ⁻³
-	-	-	-	-	rs6048544	23071031	-	2.80x10 ⁻³
-	-	-	-	-	rs17682491	23057867	-	7.81x10 ⁻³
-	-	-	-	-	rs17682515	23059279	-	8.35x10 ⁻³
-	-	-	-	-	rs3746731	23065209	missense	9.75x10 ⁻³
-	-	-	-	-	rs6076019	23064279	utr-3	1.12x10 ⁻²
-	-	-	-	-	rs6137821	23067799	near-gene-5	1.91x10 ⁻²
-	-	-	-	-	rs7492	23060257	utr-3	3.01x10 ⁻²
MGC57346	5.33x10 ⁻⁵	17	43692712	27617	rs389217	43717131	-	5.33x10 ⁻⁵
-	-	-	-	-	rs413778	43716885	-	5.59x10 ⁻⁵
-	-	-	-	-	rs439558	43717803	-	1.20x10 ⁻⁴
-	-	-	-	-	rs393152	43719143	-	1.31x10 ⁻⁴
ZNF536	5.57x10 ⁻⁵	19	30858328	195637	rs8110509	30981639	intron	1.31x10 ⁻⁶
-	-	-	-	-	rs8100439	30983806	intron	2.62x10 ⁻⁵
-	-	-	-	-	rs3786791	31026875	intron	1.92x10 ⁻⁴
-	-	-	-	-	rs12459057	30996525	intron	2.44x10 ⁻⁴
-	-	-	-	-	rs9676954	31008054	intron	2.54x10 ⁻⁴
-	-	-	-	-	rs8101081	31049031	near-gene-3	2.95x10 ⁻⁴
-	-	-	-	-	rs10518269	31028666	intron	3.24x10 ⁻⁴
-	-	-	-	-	rs919803	30987104	intron	3.85x10 ⁻⁴
-	-	-	-	-	rs7253628	31047269	intron	5.01x10 ⁻⁴
-	-	-	-	-	rs7248805	31018491	intron	7.67x10 ⁻⁴

Gene	Gene P	Chromosome	Start Position	Length	SNP	Position	Features	SNP P
-	-	-	-	-	rs6510168	31049006	near-gene-3	1.07×10^{-3}
-	-	-	-	-	rs16964244	30984109	intron	1.19×10^{-3}
-	-	-	-	-	rs1004046	30992639	intron	1.30×10^{-3}
-	-	-	-	-	rs7250841	31041411	intron	2.04×10^{-3}
-	-	-	-	-	rs7250115	31033472	intron	2.68×10^{-3}
-	-	-	-	-	rs8112930	31036269	intron	3.27×10^{-3}
-	-	-	-	-	rs1469705	31038995	coding-synonymous	4.56×10^{-3}
-	-	-	-	-	rs12980596	31015438	intron	5.99×10^{-3}
-	-	-	-	-	rs6510167	31044025	intron	1.16×10^{-2}
-	-	-	-	-	rs10421376	31028277	intron	1.53×10^{-2}
-	-	-	-	-	rs3786811	30952806	intron	2.77×10^{-2}
-	-	-	-	-	rs12974244	30954080	intron	2.83×10^{-2}
-	-	-	-	-	rs8110100	30950800	intron	3.39×10^{-2}
ZNF408	5.74×10^{-5}	11	46717317	15149	rs10769205	46723603	intron	5.74×10^{-5}
-	-	-	-	-	rs12361673	46723937	intron	4.54×10^{-4}
C17orf69	7.00×10^{-5}	17	43711341	17254	rs389217	43717131	-	5.33×10^{-5}
-	-	-	-	-	rs413778	43716885	-	5.59×10^{-5}
-	-	-	-	-	rs453997	43727061	-	7.29×10^{-5}
-	-	-	-	-	rs439558	43717803	-	1.20×10^{-4}
-	-	-	-	-	rs393152	43719143	-	1.31×10^{-4}
-	-	-	-	-	rs417968	43728376	-	3.79×10^{-4}
LOC100132570	7.16×10^{-5}	17	44339778	11282	rs2732711	44350293	-	3.72×10^{-5}
-	-	-	-	-	rs2532345	44343902	-	2.22×10^{-4}
TAF5	8.44×10^{-5}	10	105122724	31098	rs11191672	105138961	intron	3.97×10^{-5}
-	-	-	-	-	rs11191666	105127278	near-gene-5	4.45×10^{-5}
-	-	-	-	-	rs10883858	105127708	near-gene-5	4.68×10^{-5}
-	-	-	-	-	rs7905968	105135319	intron	4.95×10^{-5}
-	-	-	-	-	rs10883857	105127587	near-gene-5	5.14×10^{-5}
-	-	-	-	-	rs10883861	105129665	intron	1.08×10^{-2}

Supplementary Table 20: Gene-based analysis of mean bilateral hippocampal volume including patients correcting for Sex, Age, Age², Sex*Age, Sex* Age², MDS.

SNP *P*-values are double genome controlled.

Gene	Gene <i>P</i>	Chromosome	Start Position	Length	SNP	Position	Features	SNP <i>P</i>
HRK	1.18x10 ⁻⁵	12	117294027	30205	rs7315280	117320938	near-gene-5	1.75x10 ⁻⁶
-	-	-	-	-	rs7132910	117320658	near-gene-5	1.81x10 ⁻⁶
-	-	-	-	-	rs10507275	117294504	-	1.75x10 ⁻²
-	-	-	-	-	rs1112700	117306205	intron	3.00x10 ⁻²
PTK2	8.54x10 ⁻⁵	8	141663501	352831	rs3639	141684170	intron	1.16x10 ⁻⁵
-	-	-	-	-	rs4961287	141706320	intron	1.25x10 ⁻⁵
-	-	-	-	-	rs11997161	141738587	intron	1.37x10 ⁻⁵
-	-	-	-	-	rs13257090	141729463	intron	1.89x10 ⁻⁵
-	-	-	-	-	rs6993266	141762659	intron	2.02x10 ⁻⁵
-	-	-	-	-	rs6994744	141740868	intron	2.13x10 ⁻⁵
-	-	-	-	-	rs10111852	141937541	intron	1.15x10 ⁻⁴
-	-	-	-	-	rs7820179	141701476	intron	1.61x10 ⁻⁴
-	-	-	-	-	rs4413752	141688972	intron	4.14x10 ⁻⁴
-	-	-	-	-	rs10089107	141698451	intron	4.27x10 ⁻⁴
-	-	-	-	-	rs7831543	141847249	intron	5.29x10 ⁻⁴
-	-	-	-	-	rs11166992	141677470	intron	5.56x10 ⁻⁴
-	-	-	-	-	rs13273096	141675931	intron	5.60x10 ⁻⁴
-	-	-	-	-	rs11166990	141663972	-	5.82x10 ⁻⁴
-	-	-	-	-	rs12156014	141853518	intron	5.86x10 ⁻⁴
-	-	-	-	-	rs4961230	141722084	intron	6.34x10 ⁻⁴
-	-	-	-	-	rs7839832	141728474	intron	6.51x10 ⁻⁴
-	-	-	-	-	rs11166991	141666413	-	6.62x10 ⁻⁴
-	-	-	-	-	rs4961234	141840881	intron	7.06x10 ⁻⁴
-	-	-	-	-	rs13280245	141727310	intron	7.21x10 ⁻⁴
-	-	-	-	-	rs11166995	141719251	intron	7.63x10 ⁻⁴
-	-	-	-	-	rs4246128	141840739	intron	7.63x10 ⁻⁴
-	-	-	-	-	rs13251663	141841577	intron	7.71x10 ⁻⁴
-	-	-	-	-	rs7001591	141834000	intron	7.80x10 ⁻⁴

Gene	Gene P	Chromosome	Start Position	Length	SNP	Position	Features	SNP P
-	-	-	-	-	rs4434666	141840168	intron	7.81x10 ⁻⁴
-	-	-	-	-	rs4961237	141902493	intron	8.49x10 ⁻⁴
-	-	-	-	-	rs9650572	141831989	intron	9.70x10 ⁻⁴
-	-	-	-	-	rs10088475	141670266	intron	9.79x10 ⁻⁴
-	-	-	-	-	rs10090774	141826739	intron	9.92x10 ⁻⁴
-	-	-	-	-	rs10283368	141679817	intron	1.07x10 ⁻³
-	-	-	-	-	rs13268978	141679385	intron	1.09x10 ⁻³
-	-	-	-	-	rs7840381	141774282	intron	1.15x10 ⁻³
-	-	-	-	-	rs4961290	141751712	intron	1.21x10 ⁻³
-	-	-	-	-	rs11786116	141864096	intron	1.22x10 ⁻³
-	-	-	-	-	rs10105905	141860895	intron	1.23x10 ⁻³
-	-	-	-	-	rs13271554	141873688	intron	1.26x10 ⁻³
-	-	-	-	-	rs3923115	141754451	intron	1.31x10 ⁻³
-	-	-	-	-	rs4246126	141790892	intron	1.31x10 ⁻³
-	-	-	-	-	rs11167005	141883156	intron	1.33x10 ⁻³
-	-	-	-	-	rs4961233	141808948	intron	1.33x10 ⁻³
-	-	-	-	-	rs11775840	141883233	intron	1.33x10 ⁻³
-	-	-	-	-	rs6992780	141911621	intron	1.40x10 ⁻³
-	-	-	-	-	rs1868280	141896254	intron	1.42x10 ⁻³
-	-	-	-	-	rs4961289	141748265	intron	1.45x10 ⁻³
-	-	-	-	-	rs10875458	141779826	intron	1.45x10 ⁻³
-	-	-	-	-	rs4246123	141775168	intron	1.47x10 ⁻³
-	-	-	-	-	rs7008498	141877028	intron	1.52x10 ⁻³
-	-	-	-	-	rs11781505	141933729	intron	1.58x10 ⁻³
-	-	-	-	-	rs13255947	141911445	intron	1.72x10 ⁻³
-	-	-	-	-	rs13261338	141891821	intron	1.79x10 ⁻³
-	-	-	-	-	rs4291312	141826138	intron	1.84x10 ⁻³
-	-	-	-	-	rs4961300	141910867	intron	1.89x10 ⁻³
-	-	-	-	-	rs13279233	141946474	intron	2.02x10 ⁻³
-	-	-	-	-	rs10089610	141921613	intron	2.04x10 ⁻³
-	-	-	-	-	rs11777839	141917894	intron	2.09x10 ⁻³
-	-	-	-	-	rs13270490	141961179	intron	2.14x10 ⁻³

Gene	Gene P	Chromosome	Start Position	Length	SNP	Position	Features	SNP P
-	-	-	-	-	rs13250787	141916932	intron	2.17×10^{-3}
-	-	-	-	-	rs10111363	141928350	intron	2.31×10^{-3}
-	-	-	-	-	rs11167010	141954210	intron	2.32×10^{-3}
-	-	-	-	-	rs10106750	142004909	intron	2.33×10^{-3}
-	-	-	-	-	rs11778798	141918880	intron	2.35×10^{-3}
-	-	-	-	-	rs11785430	142009527	intron	2.49×10^{-3}
-	-	-	-	-	rs7843337	141962642	intron	2.51×10^{-3}
-	-	-	-	-	rs7816620	142004114	intron	2.59×10^{-3}
-	-	-	-	-	rs7813058	142004193	intron	2.86×10^{-3}
-	-	-	-	-	rs11167018	142003311	intron	3.08×10^{-3}
-	-	-	-	-	rs1375062	141965781	intron	3.11×10^{-3}
-	-	-	-	-	rs7831770	142000187	intron	3.18×10^{-3}
-	-	-	-	-	rs1397380	142003054	intron	3.19×10^{-3}
-	-	-	-	-	rs12680723	141994803	intron	3.36×10^{-3}
-	-	-	-	-	rs12548549	141967272	intron	3.48×10^{-3}
-	-	-	-	-	rs4440675	141975457	intron	3.96×10^{-3}
-	-	-	-	-	rs13276704	141993696	intron	4.02×10^{-3}
-	-	-	-	-	rs11167016	141995180	intron	4.11×10^{-3}
-	-	-	-	-	rs11167015	141991440	intron	4.16×10^{-3}
-	-	-	-	-	rs11781807	141994393	intron	4.23×10^{-3}
-	-	-	-	-	rs1031262	141985905	intron	4.58×10^{-3}
-	-	-	-	-	rs7007003	141966167	intron	4.94×10^{-3}
-	-	-	-	-	rs11991796	141898518	intron	7.84×10^{-3}
-	-	-	-	-	rs7839119	141705106	intron	2.74×10^{-2}

Supplementary Table 21: Gene-based analysis of mean bilateral hippocampal volume without patients correcting for Sex, Age, Age², Sex*Age, Sex* Age², MDS.

SNP *P*-values are double genome controlled.

Gene	Gene <i>P</i>	Chromosome	Start Position	Length	SNP	Position	Features	SNP <i>P</i>
LOC100421531	2.31x10 ⁻⁵	7	36166443	41191	rs10951458	36170199	-	2.21x10 ⁻⁶
-	-	-	-	-	rs2700904	36186050	-	9.18x10 ⁻⁴
-	-	-	-	-	rs4720196	36183300	-	7.23x10 ⁻³
-	-	-	-	-	rs12530870	36181501	-	7.47x10 ⁻³
-	-	-	-	-	rs11974973	36184850	-	7.53x10 ⁻³
-	-	-	-	-	rs1882062	36188719	-	7.76x10 ⁻³
-	-	-	-	-	rs17264903	36171893	-	7.79x10 ⁻³
-	-	-	-	-	rs2700897	36177089	-	9.12x10 ⁻³
-	-	-	-	-	rs2700899	36178740	-	1.09x10 ⁻²
-	-	-	-	-	rs2726072	36174104	-	1.14x10 ⁻²
-	-	-	-	-	rs11979422	36177479	-	1.27x10 ⁻²
-	-	-	-	-	rs11975199	36178054	-	1.30x10 ⁻²
-	-	-	-	-	rs6952488	36173281	-	1.57x10 ⁻²
LOC100131159	8.33x10 ⁻⁵	6	16141165	41733	rs17580572	16153962	-	1.58x10 ⁻⁵
-	-	-	-	-	rs17641827	16157119	-	1.14x10 ⁻⁴
-	-	-	-	-	rs2072779	16153745	-	1.01x10 ⁻²
-	-	-	-	-	rs2038037	16175295	-	2.91x10 ⁻²
MLF2	8.86x10 ⁻⁵	12	6837158	45478	rs7970575	6858971	intron	1.25x10 ⁻⁵
-	-	-	-	-	rs2302371	6858126	coding-synonymous	3.40x10 ⁻⁵
-	-	-	-	-	rs11064338	6846045	-	1.91x10 ⁻³
-	-	-	-	-	rs11064356	6852447	-	3.03x10 ⁻³
-	-	-	-	-	rs7296292	6854843	-	5.40x10 ⁻³
-	-	-	-	-	rs2302368	6859797	intron	1.17x10 ⁻²
-	-	-	-	-	rs1997510	6871891	-	1.29x10 ⁻²
-	-	-	-	-	rs2302367	6861043	intron	1.84x10 ⁻²
-	-	-	-	-	rs12578573	6842959	-	2.07x10 ⁻²
-	-	-	-	-	rs7135106	6871499	-	4.01x10 ⁻²

Supplementary Table 22: Gene-based analysis of mean bilateral hippocampal volume including patients correcting for Sex, Age, Age², Sex*Age, Sex* Age², MDS, ICV.

SNP *P*-values are double genome controlled.

Gene	Gene <i>P</i>	Chromosome	Start Position	Length	SNP	Position	Features	SNP <i>P</i>
RPL36P15	1.15x10 ⁻⁶	12	117326117	40319	rs7294919	117327592	-	2.42x10 ⁻⁷
-	-	-	-	-	rs7132339	117335912	-	4.87x10 ⁻⁶
-	-	-	-	-	rs4767469	117326854	-	9.44x10 ⁻⁴
HRK	1.37x10 ⁻⁶	12	117279027	60205	rs7315280	117320938	near-gene-5	1.40x10 ⁻⁷
-	-	-	-	-	rs7132910	117320658	near-gene-5	1.95x10 ⁻⁷
-	-	-	-	-	rs7294919	117327592	-	2.42x10 ⁻⁷
-	-	-	-	-	rs7132339	117335912	-	4.87x10 ⁻⁶
-	-	-	-	-	rs4767469	117326854	-	9.44x10 ⁻⁴
-	-	-	-	-	rs9669553	117315349	intron	1.73x10 ⁻²
-	-	-	-	-	rs7972948	117312199	intron	2.04x10 ⁻²
-	-	-	-	-	rs884378	117308198	intron	2.83x10 ⁻²
BRD7P6	1.32x10 ⁻⁵	2	70549227	53823	rs13394815	70564002	-	9.27x10 ⁻⁷
-	-	-	-	-	rs6751950	70560939	-	2.16x10 ⁻⁵
-	-	-	-	-	rs1478644	70576997	-	7.44x10 ⁻⁵
-	-	-	-	-	rs4852161	70562650	-	7.93x10 ⁻⁵
-	-	-	-	-	rs1871238	70574318	-	1.86x10 ⁻⁴
-	-	-	-	-	rs4852506	70554285	-	1.79x10 ⁻²
-	-	-	-	-	rs4852500	70549778	-	1.93x10 ⁻²
-	-	-	-	-	rs11126264	70572693	-	2.23x10 ⁻²
-	-	-	-	-	rs6750178	70556337	-	4.30x10 ⁻²
RPL7AP52	3.05x10 ⁻⁵	10	96622321	40785	rs4110517	96650328	-	6.37x10 ⁻⁶
-	-	-	-	-	rs9888067	96648224	-	6.96x10 ⁻⁶
-	-	-	-	-	rs4466755	96632253	-	1.10x10 ⁻³
-	-	-	-	-	rs11188105	96647117	-	1.38x10 ⁻³
-	-	-	-	-	rs11595422	96640715	-	1.64x10 ⁻³
FBXW8	7.16x10 ⁻⁵	12	117328761	160192	rs7132339	117335912	-	4.87x10 ⁻⁶
-	-	-	-	-	rs4767492	117436861	intron	9.49x10 ⁻⁴
-	-	-	-	-	rs11068296	117467372	utr-3	2.86x10 ⁻³

Gene	Gene P	Chromosome	Start Position	Length	SNP	Position	Features	SNP P
-	-	-	-	-	rs4076700	117383320	missense	5.04x10 ⁻³
-	-	-	-	-	rs4767474	117366338	intron	5.07x10 ⁻³
-	-	-	-	-	rs7973925	117476143	-	5.39x10 ⁻³
-	-	-	-	-	rs4767489	117422392	intron	5.94x10 ⁻³
-	-	-	-	-	rs4562927	117363166	intron	5.96x10 ⁻³
-	-	-	-	-	rs7302025	117442902	intron	6.06x10 ⁻³
-	-	-	-	-	rs4542506	117398448	intron	6.50x10 ⁻³
-	-	-	-	-	rs7973240	117408148	intron	6.75x10 ⁻³
-	-	-	-	-	rs4767484	117406001	intron	7.01x10 ⁻³
-	-	-	-	-	rs7297848	117443591	intron	7.71x10 ⁻³
-	-	-	-	-	rs10735102	117410159	intron	7.85x10 ⁻³
-	-	-	-	-	rs4766815	117374508	intron	8.16x10 ⁻³
-	-	-	-	-	rs10850743	117462785	intron	8.16x10 ⁻³
-	-	-	-	-	rs2393111	117382290	intron	9.56x10 ⁻³
-	-	-	-	-	rs4562925	117362453	intron	9.69x10 ⁻³
-	-	-	-	-	rs11068277	117424506	intron	9.78x10 ⁻³
-	-	-	-	-	rs4130296	117386085	intron	9.79x10 ⁻³
-	-	-	-	-	rs4767473	117365506	intron	1.02x10 ⁻²
-	-	-	-	-	rs11068264	117396097	intron	1.07x10 ⁻²
-	-	-	-	-	rs12302906	117474662	-	1.63x10 ⁻²
-	-	-	-	-	rs12299065	117442304	intron	1.98x10 ⁻²
-	-	-	-	-	rs4767490	117435016	intron	1.99x10 ⁻²
-	-	-	-	-	rs7131746	117423264	intron	2.00x10 ⁻²
-	-	-	-	-	rs7311972	117425436	intron	2.33x10 ⁻²
-	-	-	-	-	rs10774896	117435999	intron	2.60x10 ⁻²
LOC100131159	8.69x10 ⁻⁵	6	16141165	41733	rs17580572	16153962	-	1.64x10 ⁻⁵
-	-	-	-	-	rs17641827	16157119	-	8.85x10 ⁻⁴
-	-	-	-	-	rs2072779	16153745	-	1.66x10 ⁻³
-	-	-	-	-	rs2038037	16175295	-	2.91x10 ⁻³

Supplementary Table 23: Gene-based analysis of mean bilateral hippocampal volume without patients correcting for Sex, Age, Age², Sex*Age, Sex* Age², MDS, ICV.

SNP *P*-values are double genome controlled.

Gene	Gene <i>P</i>	Chromosome	Start Position	Length	SNP	Position	Features	SNP <i>P</i>
BRD7P6	3.38 x10 ⁻⁵	2	70549227	53823	rs13394815	70564002	-	2.38 x10 ⁻⁶
-	-	-	-	-	rs1478644	70576997	-	2.29 x10 ⁻⁴
-	-	-	-	-	rs6751950	70560939	-	2.81 x10 ⁻⁴
-	-	-	-	-	rs4852161	70562650	-	6.61 x10 ⁻⁴
-	-	-	-	-	rs1871238	70574318	-	1.04 x10 ⁻³
-	-	-	-	-	rs4852500	70549778	-	3.91 x10 ⁻³
-	-	-	-	-	rs4852506	70554285	-	4.03 x10 ⁻³
-	-	-	-	-	rs6750178	70556337	-	6.55 x10 ⁻³
-	-	-	-	-	rs2862843	70550490	-	8.99 x10 ⁻³
-	-	-	-	-	rs13001282	70567734	-	4.54 x10 ⁻²

Supplementary Table 24: Gene-based analysis of mean bilateral hippocampal volume including patients correcting for Sex, Age, Age², Sex*Age, Sex* Age², MDS, TBV.

SNP *P*-values are double genome controlled.

Gene	Gene <i>P</i>	Chromosome	Start Position	Length	SNP	Position	Features	SNP <i>P</i>
RPL36P15	2.74x10 ⁻⁶	12	117326117	40319	rs7294919	117327592	-	5.78x10 ⁻⁷
-	-	-	-	-	rs7132339	117335912	-	7.26x10 ⁻⁶
-	-	-	-	-	rs4767469	117326854	-	3.97x10 ⁻³
HRK	4.52x10 ⁻⁶	12	117279027	60205	rs7294919	117327592	-	5.78x10 ⁻⁷
-	-	-	-	-	rs7315280	117320938	near-gene-5	6.77x10 ⁻⁷
-	-	-	-	-	rs7132910	117320658	near-gene-5	9.27x10 ⁻⁷
-	-	-	-	-	rs7132339	117335912	-	7.26x10 ⁻⁶
-	-	-	-	-	rs4767469	117326854	-	3.97x10 ⁻³
-	-	-	-	-	rs9669553	117315349	intron	1.23x10 ⁻²
-	-	-	-	-	rs7972948	117312199	intron	1.57x10 ⁻²
-	-	-	-	-	rs884378	117308198	intron	2.33x10 ⁻²
FZD3	5.66x10 ⁻⁵	8	28331773	110209	rs164658	28441566	-	1.07x10 ⁻⁵
-	-	-	-	-	rs352214	28434641	-	6.21x10 ⁻⁵
-	-	-	-	-	rs352222	28421781	utr-3	7.57x10 ⁻⁵
-	-	-	-	-	rs7833751	28362792	intron	8.56x10 ⁻⁵
-	-	-	-	-	rs7001034	28363378	intron	9.80x10 ⁻⁵
-	-	-	-	-	rs4415271	28426419	-	1.13x10 ⁻⁴
-	-	-	-	-	rs6980605	28416551	intron	1.19x10 ⁻⁴
-	-	-	-	-	rs352217	28426263	-	1.25x10 ⁻⁴
-	-	-	-	-	rs7842884	28362459	intron	1.27x10 ⁻⁴
-	-	-	-	-	rs11779401	28435668	-	1.30x10 ⁻⁴
-	-	-	-	-	rs11783087	28404027	intron	1.57x10 ⁻⁴
-	-	-	-	-	rs13260884	28415829	intron	1.58x10 ⁻⁴
-	-	-	-	-	rs6997072	28359611	intron	1.60x10 ⁻⁴
-	-	-	-	-	rs6984655	28369097	intron	1.62x10 ⁻⁴
-	-	-	-	-	rs10092491	28411072	intron	1.78x10 ⁻⁴
-	-	-	-	-	rs352199	28441331	-	1.83x10 ⁻⁴
-	-	-	-	-	rs352203	28394701	intron	2.08x10 ⁻⁴

Gene	Gene P	Chromosome	Start Position	Length	SNP	Position	Features	SNP P
-	-	-	-	-	rs2874941	28373348	intron	2.27x10 ⁻⁴
-	-	-	-	-	rs2241802	28384712	coding-synonymous	2.34x10 ⁻⁴
BRD7P6	8.04x10 ⁻⁵	2	70549227	53823	rs13394815	70564002	-	5.66x10 ⁻⁶
-	-	-	-	-	rs6751950	70560939	-	9.05x10 ⁻⁵
-	-	-	-	-	rs1478644	70576997	-	4.06x10 ⁻⁴
-	-	-	-	-	rs4852161	70562650	-	4.70x10 ⁻⁴
-	-	-	-	-	rs1871238	70574318	-	5.35x10 ⁻⁴
-	-	-	-	-	rs11126264	70572693	-	4.27x10 ⁻²

Supplementary Table 25: Gene-based analysis of mean bilateral hippocampal volume without patients correcting for Sex, Age, Age², Sex*Age, Sex* Age², MDS, TBV.

SNP *P*-values are double genome controlled.

Gene	Gene <i>P</i>	Chromosome	Start Position	Length	SNP	Position	Features	SNP <i>P</i>
ERGIC3	1.81x10 ⁻⁴	20	34109778	55627	rs224415	34135629	intron	5.49x10 ⁻⁵
-	-	-	-	-	rs224419	34143092	intron	1.22x10 ⁻⁴
-	-	-	-	-	rs6060448	34112192	-	1.60x10 ⁻⁴
-	-	-	-	-	rs224440	34159447	-	1.84x10 ⁻⁴
-	-	-	-	-	rs224437	34154371	-	2.10x10 ⁻⁴
-	-	-	-	-	rs7264396	34154741	-	2.13x10 ⁻⁴
-	-	-	-	-	rs224435	34154087	-	2.49x10 ⁻⁴
-	-	-	-	-	rs224430	34153341	-	2.61x10 ⁻⁴
-	-	-	-	-	rs224436	34154124	-	4.85x10 ⁻⁴
-	-	-	-	-	rs17092784	34142287	intron	1.67x10 ⁻³
-	-	-	-	-	rs6119625	34160455	-	3.64x10 ⁻³
-	-	-	-	-	rs2277862	34152782	-	5.50x10 ⁻³
-	-	-	-	-	rs2104417	34127871	near-gene-5	9.68x10 ⁻³
-	-	-	-	-	rs1557203	34164463	-	4.07x10 ⁻²

Supplementary Table 26: Correlations between brain volume and intelligence measures.

Correlations were assessed between brain volume measures and the three intelligence measures in the QTIM sample in unrelated subjects only.

		Hippo	ICV	VIQ	PIQ	FIQ
Hippo	Pearson Correlation	1	.412	.189	.173	.205
	Sig. (2-tailed)		4.15x10 ⁻¹⁴	1.17x10 ⁻³	2.89x10 ⁻³	4.11x10 ⁻⁴
	N	310	310	293	293	293
ICV	Pearson Correlation	.412	1	.214	.132	.190
	Sig. (2-tailed)	4.15x10 ⁻¹⁴		2.21x10 ⁻⁴	2.39x10 ⁻²	1.1x10 ⁻³
	N	310	310	293	293	293
VIQ	Pearson Correlation	.189	.214	1	.576	.857
	Sig. (2-tailed)	1.17x10 ⁻³	2.21x10 ⁻⁴		2.65x10 ⁻²⁷	5.97x10 ⁻⁸⁶
	N	293	293	293	293	293
PIQ	Pearson Correlation	.173	.132	.576	1	.914
	Sig. (2-tailed)	2.89x10 ⁻³	2.39x10 ⁻²	2.65x10 ⁻²⁷		7.34x10 ⁻¹¹⁶
	N	293	293	293	293	293
FIQ	Pearson Correlation	.205	.190	.857	.914	1
	Sig. (2-tailed)	4.11x10 ⁻⁴	1.1x10 ⁻³	5.97x10 ⁻⁸⁶	7.34x10 ⁻¹¹⁶	
	N	293	293	293	293	293

Supplementary Table 27: Location of Manhattan and QQ plots

Cohort Level analyses	Fixed effects meta-analyses	Random effects meta-analyses
Mean Bilateral Hippocampal Volume:		
<i>Controlling for intracranial volume</i>		
Supplementary Figure 9, Supplementary Figure 10, Supplementary Figure 11 & Supplementary Figure 12	Supplementary Figure 25 & Supplementary Figure 26	Supplementary Figure 33 & Supplementary Figure 34
<i>Controlling for total brain volume</i>		
Supplementary Figure 13, Supplementary Figure 14, Supplementary Figure 15 & Supplementary Figure 16	Supplementary Figure 27 & Supplementary Figure 28	Supplementary Figure 35 & Supplementary Figure 36
<i>Without controlling for brain size</i>		
Supplementary Figure 17, Supplementary Figure 18, Supplementary Figure 19 & Supplementary Figure 20	Supplementary Figure 29 & Supplementary Figure 30	Supplementary Figure 37 & Supplementary Figure 38

References

1. Saykin, A.J. *et al.* Alzheimer's Disease Neuroimaging Initiative biomarkers as quantitative phenotypes: Genetics core aims, progress, and plans. *Alzheimers Dement* **6**, 265-73 (2010).
2. Sprooten, E. *et al.* Association of white matter integrity with genetic variation in an exonic DISC1 SNP. *Mol. Psychiatry* **16**, 688-9 (2011).
3. Sprooten, E. *et al.* White Matter Integrity in Individuals at High Genetic Risk of Bipolar Disorder. *Biol. Psychiatry* (2011).
4. Franke, B. *et al.* Genetic variation in CACNA1C, a gene associated with bipolar disorder, influences brainstem rather than gray matter volume in healthy individuals. *Biol. Psychiatry* **68**, 586-8 (2010).
5. Potkin, S.G. *et al.* Identifying gene regulatory networks in schizophrenia. *Neuroimage* **53**, 839-47 (2010).
6. Segall, J.M. *et al.* Voxel-based morphometric multisite collaborative study on schizophrenia. *Schizophr. Bull.* **35**, 82-95 (2009).
7. Schumann, G. *et al.* The IMAGEN study: reinforcement-related behaviour in normal brain function and psychopathology. *Mol. Psychiatry* **15**, 1128-39 (2010).
8. Houlihan, L.M. *et al.* Common variants of large effect in F12, KNG1, and HRG are associated with activated partial thromboplastin time. *Am. J. Hum. Genet.* **86**, 626-31 (2010).
9. Esslinger, C. *et al.* Neural mechanisms of a genome-wide supported psychosis variant. *Science* **324**, 605 (2009).
10. Inkster, B. *et al.* Association of GSK3beta polymorphisms with brain structural changes in major depressive disorder. *Arch. Gen. Psychiatry* **66**, 721-8 (2009).
11. Espeseth, T. *et al.* Accelerated age-related cortical thinning in healthy carriers of apolipoprotein E epsilon 4. *Neurobiol. Aging* **29**, 329-40 (2008).
12. de Zubicaray, G.I. *et al.* Meeting the Challenges of Neuroimaging Genetics. *Brain Imaging Behav.* **2**, 258-263 (2008).
13. Volzke, H. *et al.* Cohort profile: the study of health in Pomerania. *Int. J. Epidemiol.* **40**, 294-307 (2011).
14. Pausova, Z. *et al.* Genes, maternal smoking, and the offspring brain and body during adolescence: design of the Saguenay Youth Study. *Hum. Brain Mapp.* **28**, 502-18 (2007).
15. Rimol, L.M. *et al.* Cortical thickness and subcortical volumes in schizophrenia and bipolar disorder. *Biol. Psychiatry* **68**, 41-50 (2010).
16. Athanasiu, L. *et al.* Gene variants associated with schizophrenia in a Norwegian genome-wide study are replicated in a large European cohort. *J. Psychiatr. Res.* **44**, 748-53 (2010).
17. Psaty, B.M. *et al.* Cohorts for Heart and Aging Research in Genomic Epidemiology (CHARGE) Consortium: Design of prospective meta-analyses of genome-wide association studies from 5 cohorts. *Circ. Cardiovasc. Genet.* **2**, 73-80 (2009).
18. Cavalleri, G.L. *et al.* Multicentre search for genetic susceptibility loci in sporadic epilepsy syndrome and seizure types: a case-control study. *Lancet Neurol.* **6**, 970-80 (2007).
19. Boomsma, D.I. *et al.* Genome-wide association of major depression: description of samples for the GAIN Major Depressive Disorder Study: NTR and NESDA biobank projects. *Eur. J. Hum. Genet.* **16**, 335-42 (2008).
20. Penninx, B.W. *et al.* The Netherlands Study of Depression and Anxiety (NESDA): rationale, objectives and methods. *Int J Methods Psychiatr Res* **17**, 121-40 (2008).
21. Winkler, A.M. *et al.* Cortical thickness or grey matter volume? The importance of selecting the phenotype for imaging genetics studies. *Neuroimage* **53**, 1135-46 (2010).
22. Salvadore, G. *et al.* Prefrontal cortical abnormalities in currently depressed versus currently remitted patients with major depressive disorder. *Neuroimage* **54**, 2643-51 (2011).
23. Morra, J.H. *et al.* Automated mapping of hippocampal atrophy in 1-year repeat MRI data from 490 subjects with Alzheimer's disease, mild cognitive impairment, and elderly controls. *Neuroimage* **45**, S3-15 (2009).
24. Collins, D.L., Neelin, P., Peters, T.M. & Evans, A.C. Automatic 3D intersubject registration of MR volumetric data in standardized Talairach space. *J. Comput. Assist. Tomogr.* **18**, 192-205 (1994).
25. Smith, S.M. & Brady, J.M. SUSAN - A new approach to low level image processing. *International Journal of Computer Vision* **23**, 45-78 (1997).
26. Valdes Hernandez, M.C. *et al.* Reliability of two techniques for assessing cerebral iron deposits with structural magnetic resonance imaging. *J. Magn. Reson. Imaging* **33**, 54-61 (2011).

27. van der Kouwe, A.J., Benner, T., Salat, D.H. & Fischl, B. Brain morphometry with multiecho MPRAGE. *Neuroimage* **40**, 559-69 (2008).
28. Schnack, H.G. et al. Automated separation of gray and white matter from MR images of the human brain. *Neuroimage* **13**, 230-7 (2001).
29. Brouwer, R.M., Hulshoff Pol, H.E. & Schnack, H.G. Segmentation of MRI brain scans using non-uniform partial volume densities. *Neuroimage* **49**, 467-77 (2010).
30. Kochunov, P. & Duff Davis, M. Development of structural MR brain imaging protocols to study genetics and maturation. *Methods* **50**, 136-46 (2010).
31. Pantel, J. et al. A new method for the in vivo volumetric measurement of the human hippocampus with high neuroanatomical accuracy. *Hippocampus* **10**, 752-8 (2000).
32. Morra, J.H. et al. Validation of a fully automated 3D hippocampal segmentation method using subjects with Alzheimer's disease mild cognitive impairment, and elderly controls. *Neuroimage* **43**, 59-68 (2008).
33. Sklar, P. et al. Large-scale genome-wide association analysis of bipolar disorder identifies a new susceptibility locus near ODZ4. *Nat. Genet.* **43**, 977-83 (2011).
34. Ripke, S. et al. Genome-wide association study identifies five new schizophrenia loci. *Nat. Genet.* **43**, 969-76 (2011).